skb.se

SKB P-26-06

ISSN 1651-4416

ID 2122159

June 2026

Non-linear groundwater flow during hydraulic borehole testing in fractured rock

Mansueto Morosini

Svensk Kärnbränslehantering AB

Keywords: Packer test, Skin, Well skin, Tunnel skin, Non-Darcy, Non-laminar, Non-linear, Turbulent, Turbulence, Formation loss, Aquifer loss, Well test, Step test, Injection test, Constant head test, Constant pressure test, Constant drawdown test, Constant rate test, Fractured rock, Crystalline rock, Rate transient analysis, Pressure transient analysis, Rate superposition, Rorabaugh, Jacob, Forchheimer, K03009F01, K08028F01, Äspö.

Preface

While this study is published long after the field investigations were terminated, its outcome provided support to the on-going work on SKB's methodologies for hydraulic borehole testing. The issue and scope of works are still relevant and still with room for development and improvement, of both testing methodology as well as interpretation and analysis tools.

Many thanks are due to Lars Andersson (SKB) for support in performing the field operations and to Kent Hansson and Calle Hjerne (Geosigma AB) for support at the planning stage and for stimulating discussions on test interpretation at the time of field operations.

Summary

Hydraulic tests were performed in boreholes from a tunnel at 400 m depth in fractured crystalline rock with the objective to identify and quantify non-linear flow and fracture aperture effects. A suite of 25 hydraulic tests are executed targeting discrete fractures with apertures of 0.5 and 1 mm and a crush zone of 27 mm width. Complementary interpretation is made through Q-p cross plots, pseudo steady-state evaluation of step tests and transient interpretation of perturbation phases. Tests are performed with pressure perturbations ranging 100-3000kPa and flows ranging 0.04-7L/min. Non-linear flow to different degree is identified in all tests, from transitional flow to fully turbulent flow with flow rate exponent of n=1.5-2.

Sammanfattning

Hydrauliska tester har utförts i borrhål från en tunnel på 400 m djup i sprickigt kristallint berg med syfte att identifiera och kvantifiera icke-linjärt flöde och sprickapertur effekter. En serie av 25 hydrauliska tester har utförts på sprickor med aperturer på 0,5 och 1 mm och en krosszon som är 27 mm bred. Olika kompletterande testutvärderingar utförs genom Q-p plottar, pseudo-stationär utvärdering av stegvisa tester samt transient utvärdering av testets störningsfas. Testerna har utförts med tryckstörningar i intervallet 100-3000 kPa och flöden 0,04-7L/min. Icke-linjärt flöde i olika utsträckning har identifierades i alla tester, från övergångsflöde till fullt turbulent flöde med flödeshastighetsexponenter i intervallet n=1,5-2.

Extended abstract

Introduction/Objective

The present study is undertaken to support a revision of SKB's standard procedures for site investigations. Its primary focus is on the issue of well and near well head losses due to non-linear flow when conducting hydraulic borehole tests for determining formation- and borehole parameters and hydraulic connectivity in the formation. This provides insight/understanding of the issue in support of developing the methodology and toolbox for SKB´s site characterization and investigations with particularly aim at the extension and construction of underground repositories for radioactive waste at Forsmark, Sweden.

The direct trigger for the present study is some elevated/abnormal results of skin factors encountered in borehole K03009F01which were suspected to be caused by non-linear flow (Morosini, 2018). Although quite high skin factors is not a new issue and have been encountered from time to time during investigations at Äspö HRL.

A hydraulic borehole testing programme was executed to provide in-situ data towards development and revisions of SKB's toolbox for hydrogeological investigations with particular focus on non-linear flow effects.

The primary objective of the study is to perform and analyse hydraulic borehole tests to identify and quantify non-linear flow and possibly fracture aperture effects and to gain some further understanding on reasons for some abnormally high skin factors.

Methodology

The testing campaign comprised four borehole sections in two sub-horizontal boreholes in sparsely fractured crystalline rock situated at 400 m depth at the Äspö HRL in southeastern Sweden, where a total of 25 tests were executed comprising different test types.

- a combination of step tests with variable flow (i. e. constant head)
- a combination of step tests with variable pressure (i. e. constant rate)
- constant rate injection tests
- constant head injection tests.

The tests targeted discrete fractures with apertures of 0.5 and 1 mm and a crush zone of 27 mm width. Pseudo steady-state evaluation of step test was the main tool for assessing non-linearity through Q-p plots and Rorabaugh analysis. These were complemented with constant perturbation tests at different perturbations for full transient analysis as a mean to checking and validating the pseudo steady-state conditioned step test result. Test were performed with pressure perturbations ranging 100-3000 kPa and flows 0.04-7 L/min. The tests were performed with SKB´s equipment, comprising.

- Downhole: pressure gauges, inflatable packers, hose and aluminium pipe string
- Borehole collar: valves, pressure and flow gauges, pressure vessel and a high-pressure water injection controller unit (HWIC).

Test sections are sealed with packers from Petrometalic with sliding sleeve and 0.94m sealing length. Groundwater pressure is measured with absolute pressure gauges. The test valve to the test section is situated outside of the borehole, at the borehole collar. The equipment is schematically outlined in the Figure 3-1.

All tests are single hole as either constant perturbation tests or stepwise variable perturbation tests (step tests). These are evaluated in different ways, with the main objectives to a) identify indicator(s) for non-linear flow and b) quantify the non-linear flow component.

The interpretation is based on the well loss concept where the additional nonlinear head loss is expressed through a power law of flow rate. For definitions and nomenclature see chapter 4 and 5.

Three lines of interpretation were identified and are pursued on the field data:

- **Q-p evaluation:** Produce linear plots of pressure change and specific capacity respectively, as a function of volumetric flow rate (i.e. *dp* vs *dQ* and *dQ/dp* vs *dQ*) to indicate deviation from linearity, see Figure 5-2. The main objective with this type of interpretation is to identify if non-linear flow is present. This type of interpretation is done on all step tests.
- **Step test evaluation:** Adopts Jacob's well loss concept through application of Rorabaugh´s method of interpretation. The main objective with this type of interpretation is to identify and quantify non-linear flow through the CQ^n-term.
- **Transient evaluation:** A batch of tests are performed at different consatant head. Interpretation of the perturbation phase yield flow geometry, transmissivity and skin factor. The test and interpretation are based transient conditions.

Results

Non-linear flow was identified in all tests, from transitional flow to fully turbulent flow with flow rate exponent of n=1.5-2.

Well efficiency is ranging 2-50%. It was estimated that the non-linear energy loss is causing a reduction in transmissivity in the range 11-65% with an exponentially decaying functional form, albeit it is close to linear the crush zone.

Tests targeting singular discrete fractures all developed radial formation flow geometry while the crush zone displayed radial flow followed by a transition towards a second radial flow albeit with lower skin.

Discussion/Implication

The presence of non-linear flow will have no or little impact on the derived transmissivity from constant rate tests when transient interpretation is made. It will however cause a larger total skin factor, as the effect of geometrical skin and non-linear skin are lumped together, the amounts of which depends on the individual components. The impact also depends on whether the test is performed/evaluated according to transient flow or pseudo steady-state flow theory, the latter does not account for skin at all.

Constant head tests are sensitive to non-linear flow. These are rate-transient with decreasing flow during the perturbation phase, the magnitude of which depends on the degree of non-linearity. The impact is on the transient flow since the targeted constant drawdown (dh) is to a certain extent composed of and exaggerated by non-linear losses. This requires additional flow to maintain the specified head and, if not accounted for, gives a misrepresented transient flow evolution and underestimates the calculated transmissivity.

The presence of non-linear flow may also have an impact on the diagnostic interpretation of flow geometry. If an extensive non-linear flow regime develops near the borehole, it may be interpreted as the formation being of lower transmissivity instead of a flow-induced effect. This is exhibited as a radial composite flow geometry leading to the identification of a lower transmissive zone near the wellbore rock while it in fact does not exist. Hence, this will give a wrong conceptualization and potentially also feed incorrect parameters into the statistics supporting the homogenization/parameterization process during the conceptual modelling exercise.

Conclusion

Non-linear flow is identified in all test sections, from transitional flow to fully turbulent flow. It is much more pronounced in small open fractures than in a crush zone environment. The presence of non-linear flow is mainly impacting the skin factor/well loss component which may extend into the rock forming a two-regime flow system of non-linear/linear flow proximal to the borehole. To summarize it was found that:

- non-linear flow is present in all test sections covering different hydraulic features small open fractures, crush zone and low transmissive deformation zone. The flow regime ranges from transitional to fully turbulent with a flow exponent of n = 1.5-2.0 which reduces the well efficiency to between 50 – 2 %,
- for small open fractures high total skin factors occur when non-linear flow is present during the test and not accounted for in the evaluation,
- for the crush zone the skin factors are low, even when non-linear flow is present. Suggesting the non-linear flow component is modest under otherwise same conditions,
- much higher skin factors are present in small open fractures than in the crush zone, up to a ten-fold difference,
- transmissivities derived from steady-state evaluations are always prone to underestimate the actual transmissivity when positive skin is present. When the skin is also caused by non-linear flow the estimated transmissivity can be exceptionally wrong, by an order of magnitude,
- through analogy between borehole and tunnel, it is inferred that principles for non-linear flow and very high skin factors for boreholes in this investigation are equally applicable for tunnel inflow and associated head distribution around a tunnel,
- a distinct fracture aperture and/or gouge remobilisation effect was observed for the crushed zone section (Test 12).

Content

1 Introduction

The present study has the primary focus on the issue of well and near well losses due to non-linear flow and fracture aperture effects when conducting hydraulic borehole tests. Generaly, such tests aim at determining formation- and borehole parameters as well as hydraulic connectivity in the formation. This provides insight/understanding of the issue in support of developing the methodology and toolbox for SKB´s site characterization and investigations.

SKB has performed geoscientific site investigation over many years and maintain a suite of standard procedures for their execution. The procedures set general demands on geoscientific investigation methods, their uncertainty, technical execution as well as quality assurance and quality control. The present investigation is in support of a revision exercise of SKB's site investigation procedures to provide data on non-linear flow.

Hydraulic tests to address non-linear flow effects are performed in two horizontal boreholes at 400m depth at Äspö Hard Rock Laboratory (ÄHRL), K03009F01 and K08028F01. Geometrical borehole data is compiled in Table 1-1 and their location in the ÄHRL tunnel system is shown in Figure 1-1.

Table 1-1. Geographical and geometrical borehole information.

Borehole id:	K03009F01	K08028F01
Location	Äspölaboratoriet, TAS03	Äspölaboratoriet, TAS08
Coordinate system (xy/z)	RT90/RHB70	RT90/RHB70
Start coordinate (m)	Northing: 6367 996.02m Easting: 1551 627.02m Elevation: -399.23masl	Northing: 6368 033.71m Easting: 1551 637.79m Elevation: -396.56masl
Azimuth (°)	319,18	308,68
Inclination (°)	-0.37 (down)	2.10
Diameter (mm)	75.8	75.8
Length (m)	100.92	94.39
TOC from reference point of rock face (m)	0.238	0.35
Casing length (m)	2.44	2.28
Casing inner diameter (mm)	80	76.2

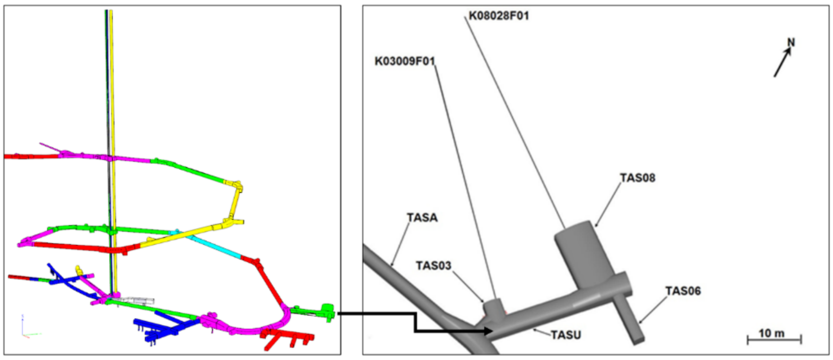

Figure 1-1. *Location of tested boreholes K00009F01 and K08028F01, about 40m apart, situated at about 400m depth in the Äspö Hard Rock Laboratory.*

The investigations and activities are undertaken in the framework of SKB's quality assurance system through SKB's internal controlling document according to Table 1-2. The activity plan provides detailed specification on what, whom, when, where and deliverables while the method description specifies requirements on data output and execution from the test.

Table 1-2. SKB`s internal controlling documents

Document	Number	Version
Aktivitetsplan Skintester i borrhål K03009F01	AP TD F49-15-006	1.0
Metodbeskrivning för Hydrauliska enhålstester i tunnelborrhål	SKB MD 324.009	2.0
Metodinstruktion för analys av hydrauliska injektions- och enhålspumptester.	SKB MD 320.004	3.0

After some consideration, the term "non-linear" has been adopted throughout the report. It shall be understood as synonymous to "non-Darcy" and to "non-laminar" with regards to groundwater flow. This non-linearity in flow includes the transitional phase up to fully turbulent flow and beyond. Non-linear flow effects can also be observed at the lower end of flow rates, involving molecular effect, but this is not included or addressed in the present study. Conversely, "linear flow", "laminar flow" and "Darcy flow" are regarded as synonymous with the meaning of the flow being attributed exclusively to viscous forces, termed a potential flow in the field of physics.

"Linearity" between variables is another often used term, not to be confused with linear flow.

2 Objective and scope

2.1 Objective

The present study is undertaken with the objective to provide data and insight on the presence of non-linear flow and fracture aperture effects during hydraulic borehole testing. It aims to include a couple of hydrogeological environments which are typically encountered in tunnel drilled boreholes in crystalline rock i.e. open fractures and crush zones.

Although quite high skin factors is not a new issue and have been encountered during investigations at Äspö HRL, the direct trigger for the present activity is from elevated/abnormal skin factors which are suspected to be caused by non-linear flow (Morosini, 2018) or possibly fracture aperture effects or a combination of both.

A hydraulic borehole testing programme was executed with the objective to identify and quantify non-linear flow and fracture aperture effects, if any.

The primary objective with this report is to compile and present the measured data/variables along with their execution and basic data treatment/evaluation into parameters, secondly, to state if and how the objectives of the study have been achieved and possibly to make conclusions and inferences based on the test results.

Target audience for this report are expert professionals involved with hydraulic borehole testing.

2.2 Scope

The testing campaign comprised four borehole sections in two sub-horizontal boreholes situated at 400m depth at the Äspö HRL. Three sections in borehole K03009F01 were tested during March 30 - April 30, 2015 targeting discrete open fractures and one section in borehole K08028F01 during March 23 – April 5, 2016 targeting a crush zone. A total of 25 tests were executed comprising a suite of test types

- a combination of step tests with variable flow (i. e. constant head)
- a combination of step tests with variable pressure (i. e. constant rate)
- constant head injection test
- constant rate injection test.

The test programme is summarised in Appendix 1.

Following the initial test evaluation, preliminary results from K03009F01 were presented and discussed within SKB in September 2015 it was decided to perform complementary tests in one section in borehole K08028F01 to target a crush zone.

3 Execution

Tests are conducted by either withdrawing water from or injecting water to the test section. Both modes constitute a perturbation of the prior pressure and flow situation in the test section and in the formation. Consequently, withdrawing or injecting water is termed a perturbation and perturbation phase, which is followed by a recovery phase where pressure and flow tend to return to its original state.

3.1 Hydrogeological environment

The tested sections are situated in sparsely fractured rock of fine-grained granite, diorite and granodiorite where the hydraulic features are predominantly subvertical and trending NE. A couple of crush zones are intercepted through the tested borehole sections, of relatively low transmissivity. A deformation zone (DZ) is present at 10-32m borehole length in K03009F01. This deformation zone has highly transmissive contact with the surrounding competent rock. The high water-yielding contact zone at 10.5m in K03009F01 was grouted during the drilling operations and hydraulically tested prior to grouting (Morosini 2018). Hydraulic connectivity modelling suggests this DZ is sub-vertical trending NW-SE. A deformation zone was also identified at 77-100m in K03009F01 which proved to be hydraulically insignificant. Otherwise, small discrete fractures carry most of the water. From the general understanding of rock stress at Äspö HRL (Hakami, 2003) it is inferred that the major principal stress Sigma1 of 30MPa is subvertical with a NS trend.

3.2 Tested features

The very high skin values which had previously been identified in K03009F01 (Morosini, 2018) provided the prime motivation as target for our investigations. The prior characterisation of the borehole, with geological mapping and flow logging provided good support in target selection, target objectives, programme formulation and test interpretation. Targeted features and its support data are summarised in Table 3-1.

Selection of 14.20-17.19m in K03009F01 is based on the high skin (538) that was previously calculated and on the fact its inflow when drilling was relatively low (0.7L/min). Section 17.20-20.19m was selected because it had ten times higher inflow (7L/min) while the evaluated skin was ten times lower (51), for approximately same borehole drawdown.

Section 37-39m in K08028F01 comprise a relatively low transmissive crush zone with relatively consistent parameters evaluated from a prior test (Hjerne et.al, 2016).

The tests in K08028F01 are complementary to those in K03009F01, with main objectives to

- test the hydraulic behaviour of a crush zone.
- perform a more refined step test, with more and smaller steps, 16 steps instead of 7.

Table 3-1. Flow features identified in the tested borehole sections

Test section and target (feature)	Inflow during drilling[1)] [L/min]	Open fractures Borehole[2)] length[m]	Fracture aperture [mm] [2)]	Fracture flow log [L/min] [3)]	Fracture transmissivity (m²/s) [3)]
Borehole K03009F01					
14.20-17.19m (fractures)	1	15.42	0.5	0.010 at 15.6m	5.9E-10
		15.95	1		
		16.1	1	0.410 at 16.2m	1.9E-8
17.20-20.19m (fracture)	1	17.21	0.5	0.173 at 17.2m	8.5E-9
		17.26	0.5		
15.30-16.79m (fractures)	1	15.42	0.5	0.010 at 15.6m	5.9E-10
		15.95	1		
		16.1	1	0.410 at 16.2m	1.9E-8
Borehole K08028F01					
37.00-39.00m (crush zone)	1.3	37.560-37.587	27	0.395 at 37.6m	2.3E-8

1) Report P-15-10, Nilsson, G., 2017. Steered core drilling of boreholes K03009F01 and K08028F01 at the Äspö HRL.

2) Internal memo:1475597, Hultgren & Mattsson, 2015. Geological single-hole interpretation of K03009F01.

3) Report P-15-13, Komulainen & Pöllänen, 2016. Difference flow logging in boreholes K03009F01 and K08028F01.

3.3 Testing programme

The testing programme comprises twenty-five tests of four test types in four borehole test sections, Table 3-2. The full test programme specification is presented in Appendix 1.

Table 3-2. Tested sections and type of tests

Test type (acronym)	Test section & Test No (see Appendix 1 for details)			
Test section: Target object:	K03009F01 14.20-17.19m fracture	K03009F01 17.20-20.19m fracture	K03009F01 15.30-16.79m fracture	K08028F01 37.00-39.00 crush zone
Step constant rate withdrawal & recovery (sCRwr)	1	9	10	13
Constant head withdrawal & recovery (CHwr)	2-6	9a-9e		14-18
Step constant head injection & recovery (sCHir)	7	9f	11	12
Constant head injection & recovery (CHir)	8			19

The basic rationale for the adopted type of tests is to use step tests to a) obtain indication and measure of non-linear flow and b) an indication of fracture aperture effect. Constant perturbation tests with transient evaluation provide a reference to commonly used procedures for comparison as a mean to bench mark the step tests, particularly those requiring pseudo steady-state flow. Test specific objectives are summarised in Table 4-1.

Each test comprises two phases, a perturbation (stepped or constant) and recovery phase respectively.

For the injection tests fresh tap water was utilised traced with uranin (0.2mg/L). The testing programme is summarised in Appendix 1.

The logging time for pressure and flow in the test section was set in the testing control unit (HWIC) as follows,

- measurement period 5min prior and after change of flow rate (i. e. start & stop): log time=1s
- measurement period 5min – 60min: log time=10s
- measurement period 60min – 5min prior to change of flow rate: log time=60s.

Logging time in the observation sections inner and outer of the test section is set to 20s throughout the tests.

3.4 Testing equipment

The tests were performed with SKB´s equipment schematically outlined in Figure 3-1 and in Appendix 2, comprising

a) Downhole: pressure gauges, inflatable packers, hose and aluminium pipe string

b) Borehole collar: valves, pressure and flow gauges, pressure vessel and a high-pressure water injection controller unit (HWIC).

The packers are from Petrometalic with sliding sleeve and 0.94m sealing length. Groundwater pressure is measured with absolute pressure gauges.

The test valve to the test section is situated outside of the borehole, at the borehole collar.

The control unit (HWIC[1]) is comprised of various pumps, valves, gauges, data loggers and computerised control unit for regulating pressure and flow during a hydraulic test and housed in a box measuring 1.3*0.8*1.2m. It automatically converges towards an operator-specified pressure or flow capable of performing constant head or constant pressure withdrawal or injection tests in tunnel boreholes at large depths. The constant head tests can be made in the flow range 0.002-50L/min with a formation pressure of up to 5MPa. Pressure disturbance in the test section can be made in the range 0.1-2MPa with a resolution of about 0.001MPa. For constant flow tests the unit is capable to perform with flow in the interval 0.05-40L/min. The unit is set to automatically converge towards the set (desired) constant pressure or flow, which is achieved within 1 minute for most field conditions and then kept constant at the set value throughout the test phase.

Part of the test equipment is installed in the borehole of 0.076m diameter drilled in fractured crystalline rock at 400m depth. Part of the equipment is installed outside of the borehole, where pressure and flow in the HWIC control unit situated about 3m from the borehole collar. The tubing (pipe string) inner diameter is 21 mm stainless steel which at borehole collar is connected to same diameter plastic hose connected to the flow gauges 3m from the borehole collar in the control unit HWIC.

Flow is from/to test section which is isolated with hydraulic packers and a guard packer close to casing sealing the borehole outflow.

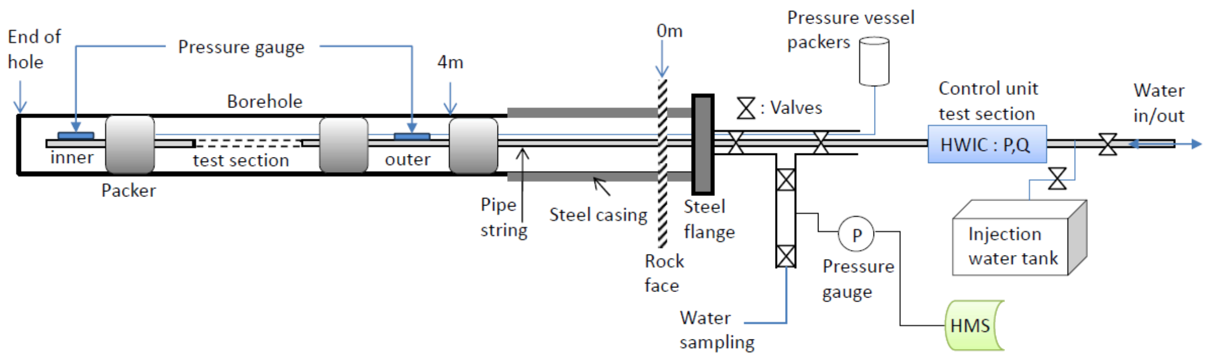

Figure 3-1. Schematics of the test system, down-hole and at the borehole collar. See Appendix 2 for test site and equipment photos. HMS is SKB´s time series database Hydro Monitoring System. Inner section is sometimes termed below section and outer section sometimes termed above section.

[1] HWIC : High pressure Water Injection Control is an SKB developed control system.

Head losses due to friction through pipe and packer have been calculated for various flows according to Table 3-3. For the flows encountered in these tests (0.05 to 7 L/min for 20m length) it is concluded these losses are so small that they may be neglected.

Table 3-3. Friction losses in PSS-pipes[2] with inner diameter of 21 mm, including two Petrometalic Bimbar 1-54 packers (Kent Hanssson, 2015 personal communication through internal memo).

Flow (L/min)	Friction losses. 20 m pipe (mH_2O)	Friction losses. 100 m pipe (mH_2O)	Friction losses. 300 m pipe (mH_2O)
1	0,006	0,03	0,09
10	0,03	1,5	4,5
20	1,1	5,3	15,9
30	2,2	11,0	33
40	3,7	18,3	54.9
50	5,4	27,2	81.6
70	9,9	49,6	148,8
100	18,7	93,6	280,8

The pressure in sections above and below the test section were logged throughout the testing campaign according to Table 3-4 and responses are presented in Appendix 3. These responses are not interpreted/evaluated in the present report.

Table 3-4. Test sections delimited by hydraulically controlled rubber packers of 0.94m length.

Borehole	S1 below	S2 test sec.	S3 above	Start date	Stop date
K03009F01	100.92-18.13m	17.19-14.20	13.26-4.02m	2015-03-30	2015-04-09
	100.92-21.13m	20.19-17.20	16.26-4.02m	2015-04-15	2015-04-23
	100.92-17.73m	16.79-15.30	14.36-4.12m	2015-04-28	2015-05-06
K08028F01	94.39-39.94m	39.00-37.00	36.06-4m	2016-03-22	2016-04-05

3.5 Data collection

Recorded data was from test section pressure, flow rate with two gauges for high and low flow respectively and for air pressure. It was collected digitally in the HWIC control unit every 10 second but increased to every second at rate change or pressure change.

Test data is logged in the control unit (HWIC) and transferred to USB-memory after each test for delivery to the responsible hydrogeologist for a first check of data integrity. No barometric or tidal compensation was made of the groundwater pressure data since we are evaluating perturbations and tests are of relatively short duration. After controlling data integrity the responsible hydrogeologist signals a go-ahead for the next test to field personnel. Once all tests have been performed, the data quality has been controlled, and a first test evaluation done then the complete data set is delivered to SKB´s site characterisation database (SICADA).

Pressure data was collected from the inner and outer sections relative to the test section but these are not analysed in the framework of this report but are presented in Appendix 3.

[2] PSS (Pipe String System) is the SKB-developed hydraulic testing system for surface drilled boreholes. Pipes from that system were utilised for the present hydraulic tests.

3.6 Quality control

Quality control is made throughout the test campaign with respect to i) that the tests are performed correctly and ii) with respect to data integrity, in the following general steps

- issuing a detailed activity plan to the field personnel on specifying all details of the execution
- calibrating the control unit prior to testing, including all gauges
- double checking and documenting that the packers are indeed set at the specified position (self-check by field personnel)
- checking and documenting the pressure in the test section with a manometer as well as gauging with a transducers
- performing manual flow rate control measurement for outflow tests to check against the flow gauge data
- plotting the data after each test to check that it is reasonable and controlling for abnormalities or outliers
- having a close and continuous dialogue between field personnel and the responsible hydrogeologist throughout the test campaign

3.7 Nonconformities

An activity plan for the tests in borehole K08028F01 (Test 12-19) was not issued or activity plan for K03009F01 updated.

Pressure data from inner and outer observation sections in K03009F01 during test #9a-11 are missing.

Data from the failed tests 9b, 9c and 9d are missing due to a corrupt memory card of the testing system which consequently did not collect data.

4 Interpretation

All performed test are single hole tests which may be classified as constant perturbation tests and stepwise variable perturbation tests (step tests). These are evaluated in different ways, with the main objectives to a) identify indicator(s) for non-linear flow and b) quantify the non-linear flow component.

As an alternative approach, the variation of total skin with drawdown and flow rate is also assessed (Tests 2-6, 9a-9e and 14-18). This is further elaborated by Morosini (2026) through the rate-dependent skin concept.

Our basic understanding of well losses (linear and non-linear) is summarised in Chapter 5 from which three lines of interpretation were identified and are pursued on the field data, briefly outlined below and explained in chapters 4.2 and 4.3:

- **Q-p evaluation:** Produce linear plots of pressure change and specific capacity respectively, as a function of volumetric flow rate (i.e. *dp* vs *dQ* and *dQ/dp* vs *dQ*) to indicate deviation from linearity, see Figure 5-2. The main objective with this type of interpretation is to identify if non-linear flow is present. This type of interpretation is done on all step tests. The test and interpretation are based on pseudo steady-state conditions.
- **Step test evaluation**: Adopting Jacob's well loss concept through application of Rorabaugh´s method of interpretation. The main objective with this type of interpretation is to identify and quantify non-linear flow through the CQ^n-term. The test and interpretation are based on pseudo steady-state conditions.
- **Transient evaluation:** A batch of tests are performed at different consatant head. Interpretation of the perturbation phase yield flow geometry, transmissivity and skin factor. The test and interpretation are based transient conditions.

Q-p evaluation according to steady-state well equation is described in chapter 5.1 and evaluation according to Rorabaugh´s transient state equation in chapter 5.2. Specific objectives of the test evaluation are summarised in Table 4-1.

Table 4-1. Specific test objectives for each test type

				For each of the test sections a suite of test types were performed :	
Borehole id.	Test section	Test#, App1.	Test type[1]	Objective with test evaluation	Flow regime
K03009F01	14-17m	1		identify nonlinearity with Q-p plot	Pseudo steady-state
K03009F01	17-20m	9	sCRwr	identifyt nonlinearity with Q-dQ/dp plot providing functional relation with Q-T plot	Pseudo steady-state
K03009F01	15-17m	10	x 1	quantify n in nonlinear exponent of CQ^n	Pseudo steady-state
K08028F01	37-39m	13			
K03009F01	14-17m	2-6		identify nonlinearity with Q-p plot	Transient state
K03009F01	17-20m	9a-9e	CHwr	identifyt transient flow regime and quantify T and total skin $\xi_T = \xi_0 + \xi_n$	Transient state
K08028F01	37-39m	14-18	x 5	identify nonlinearity with Q-p plot from T, ξ_T of each test	Transient state
				Cross check parameters between PSS (sCRwr) and TS (CHwr)	Transient state
K03009F01	14-17m	7		Check testing effects on fracture T, aperture or gouge (Test 12)	Pseudo steady-state
K03009F01	17-20m	9f	sCHir	nonlinearity with Q-p plot	Pseudo steady-state
K03009F01	15-17m	11	x 1	nonlinearity with Q-dQ/dp plot providing functional relation with Q-T plot	Pseudo steady-state
K08028F01	37-39m	12			
K03009F01	14-17m	8	CHir	Objective for these tests is not directly related to the non-linear flow issue.	Transient state
K08028F01	37-39m	19	x 1	Cross check consistency with CHwr with dp=1000kPa, Test 4 and 16.	

1) sCRwr: step Constant Rate withdrawal & recovery
CHwr: Constant Rate withdrawal & recovery
sCHir: step Constant Head injection & recovery
CHir: Constant Head injection & recovery

Test interpretations are presented in Chapter 6 for borehole K03009F01 and Chapter 7 for borehole K08028F01. Basic field data comprise time series of flow and pressure from the tests listed in Appendix 1. The data is visualised through cross plots and results from the evaluation presented in Appendix 4 and 5. Evaluated hydraulic formation parameters are compiled in Appendix 7.

4.1 Data processing and interpretation

The processing and evaluation of test data follows the basic SKB´s standard procedure (SKB MD 320.005) for single hole tests with some additions for step tests. Basic variables for evaluation were the measured absolute gauge pressure in kPa (uncorrected for atmosphere or tidal) and the measured volumetric flow in L/min.

No barometric compensation was applied to the absolute pressure data since we are dealing with pressure difference and test are of relative short duration, Appendix 3. Therefore, its effect is at most marginal and neglected.

The fluctuation of air pressure during a test is maximum 0.5kPa and consequently the barometric amplitude is 0.25kPa (tests 9,12,16,17). Whereas the tidal amplitude is about 0.5kPa (e.g. for Test 7).

4.2 Q-p interpretation

This type of test evaluation is based on the relation between head perturbation and specific capacity as a function of flow to see deviation from linearity which is helpful for understanding the behaviour of the rock mass and fracture, see e.g. Houlsby (1976) and Stille (2015). The basis for linearity is that steady state flow conditions have been achieved during the test, which it is when *dh/dt=0* for a constant rate test. Since steady-state is difficult to achieve then pseudo steady-state is deemed a sufficient approximation instead. In such case the perturbation varies linearly with time and *dh/dt=constant*. See chapter 5.1 for discussion of this issue.

4.3 Step test interpretation

4.3.1 Step constant head injection tests

This type of testing is a standard approach in rock engineering, particularly to assess hydromechanical coupling, see e.g. Rutqvist & Stephansson (2003) and Quinn et.al. (2011). These tests were performed with steps of constant head during the perturbation phase followed by a recovery phase.

4.3.2 Step constant rate withdrawal tests

This type of test is standard for assessing the turbulent well loss, originated by Jacob (1946) with many variants developed ever since, see e.g. Kruseman and de Ridder (1991), Batu (1998). These tests were performed with steps of approximately constant rate during the perturbation phase followed by a recovery phase. Evaluation of these tests was done according to Rorabaugh (1953) to derive the non-linear flow exponent (n) in equation 4-2.

This type of test was performed for Tests 1, 9, 10, 13.

4.4 Transient interpretation

4.4.1 Constant head tests

This type of test is conducted with a perturbation phase of constant head as either injection or withdrawal, followed by a recovery phase. Transient evaluation of this type of test was originated by Jacob and Lohman (1952) and is well described with theory and practice by da Prat (1990) and Doe and Geier (1990). Test evaluation generally follows SKB MD 320.005 based on the application of type curves and pressure derivatives and multi-rate superposition in time. This type of test was performed for Tests 2-6, 9a-9e and 14–18.

The transient evaluation is done for the perturbation phase. For each test phase this comprise to produce a diagnostic log-log plots to identify flow regimes and hydraulic boundaries which is providing the basis for selection of an appropriate geometric flow model to apply. Formation parameters were then calculated based on this conceptual understanding of flow geometry and hydraulic boundaries; results are compiled in Appendix 4.

4.5 Interpretation software and workflow

Software tools for test evaluation are OriginPro (OriginLab) for Q-p plots and step tests and Aqtesolv Pro v4.5 (HydroSOLVE Inc., 2007) for constant head tests.

Additionally, the step outflow tests (sCRwr) were evaluated with the Rorabaugh step test solution implemented in a spreadsheet software (OriginPro).

The workflow for the evaluation of the tests comprise following:

- Produce history plot for overview for checking consistency, quality of test and data and tidal signature if any.
- Data processing, including quality control and synchronization of pressure and flow.
- Produce Log-Log and Lin-Log plots of the test phase.
- Identify flow regimes and appropriate model from Log-Log plot, in particular the formation flow regime.
- Perform non-linear regression and calculate transmissivity and skin factors.
- Check visually that matching that model/data for each test phase is satisfactory.

5 Formation and well losses

The total drawdown in groundwater pressure (dp_T) when flowing a borehole may theoretically comprise the aggregate of energy losses (drawdown) due one or several reasons,

- linear flow (aquifer/formation and pipe) $[dp_l]$
- non-linear flow (formation, wellbore, casing) $[dp_n]$
- wellbore skin effects (screen and gravel pack) $[dp_s]$
- two-phase flow (e.g. due to degassing) $[dp_g]$
- fracture aperture changes (gouge redistribution, rock stress) $[dp_a]$
- formation compaction (loss of storage) $[dp_c]$
- restrictions in stream lines (e.g. partial penetration) $[dp_p]$

Hence, the total drawdown in pressure is a sum of different components. Their relative contribution towards the total drawdown is unknown when conducting the test but may to some degree be alleviated through some external knowledge of the hydrogeological environment, conducting the appropriate type of tests and by accounting for the effects in the analysis procedure.

As mentioned above, the focus of this study is non-linear flow so that test type and test design has been focused with this in mind and the total energy loss considered here is

$$dp_T = dp_l + dp_n + dp_s \qquad Equation\ 5-1$$

The scientific literature on well and aquifers losses is prolific. The overwhelming number of studies relate to homogeneously distributed porous media flow in confined aquifers (or reservoirs) with relatively small drawdown. Whereas the present situation is indeed in a confined system but of sparsely fractured crystalline rock where the drawdowns can be quite large (up to 350m at Äspö HRL).

Houben (2015a and 2015b) revived the issue of well losses, which mostly focused on steady state flow although did account for transient flow in one section of the Houben (2015b) paper.

In order to discriminate between the different types of losses mentioned above (at least to some degree) it is necessary to perform tests at different flow rates.

To calculate the well loss the non-linear flow approach where flow is a power law function was adopted (ch. 5.1 and 5.2).

5.1 Forchheimer/Thiem steady state equation

The basic assumption for this type of interpretation assumes the formation is homogeneous and the flow is at steady-state. Energy losses due to linear well flow (i.e. *dp* being linearly dependent on flow velocity *q*) are basically described by the Thiem equation for steady state flow (Thiem, 1906) and by the Theis equation for transient flow (Theis, 1935), including variations and developments thereof. However, experiments at steady state showed that when the flow rate is high the flow may become turbulent whereby there is a non-linear dependence between the gradient *dp/dr* and the flow velocity *q*. A parabolic dependence was arrived at by Forchheimer (1901)[3]

$$\frac{dp}{dr} = Bq + C_F q^2 \qquad Equation\ 5-2$$

where *B and* C_F are constants, *r* is length, *p* is pressure and *q* is the flow velocity (specific discharge). C_F is sometimes called the Forchheimer friction factor.

---

[3] This was originally suggested by Dupuit through extension of Darcy's law (Bear et.al., 1968).

For a well with concentric flow geometry pumping with constant rate i.e.

$$dQ_w = A \cdot dq = constant \qquad Equation\ 5-3$$

$$A = 2\pi rH \qquad Equation\ 5-4$$

Bear (1979, p307) integrated Eq 5-2 to obtain a well flow equation with a non-linear term included, constituting an extension of Thiem´s equation,

$$dp = \frac{dQ}{2\pi T} \cdot ln\left(\frac{R}{r_w}\right) + \frac{b \cdot dQ_w^2}{4\pi^2 H^2}\left(\frac{1}{r_w} - \frac{1}{R}\right) \qquad Equation\ 5-5$$

where H is the formation thickness and b is the Forchheimer friction factor.

Expand that by adding a geometrical skin ($dp_{\xi 0} = \frac{dQ_w}{2\pi T} \cdot \xi$) and allowing the non-linear flow rate exponent to be variable (n)

$$dp_w = \frac{dQ_w}{2\pi T} \cdot ln\left(\frac{R}{r_w}\right) + \frac{dQ_w}{2\pi T} \cdot \xi + \frac{b \cdot dQ_w^n}{4\pi^2 H^2}\left(\frac{1}{r_w} - \frac{1}{R}\right) \qquad Equation\ 5-6$$

Adopting this relation to our situation, i.e. for a flowing borehole with r_w = 0.038m and assuming R=50m[4] (Table5-1) and thus neglecting[5] *1/R* since $R >> r_w$ then we obtain

$$dp_w = \frac{dQ_w}{2\pi T}(1.14 + \xi) + \frac{b \cdot dQ_w^n}{4\pi^2 H^2}\frac{1}{r_w} \qquad Equation\ 5-7$$

from which it may deduced that the Forchheimer friction factor (b) has the dimension of [LT].

Upon perturbation the rate of flow may change exponentially with increasing distance and depending on the magnitude of different flow domain may develop. From non-linear near the borehole to linear further away. In the transition between non-linear and linear flow the exponent n may be between 1 and 2, where 1 is linear Darcy flow and 2 is fully turbulent flow, schematically shown in Figure 5-1. Temporally, the flow is always in a transient state when inducing the perturbation, this will develop into a pseudo steady-state flow regime. Within the time frame of a hydraulic tests the inflow and outflow of the system do not have time to be balanced and a steady-state flow regime is not developed, Figure 5-1. All hydraulic tests are performed with transient flow conditions which may develop into steady-state flow conditions, Figure 5-1.

---

4 Thiem's equation is also utilised during SKB:s difference flowlogging campaigns where R is assumed to be 500m (see e.g. Komulainen & Pöllänen, 2016)).

5 Neglecting the term 1/R means R is at infinite distance. Scoping calculations show that by neglecting 1/R then the radius term overestimated by 8% at the most, probably by much less.

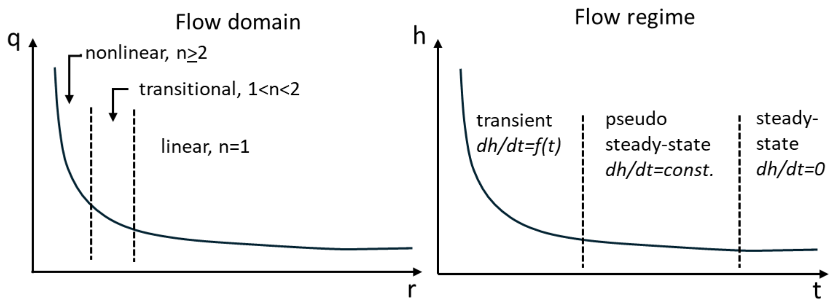

***Figure 5-1.** Schematic variation of flow velocity with radial distance from source of perturbation, borehole or tunnel, (left) and of hydraulic head with time (right).*

This conceptual understanding of the test dynamics, how different flow regimes develop over time, flow rate and flow domains may be present is summarised in Figure 5-1 and 5-2.

However, in practice steady-state flow never develop under a test. It would require that the recharge/discharge to/from the formation are in equilibrium, i.e. obeying the Laplace equation where *dh/dt=0*. This is not feasible under the timeframe and perturbation of a hydraulic test.

Rather, it is an apparent steady-state that may be observed/interpreted. Such pseudo state-state flows obey a Poisson equation where *dh/dt=constant*. It is often considered that pseudo steady-state conditions are a sufficient approximation for steady-state conditions and can be detected in field data through a linear relation between hydraulic head and time, the slope is sufficiently small (Aarstad, 1987). This means that during pseudo steady-state conditions, the steady-state relations are approximately valid. Then, the steady-state well flow equations are valid approximation e.g. Thiem's well equation become

$$dp_w \approx \frac{dQ}{2\pi T} \cdot ln\left(\frac{R}{r_w}\right) \qquad Equation\ 5-8$$

which after reshaping, gives

$$T \approx \frac{dQ}{dp} \cdot \frac{1}{2\pi} ln\left(\frac{R}{r_w}\right) = \frac{dQ}{dh} \cdot G \qquad Equation\ 5-9$$

where *G* is geometric constant, *R* is radius of influence, and r_w is well radius. The radius of investigation is unknown but it judged from Table 5-1 that it is more like to be about 1. Hence, in this context G is set to G=1 and the specific capacity (*dQ/dh*) is approximately equal to the transmissivity (*T*)

$$T \approx \frac{dQ}{dh} \qquad Equation\ 5-10$$

Table 5-1. Geometric constant for Thiems equation (G) for different radius of investigation (R).

rw (m) :	0,038	0,038	0,038	0,038
R (m) :	0,5	5	50	500
G (-) :	0,4	0,8	1,1	1,5

Then for a given test we see that

- *dh* vs *dQ* plots along a straight line if the flow is linear (laminar) and deviates from a straight linear if it is non-linear (turbulent or transitional)
- *dQ/dh* vs *dQ* plots as a straight horizontal line if the flow is linear) and deviates from a straight linear if it is non-linear (turbulent or transitional).

The different type of well and aquifer losses may be identified by conducting an isochronal step test with successively increasing flow rates and plotting the *dp* vs *dQ* according to Figure 5-2. These are implemented in the interpretation and presented in the results chapters 6 and 7.

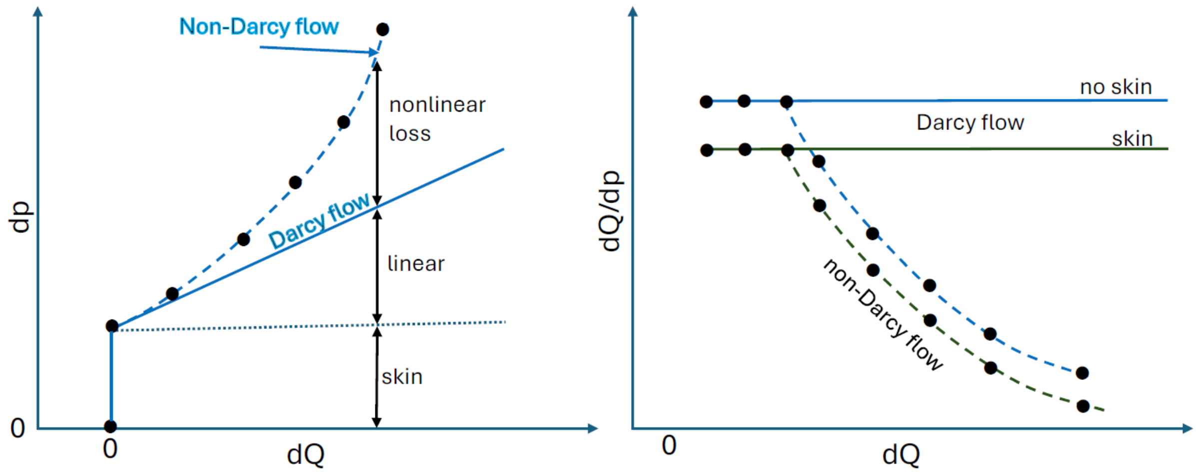

Figure 5-2. *Relations of well and aquifer loss components for hydraulic test at different flow rates under steady-state flow conditions. Darcy flow is synonymous to linear flow.*

5.2 Rorabaugh's constant rate solution

The deviation from linear flow in porous media is proposed to be attributed to inertial forces (Scheidegger, 1974) since these forces are proportional to the squared velocity, whereas in pipe flow it is attributed to viscous forces (Darcy-Weisbach), see Bear 1972, page 178).

Jacob (1946) proposed that the there is an additional pressure loss at relatively high velocities, through the screen and casing. This well loss is approximately proportional to some power of the flow rate (Q), commonly exceeding the first power and approaching the second power of Q. As a first approximation he set this well loss to CQ^2, where C is a constant. Hence the total drawdown is composed of the linear component due to laminar flow in the aquifer according to Theis (1935) and the non-linear flow through screen and casing called the well loss component,

$$dp(t) = B(t)Q + CQ^2 \qquad Equation\ 5-11$$

where Q is volumetric flow rate. CQ^2 is the dp_n-term in eq. 5-1.

Based on Jacob (1946), Rorabaugh (1953) developed a methodology to evaluate constant rate steady-state step test where the well loss is a function of Q^n instead of Q^2 and B and C are constants

$$dp = BQ + CQ^n \qquad Equation\ 5-12$$

and presented a scheme to calculate the exponent *n*. This equation was utilised for calculation the non-linear well loss. Jacob (1950) recognised that the exponent n could vary considerably with Q "especially if there were appreciable departure from laminar flow within the formation".

Here, B is not constant due to the transient nature of the flow it depends on both the distance from well and the on the time. Hence, B(r,t) represents the hydraulic resistance of the formation, from the face of the borehole to a distance into the formation where the drawdown is virtually zero, i.e. the radius of influence. For transient conditions and in its simplest form the BQ term is obtained from Theis non-equilibrium line source equation

$$dp(t) = \frac{Q}{4\pi T}\left(W(u) + 2\xi \right) \qquad Equation\ 5-13$$

where ξ is the skin factor and W(u) is the well function which for the Theis solution is the exponential integral function Ei(-u) which may be approximated the first two terms of an infinite series representation, $W(u) \approx -0.5772 - \ln(u)$

where $u = \frac{r^2 S}{4Tt} = \frac{r^2}{4t} \cdot \frac{1}{\eta}$ and η = T/S is the hydraulic diffusivity for the formation and then

$$dp(t) \approx \frac{Q}{4\pi T}\left(-0.5772 - \ln\left(\frac{r^2 S}{4Tt}\right) + 2\xi \right) \qquad Equation\ 5-14$$

The approximation is acceptable for u < 0.02 which is the case for small *r* (i.e. the flowing well) or at long flowing times (Cooper & Jacob, 1946). The underlying assumption of radial formation flow geometry for the Theis solution (Eq. 5-7) must also be valid.

For our application, in this volume of rock, the transmissivities and storage coefficients obtained from interference tests between boreholes K03009F01 and K08028F01 from 52 (37 and 15 respectively) observation sections respectively, provided values of formation diffusivities in the following range $0.0046 < T_o/S_o < 57$ (Hjerne et.al., 2016) while investigations of a larger adjacent rock volume provided hydraulic diffusivities from 142 observation section in the range $0.02 < T_o/S_o < 9.9$ (Morosini et.al., 2018).

Mathias and Todman (2010) derived an analytical relationship between *C* in the Jacob equation (*Eq. 5-5*) and the Forchheimer parameter C_F *(Eq. 5-2)*

$$C = \frac{C_F}{(2\pi H)^2 r_w g} \qquad Equation\ 5-15$$

where H is the thickness of the formation and r_w the radius of the borehole. Mathias et.al. (2008) argue that a proper numerical solution of the Forchheimer (1901) equation leads to a transient C_F coefficient and hence, it is inferred, a transient C coefficient of the Jacob (1946) equation. Mathias and Todman (2010) also recognised that since non-Darcy losses grow in time before reaching a steady state, the step duration of the test is important when analysing according to Jacob (1946) or Rorabaugh (1953) equations, since these assume a constant and equal steady-state value of the non-Darcy losses. In practice, if a test is analysed according to Jacob (1946) or Rorabaugh (1953) while the actual flow is still in the transition state from laminar to turbulent flow then the turbulent drawdown component will be overestimated in the calculation compared to the measured drawdown.

6 Results K03009F01, Test 1-11.

The present chapter summarises the execution and presents the results for the conducted hydraulic tests in each test section with separate chapters for each test. Basic and detailed test results, including all test plots, are presented in Appendix 4 and 5. Interpreted hydraulic formation parameters are compiled in Appendix 7.

6.1 Test section K03009F01 14.20-17.19m, Test 1-8

6.1.1 Test 7 Step constant head injection and recovery test (sCHir)

The step constant head and recovery test was performed from an initial formation pressure of 3264kPa with four sequentially increased constant head steps, each of 30min duration, up to 4557kPa and then four sequentially decreasing constant head steps back to initial formation pressure, Figure 6-1.

Total duration was 3.5h for injection phase and 20h for recovery phase. The much longer recovery phase displayed tidal components after 3.5h of recovery with amplitude of about 0.5kPa and wavelength of about 12.5h.

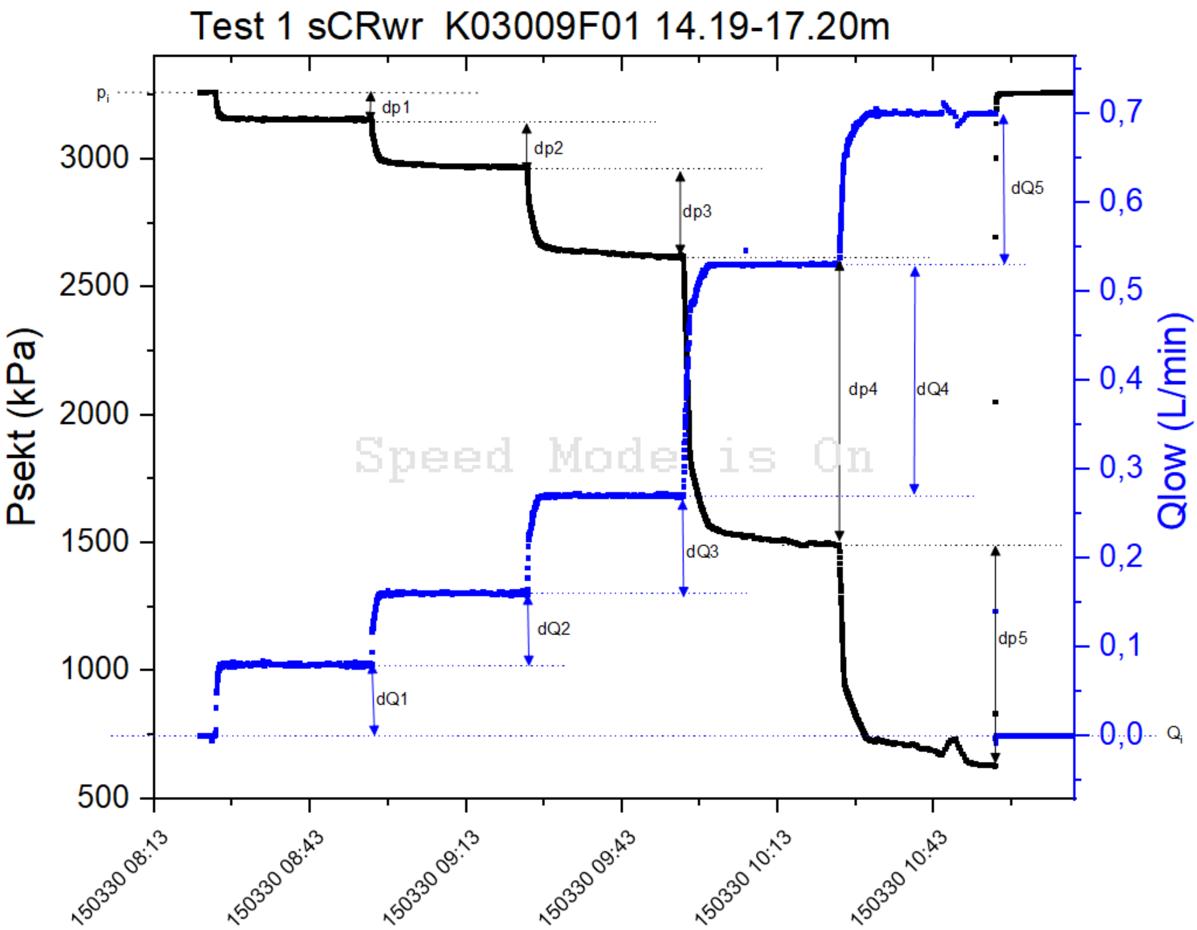

Figure 6-1. *History plot of step injection and recovery test of test section K03009F01 14.19-17.20m, also showing principle for extrapolated values for the calculation of specific capacity (dQi/dpi).*

Q-p evaluation

Q-p results are compiled in the two graphs of Figure 6-2, as pressure change versus flow and as specific capacity (*dQi/dpi*) versus flow. The latter were calculated for the *dQi* and *dpi* at the end of each step and plotted as a function of the flow rate. When flowrate did not stabilize it was linearly extrapolated from prior step when calculating dp for the following step.

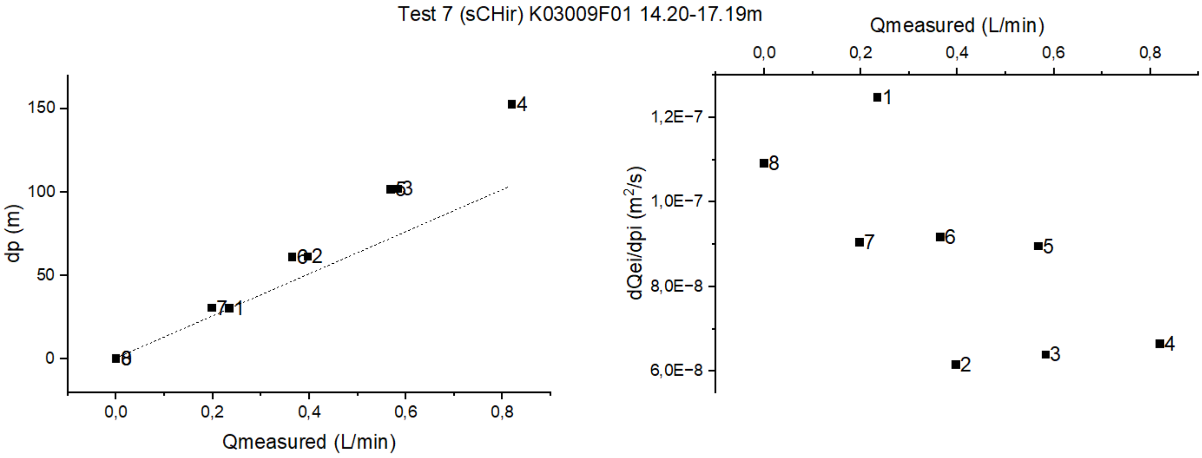

Figure 6-2. *Pressure change (left) and specific capacity (right) at end of each step versus final volumetric flow rate of section K03009F01 14.19-17.20m.*

The plot on the left of Figure 6-2 show that flow is linear from 0L/min up to when it starts to deviate from linearity at a rate somewhere between 0.2 and 0.4L/min, larger deviation the higher the rate. The same but reversed behaviour is evident when decreasing the rate.

The plot on the right of Figure 6-2 show that the specific capacity (as approximate proxy for transmissivity) is generally decreasing with increasing flow rate and vice versa. Nevertheless, maintaining specific capacity as a proxy for transmissivity, Figure 6-3 suggest an exponential decrease relation of transmissivity with flow rate. For the decreasing Q (and dp), step 1–4 suggests the relation is of the form

$$T \approx T_0 + A_1 \cdot e^{(-Q/t_1)} \qquad Equation\ 6-0$$

where A_1 and t_1 are constants, T_0 (dQ_i/dp_i) for the highest Q of the data set. Units are m^2/s for T and L/min for Q.

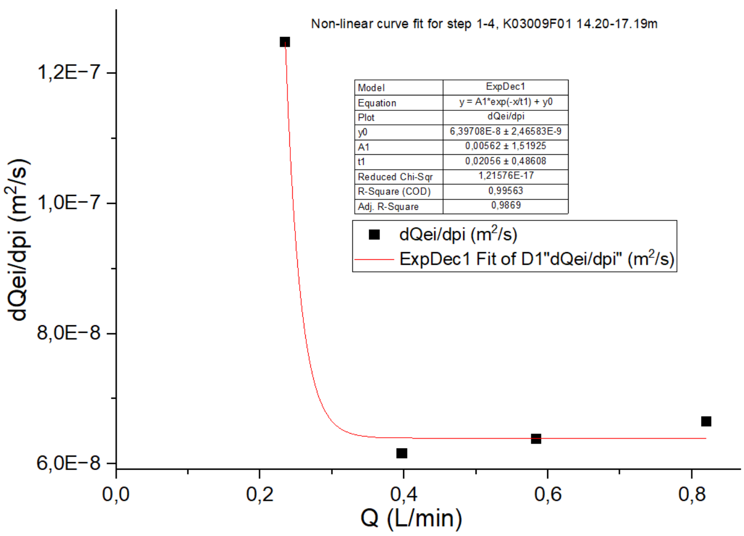

Figure 6-3. *Non-linear curve fit of steps 1–4 when flow is increasing in Figure 6-2 (right).*

This specific capacity varies 6.6E-08 to 1,2E-07m^2/s is not corrected or adjusted for any energy losses. This shows a clear decrease of specific capacity with increasing flow rate (and pressure).

These Q-p and dQ/dp behaviour are consistent with the presence of a non-linear flow component when the flow rate exceeds a certain value, generating additional energy loss.

6.1.2 Test 1 Step constant rate withdrawal and recovery test (sCRwr)

This test comprised a withdrawal phase with five steps of each 30min duration where the rate was held constant in each step, 0.08 to 0.7L/min, generating a total drawdown of 2633kPa. This was followed by a recovery phase back to initial formation pressure of 3 260 kPa, see Figure 6-4.

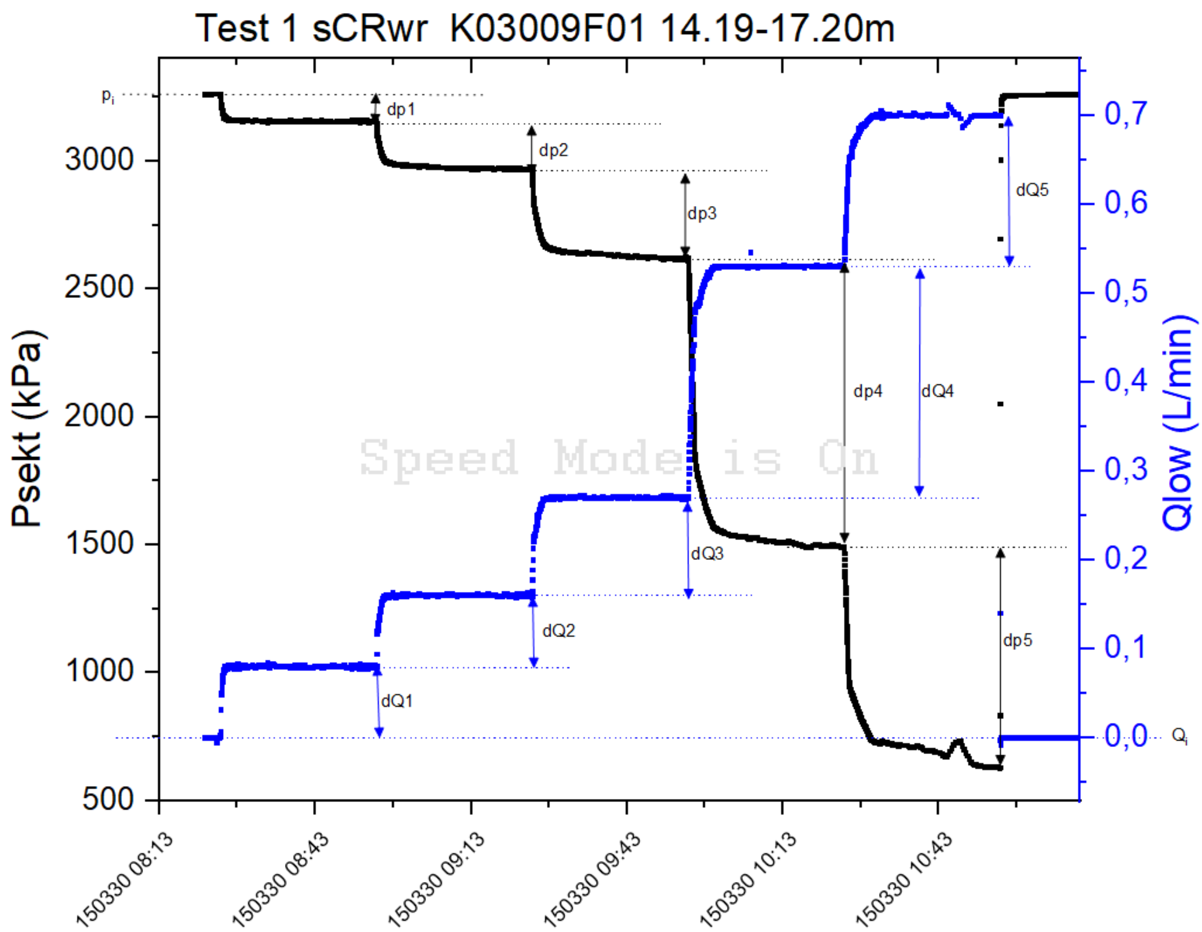

Figure 6-4. *History plot of step withdrawal and recovery test of test section K03009F01 14.19-17.20m, also showing principle for extrapolated values for the calculation of specific capacity (dQi/dpi).*

Q-p evaluation

Q-P results are compiled in the two graphs of Figure 6-5, as pressure change versus flow and as specific capacity (dQ_i/dp_i) versus flow. The latter were calculated for the *dQi* and *dpi* at the end of each step and plotted as a function of the flow rate. When flowrate did not stabilize it was linearly extrapolated from prior step when calculating dp for the following step.

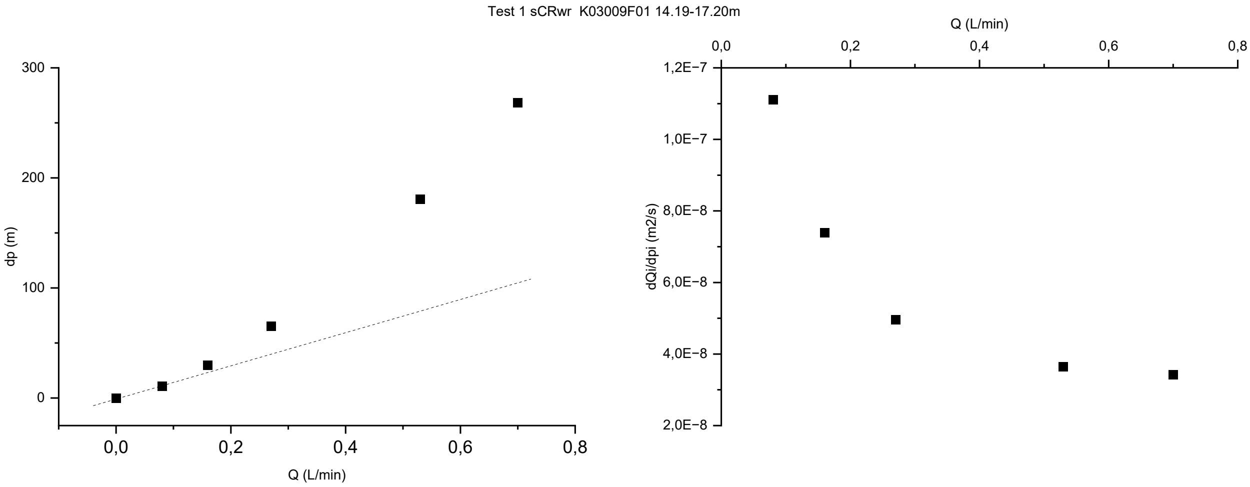

Figure 6-5. *Pressure change (left) and specific capacity (right) at end of each step versus final volumetric flow rate of section K03009F01 14.19-17.20m.*

The plot on the left of Figure 6-5 show that flow is linear from 0L/min up to when it starts to deviate from linearity at a rate somewhere between 0.1 and 0.2L/min, larger deviation the higher the rate.

The plot on the right of Figure 6-5 show that the specific capacity (as approximate proxy for transmissivity) is decreasing with increasing flow rate. Specific capacity decreased by almost one order of magnitude in this flow range 0.1-0.7L/min. As for Test 7 (see chapter 6.1.1) a good fit was obtained with an exponential decrease type relation of transmissivity with flow rate with R^2 = 0.99987.

Rorabaugh evaluation

Analysis according to Jacob (1946) and Rorabaugh (1953) showed we do not have a fully developed turbulent flow but are still in transition state of non-Darcy flow going from laminar to turbulent. This is evidenced in Figure 6-6 with n=1.51 with an excellent line fit determination coefficient of R^2 = 0.99949. This means that the proper analytical relation describing the drawdown for this test section should include a non-Darcy flow component according 6-1 and 6-2, depending on flow regime.

$$dp(t) = B(t)Q + CQ^n \qquad transient\ state \qquad Equation\ 6-1$$

$$dp \approx BQ + CQ^n \qquad pseudo\ steady-state \qquad Equation\ 6-2$$

For Rorabaugh evaluation B and C are treated as constants the flow is pseudo steady-state and Eq 6-2 is applied. Values for B, C and n are extracted from the Rorabaugh best-fit line, Figure 6-5, with basic units in meter and second. The functional form of B(t) and B will depend on the formation geometry and flow regime.

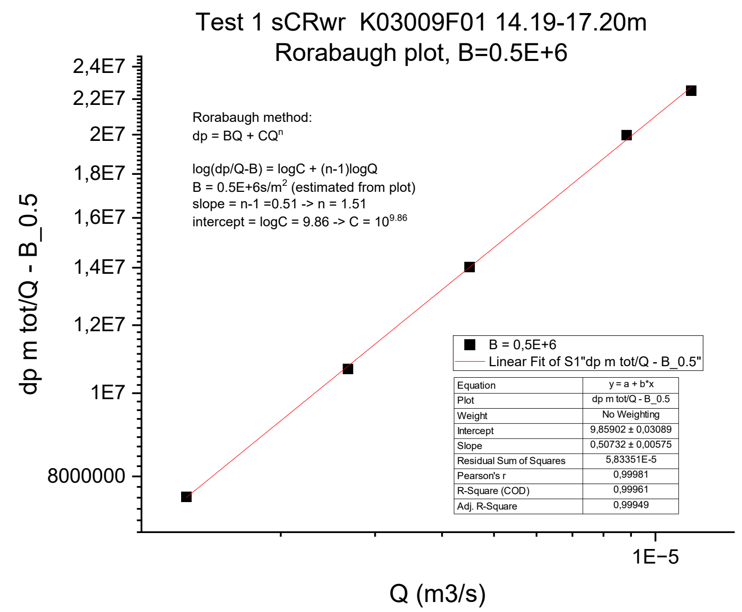

Figure 6-6. *Rorabaugh plot of step test 1 (sCRwr) of test section K03009F01 14.19-17.20m.*

Results of test simulation of drawdown at end of steps and of complete test history show good agreement with measured data, see Appendix 5, providing further confidence in the test evaluation and analysis. In this case we see from Appendix 5, Test 1 that there is a rather dramatic effect of the non-linear losses which amount to about 90% of the total drawdown.

6.1.3 Tests 2-6 Constant head withdrawal and recovery tests (CHwr)

These are five separate tests conducted at constant but different drawdown. Prior to the tests the static formation pressure in this section was 3261kPa. The five constant head withdrawal tests of equal duration were performed with dp= -300, -600, -1000, -2000 and -3000kPa, each followed by a recovery phase of longer duration than the withdrawal phase.

These tests showed an increasing final outflow rate for the step dQ= 0.08, 0.16, 0.27, 0.53 and 0.70 L/min.

Q-p evaluation

The specific capacity clearly decrease with increasing dp and dQ, Figure 6-7, where dQ taken just prior to shut-in. The specific capacity decrease from 7E-8 to 4E-8 m^2/s over the tested dQ interval.

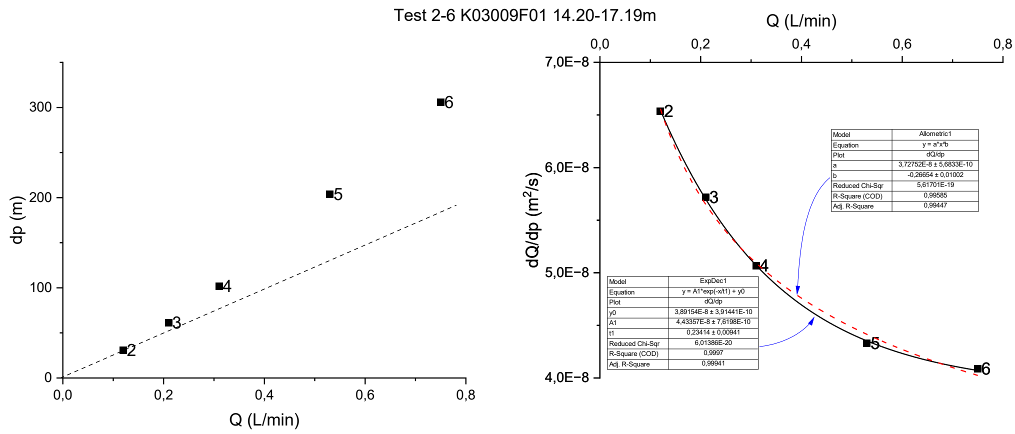

Figure 6-7. *Pressure change (left) and specific capacity (right) plot of the step withdrawal phases of Tests 2-6 in section K03009F01 17.20-207.19m.*

Transient evaluation

A transient evaluation excluding any non-linear well loss component in the fitted model was performed of the withdrawal phase. Basic test data with input variables, data plots and evaluated parameters are compiled in Appendix 4. A log-log evaluation is made of the withdrawal phase for each test, Figure 6-8. Resulting transmissivity (T) and skin factor (ξ) are compiled in Table 6-1 co-plotted Figure 6-8.

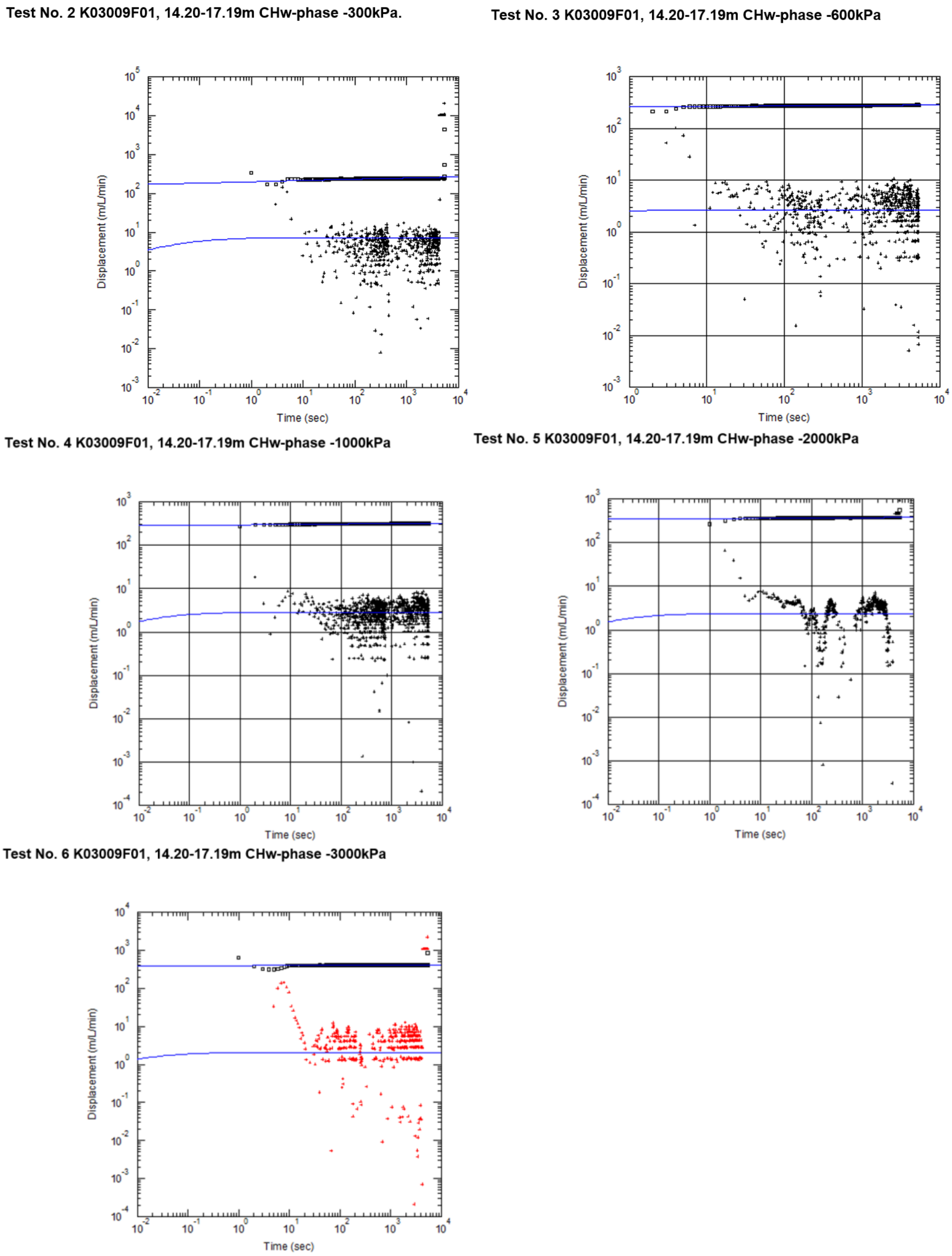

Figure 6-8. *Log-log diagnostic plots from constant head withdrawal phase of Test 2-6.*

Log-log plots Figure 6-8 display a consistent diagnostic behaviour with an initial phase of convergence a few seconds towards specified dp. This is followed by a phase with transient flow change (10-100 s) towards a linear flow with a noisy but stable derivative interpreted as radial formation flow.

Test 3 and 5 there was an initial flow leak just prior to staring the test so the initial pressure is a bit too low, 3247 and 3244kPa. The proper initial pressure should have been about p_i=3262kPa which was derived from the stabilized pressure data prior to the flow leak. For test 4 the pressure data prior to flow start is missing altogether and the value it ought to have had was derived from late recovery data of the test.

Table 6-1. Transmissivity and skin from transient interpretation from constant head withdrawal phase of Test 2-6.

Test no.	Test phase	p_i (kPa)	Applied dh (kPa)	dQ at shut-in (L/min)	Skin (m)	Transmissivity (m^2/s)	Comment
2	Withdrawal	3259.34	-300	0.12	11	1,8E-07	
3	Withdrawal	3247.32 (3262.01)	-600	0.21	47	5,1E-07	Leaky flow prior to test start.
4	Withdrawal	3262.36	-1000	0.31	49	4,6E-07	Missing pressure data at flow start. p_i from late recovery.
5	Withdrawal	3243.99 (3262.32)	-2000	0.53	71	5,5E-07	Leaky flow prior to test start.
6	Withdrawal	3261.20	-3000	0.75	92	6,4E-07	

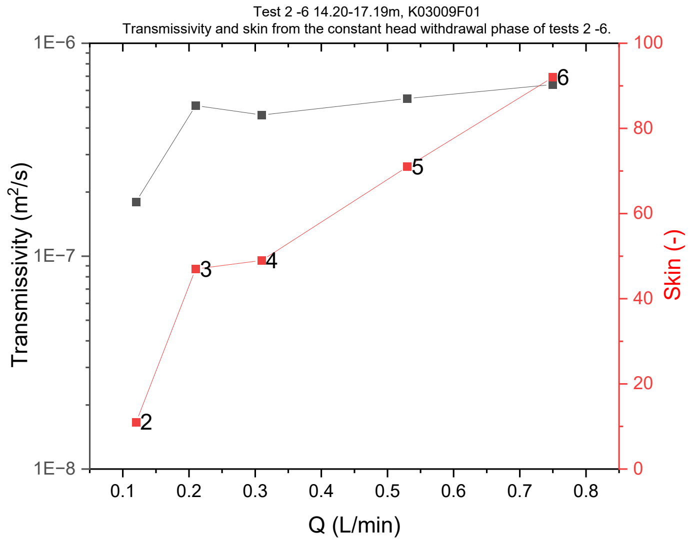

Figure 6-9. *Results from Log-Log evaluation for transmissivity and skin from drawdown phase as a function of flow rate at shut-in in section 14.20-17.19m in borehole K03009F01.*

From Figure 6-9 we note that with increasing flow rate the transmissivity increases three-fold, from 2E-7 to 6E-7m^2/s while the skin increases nine-fold, from 10 to 90. The substantial increase in skin with increasing flow rate isa taken as an indication of non-linear flow.

6.1.4 Test 8 Constant head injection and recovery (CHir)

The main rationale of this test is to compare and confirm that injection and withdrawal tests produce similar results when performed in otherwise same conditions. They are performed with the same constant dp of 1000kPa, Test 8 as injection and Test 4 as withdrawal. This chapter strictly present the results from Test 8. The comparison of test 4 and 8 is presented in Appendix 6.

Transient evaluation

A transient evaluation excluding any non-linear well loss component in the fitted model was performed of the withdrawal and recovery phase respectively. Basic test data comprising with input variables, data plots and evaluated parameters are compiled in Appendix 4, (Test 8). The evaluation is made for perturbation phase.

6.2 Test section K03009F01 17.20-20.19m, Test 9 and 9a-9f

6.2.1 Test 9 Step constant rate withdrawal and recovery test (sCRwr)

This test comprised five steps of equal 30min duration with constant steprate from 0.8 L/min to 7L/min generating a total drawdown of 2990kPa followed by a recovery to initial formation pressure of 3266kPa, see Figure 6-10.

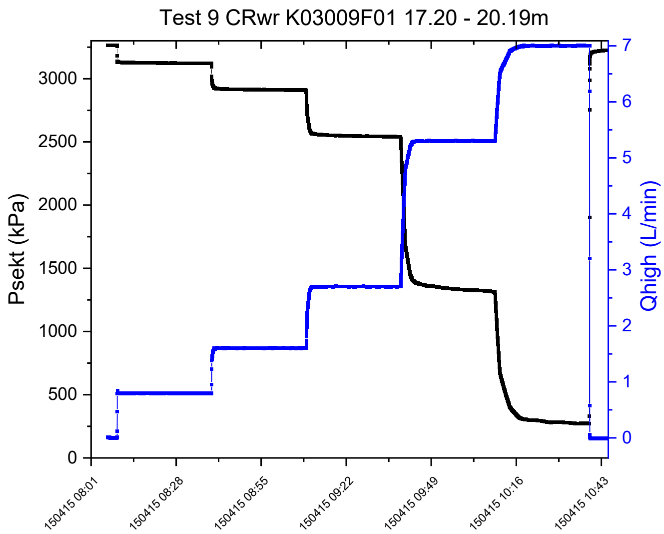

Figure 6-10. *History plot of step withdrawal and recovery test of test section K03009F01 17.20-20.19m.*

Q-p evaluation

The test showed a type of exponentially decreasing specific capacities (dQi/dpi) with increasing flowrate, from 9.62E-7 m^2/s to 3.83E-7 m^2/s. An exponential decrease function was fitted with a determination coefficient of R2 = 0.99509, see Figure 6-11

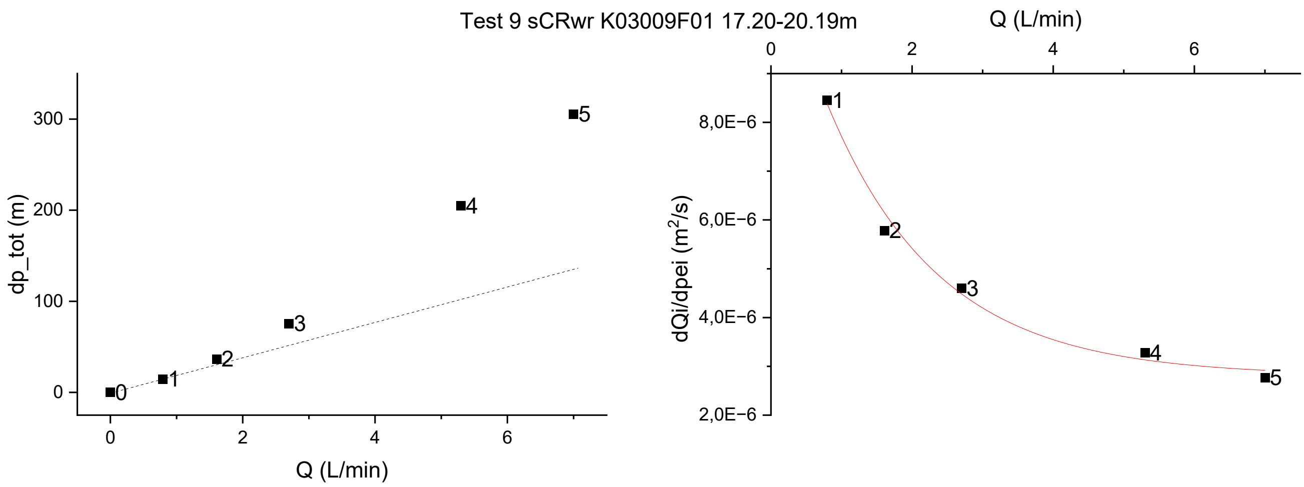

Figure 6-11. *Pressure change (left) and specific capacity (right) plot of the step withdrawal phase section K03009F01 17.20-207.19m.*

Rorabaugh evaluation

Analysis according to Jacob (1946) and Rorabaugh (1953) showed we do not have a fully developed turbulent flow but are still in transition state of non-linear flow going from laminar to full turbulent flow. This is evidenced in Figure 6-12 where the data on the Rorabaugh plot resulted in a straight line for an exponent of n=1.63 with a very good fit (R^2 = 0.99932). This means that the proper analytical relation describing the drawdown for this test section should include a non-Darcy flow component according to

$$dp \approx BQ + CQ^n$$

where units are in meters and seconds.

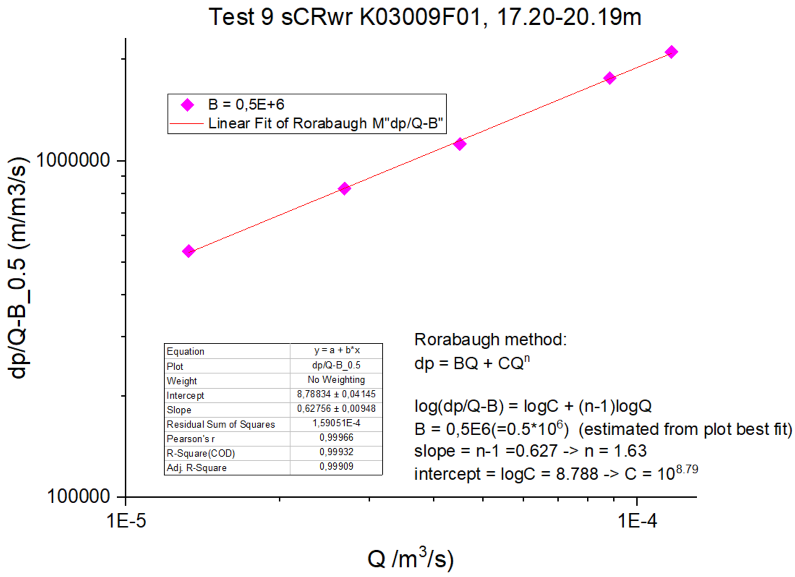

Figure 6-12. *Rorabaugh plot of step withdrawal test of test section K03009F01 17.20-20.19m.*

6.2.2 Test 9f Step constant head injection and recovery test (sCHir)

The step constant head and recovery test was performed from an initial formation pressure of 3265kPa with four sequentially increased constant head steps, each of 30min duration, up to 4756kPa and then four sequentially decreasing constant head steps back to initial formation pressure, Figure 6-13

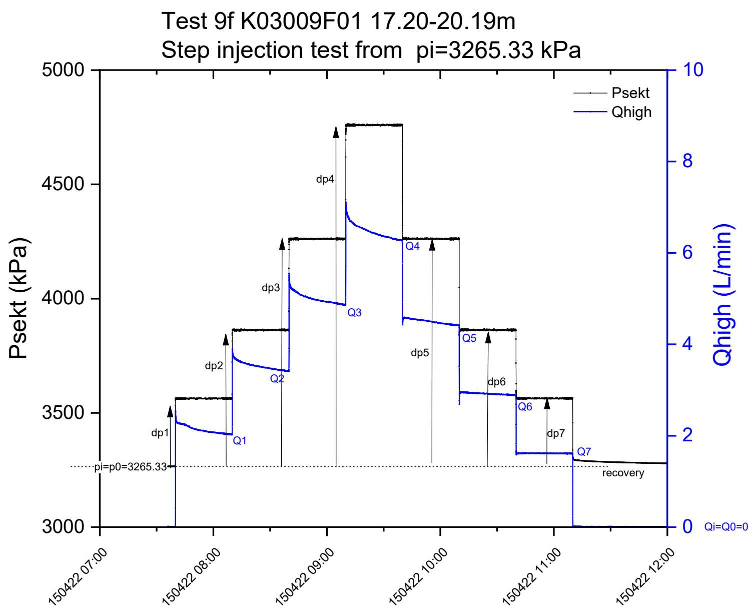

Figure 6-13. *Step constant head injection test of test section K03009F01 17.20-20.19m.*

Q-p evaluation

Q-p results are compiled in the two graphs of Figure 6-14, as pressure change versus flow and as specific capacity (*dQi/dpi*) versus flow. The latter were calculated for the dQ_i and dp_i at the end of each step and plotted as a function of the flow rate. When the flow rate did not stabilize it was linearly extrapolated from the prior step when calculating dp for the following step.

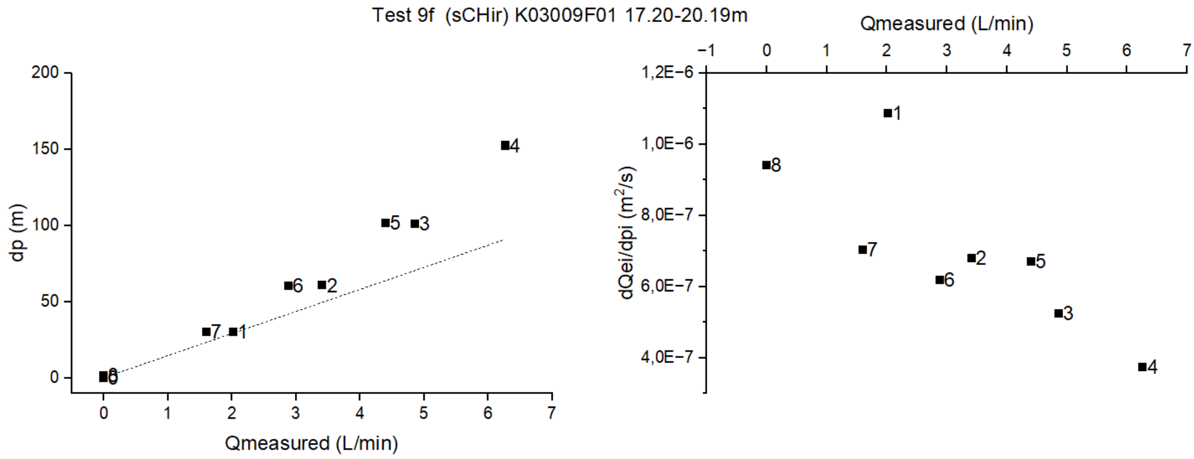

***Figure 6-14.** Plot of pressure change (left) and specific capacity (right) as a function of the flow rate of the step withdrawal phases of Test 9f in section K03009F01 17.20-20.19m.*

The plot on the left of Figure 6-14 show that flow is linear from 0L/min up to when it starts to deviate from linearity at a rate somewhere between 2 and 3.5L/min, larger deviation the higher the rate. The same but reversed behaviour is evident when decreasing the rate.

The plot on the right of Figure 6-14 show that the specific capacity is generally decreasing with increasing flow rate and vice versa. Adopting the specific capacity as an approximate proxy for transmissivity, Figure 6-15 suggest an exponential decrease relation of transmissivity with flow rate. For the decreasing Q (and dp), step 1-4 suggest the relation is of the form

$$T \approx T_0 + A_1 \cdot e^{(-Q/t_1)} \qquad Equation\ 6-0$$

where A_1 and t_1 are constants, T_0 is the transmissivity unaffected by non-linear flow which could be set approximatelly as dQ_i/dp_i for the lowest flow rate although we would need data at low rates to support this.

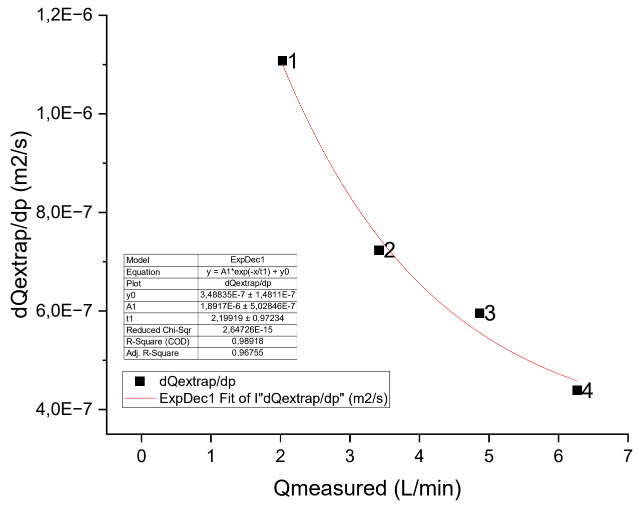

***Figure 6-15.** Non-linear curve fit between specific capacity (dQ/dp) and flow rate (Q) for steps 1-4 showing and exponentially decreasing relation.*

This specific capacity varies 1.1E-06 to 4.4E-07m^2/s is not corrected or adjusted for any energy losses. This shows a clear decrease of specific capacity with increasing flow rate (and pressure) supporting the presence of non-linear flow during the test.

Hence, both Q-p and dQ/dp behaviour are consistent with the presence of a non-linear flow component when the flowrate exceeds a certain value, generating additional energy loss.

6.2.3 Tests 9a-9e Constant head withdrawal and recovery tests (CHwr)

Prior to the tests the static formation pressure in this section was 3266kPa. Five constant head withdrawal tests of equal duration were performed with dp= -300, -600, -1000, -2000 and -3000kPa each followed by a recovery phase. These tests showed an increasing final outflow rate for the step dQ= 1.35, 2.24, 3.46, 5.3 and 6.75 L/min.

Q-p evaluation

Q-p results are compiled in the two graphs ofFigure 6-16, as pressure change versus flow and as specific capacity (dQi/dpi) versus flow. The latter were calculated for the *dQi* and *dpi* at the end of each step and plotted as a function of the flow rate. When flowrate did not stabilize it was linearly extrapolated from prior step when calculating dp for the following step.

The plot on the left of Figure 6-16 show that flow is linear from 0L/min up to when it starts to deviate from linearity at a rate of about 2L/min, larger deviation the higher the rate.

The specific capacity clearly decrease with increasing *dp* and *dQ*, Figure 6-16, with dQ taken just prior to shut-in. The specific capacity decrease from 7.35E-7 to 3.65E-7 m2/s over the tested dQ interval.

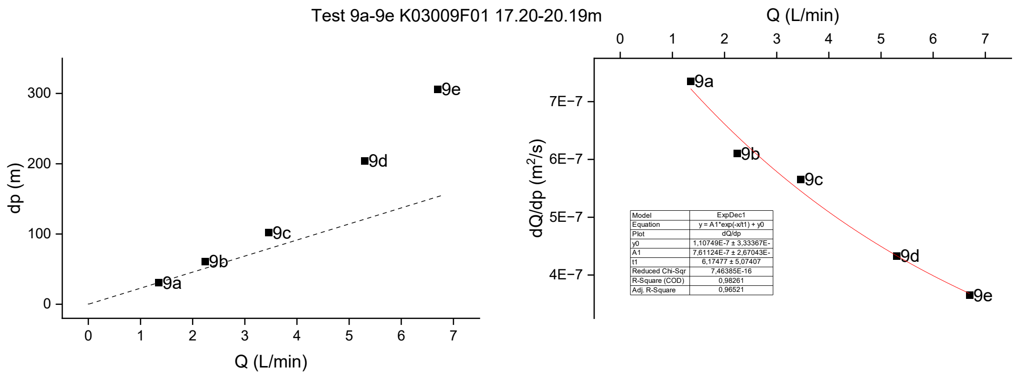

Figure 6-16. *Pressure change (left) and specific capacity (right) plot of the step withdrawal phases of Tests 9a-9e in section K03009F01 17.20-20.19m.*

The plot on the right of Figure 6-16 show that the specific capacity (as approximate proxy for transmissivity) is decreasing with increasing flow rate. It decreases about 50% over the tested. An exponentially decreasing model was fitted to the data with a coefficient of determination of R^2 = 0.9652.

Transient evaluation

Transient evaluations were made for each test where the drawdown phase display noisy or fluctuating derivative signature, Figure 6-18 display a consistent diagnostic behaviour with an initial phase of convergence a few seconds towards specified dp. This is followed by a phase with transient flow change (10-100s) towards a linear flow with a noisy but stable derivative interpreted as radial formation flow.

Resulting parameter are compiled in Table 6-2 and Figure 6-17 from which we note rather narrow spread of transmissivities, ranging 2E-6 to 5E-6m^2/s.

Table 6-2 . Transmissivity and skin from transient interpretation from constant head withdrawal phase of Test 9a-9e.

Test no.	Test phase	p_i (kPa)	Applied dh (kPa)	dQ at shut-in (L/min)	Skin (m)	Transmissivity (m^2/s)
9a	Withdrawal	3266.28	-300	1,35	30	4,6E-06
9b	Withdrawal	3263.69	-600	2,24	37	4,5E-06
9c	Withdrawal	3265.64	-1000	3,46	16	2,2E-06
9d	Withdrawal	3262.73	-2000	5,30	19	1,9E-06
9e	Withdrawal	3262.26	-3000	6,75	73	4,9E-06

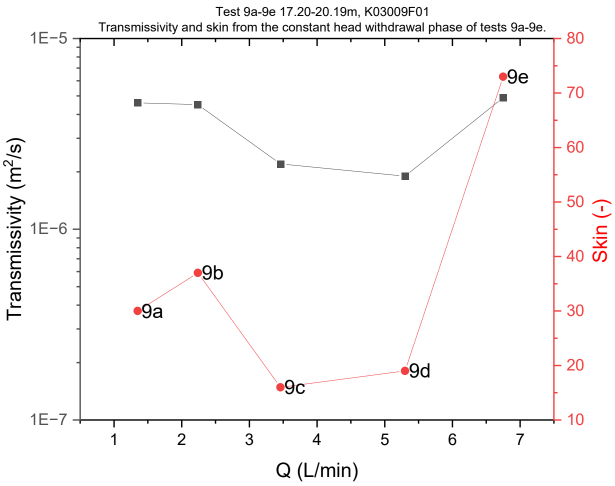

Figure 6-17. *Results of log-log analysis for T and skin from the withdrawal phase of tests 9a- 9e as a function of flow rate (at shut-in) in section 17.20-20.19m in borehole K03009F01.*

The evolution of skin with increasing flow is unexpected, substantial skin factors in the range 16-73 but devoid of any flow trend resemblances. In contrast to the Q-p plot analysis, the compounded transient interpretations of transmissivity and skin do not provide support for increased energy losses with increased flow and hence no support for non-linear flow. Although it does not discard it either and tests are inconclusive in this respect.

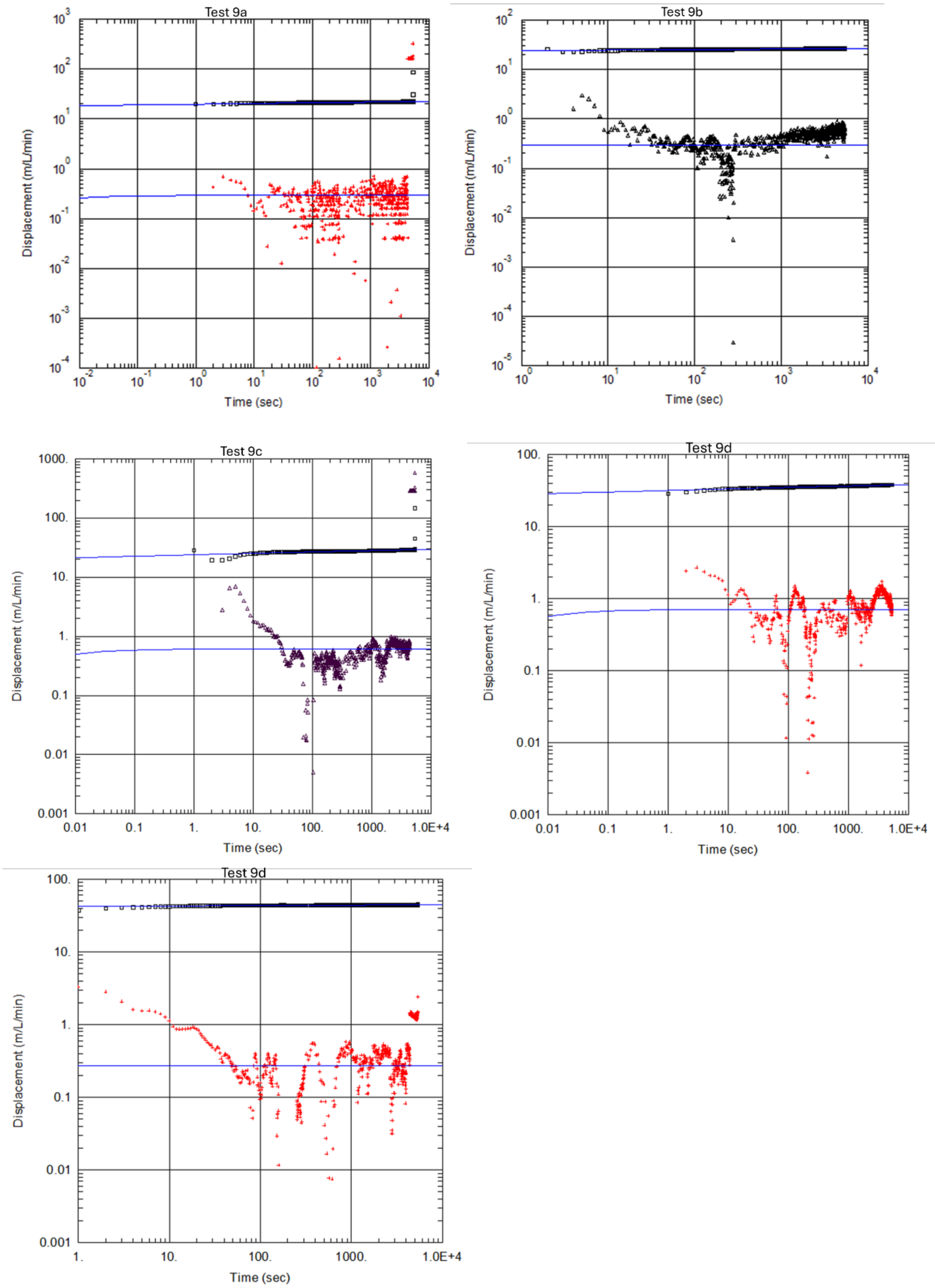

Figure 6-18. *Log-log diagnostic plots from constant head withdrawal phase of Test 9a-9e.*

6.3 Test section K03009F01 15.30-16.79m, Test 10-11.

These tests are straddling the same two flow anomalies as test 1-9 presented in chapter 6.1 but with shorter section length of 1.5m instead of 3m, to possibly assess effects and results due to a re-distribution of flow (if any) due to section length. To this effect only step tests were executed, step withdrawal and step injection respectively.

6.3.1 Test 10 Step constant rate withdrawal and recovery test (sCRwr)

The test was performed in five isochronal steps over a flow range of 0.05-0.5L/min which generated drawdown of up to 55m. History plot show that steady state flow conditions were achieved for all steps, Figure 6-19, and no extrapolation was done.

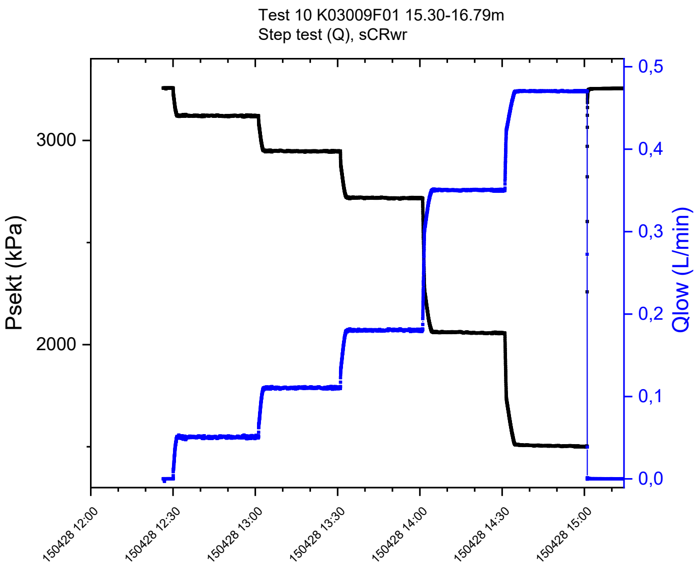

Figure 6-19. *History plot of pressure and flow for Test 10 in K03009F01 15.30-16.79m.*

Q-p evaluation

Q-p results are compiled in the two graphs of Figure 6-20, as pressure change versus flow and as specific capacity (dQi/dpi) versus flow. The latter were calculated for the *dQi* and *dpi* at the end of each step and plotted as a function of the flow rate. Stabilized steady-state condition were achieved for each step and no extrapolation was done.

The plot on the left in Figure 6-20 show that flow is linear from 0L/min up to when it starts to deviate from linearity at a rate of about 0.2L/min, larger deviation the higher the flow rate.

With regard to specific capacity (*dQi/dpi*) it is clearly decreasing with increasing rate but the decrease would appear almost linear, Figure 6-20. Although the exponential decrease relation was matching the data quite well with an adjusted coefficient of determination of R2=0.99704. The decreases is about 33%, from 6.1E-8m2/s to 4.4E-8m2/s over the tested flow range.

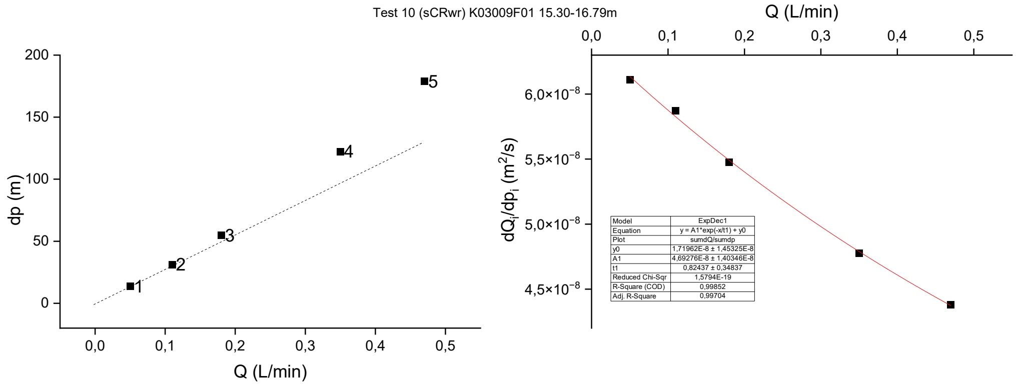

Figure 6-20. *Pressure change (left) and specific capacity (right) plot of the step withdrawal phases of Tests 10 in section K03009F01 15.30-16.79m.*

Rorabaugh evaluation

Analysis according to Rorabaugh (1953) showed we do have a fully developed turbulent flow as evidenced in Rorabaugh plot of Figure 6-21 where the data resulted in an actual flow rate exponent of n=2.02 with a line fit determination coefficient of R^2 = 0.99328. This means that the proper analytical relation describing the drawdown for this test section should include a non-Darcy flow component according to

$$dp \approx BQ + CQ^n$$

where units are in meter and second.

Considering the results from section 14.20-17.19m (Chapter 6.1.2) which contain the same flowing fractures as the present section and which yielded the non-Darcy flow exponent to be n=1.49, we may establish that the tests give two different flow regimes, namely a transitional and a fully turbulent, for tests of the same flowing features and with same pressure- and time steps, the difference being the final flow rate which was 0.70L/min and 0.47L/min respectively.

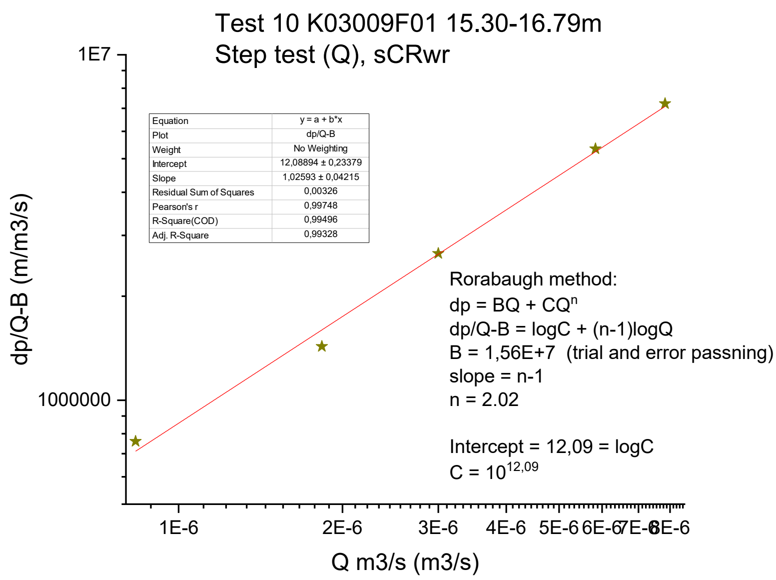

Figure 6-21. *Rorabaugh plot of step withdrawal test of test section K03009F01 15.30-16.79 m*

6.3.2 Test 11 Step constant head injection and recovery (sCHir)

The step constant head and recovery test was performed from an initial formation pressure of 3256kPa with four sequentially increased constant head steps, each of 30min duration, up to 4756kPa and then fours sequentially decreasing constant head steps back to initial formation pressure, Figure 6-22. These pressure perturbations in the interval 30-150m generated flow in the range of 0.1-0.5L/min.

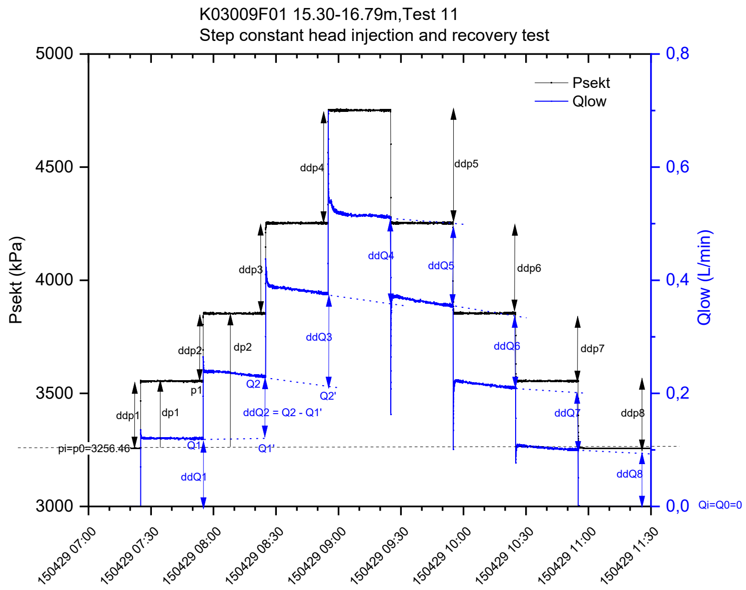

Figure 6-22. *Perturbation phase of step injection Test 11 in K03009F01 15.30-16.79m.*

Q-p evaluation

Q-p results are compiled in the two graphs of Figure 6-23, as pressure change versus flow and as specific capacity (dQi/dpi) versus flow. The latter were calculated for the dQi and dpi at the end of each step and plotted as a function of the flow rate. When flow rate did not stabilize it was linearly extrapolated from prior step when calculating dp for the following step.

The plot on the left of Figure 6-23 show that the flow is largely linear over the present flow range, deviating slightly towards the higher of 0.4-0.5L/min.

Figure 6-23 show a small decrease of specific capacities but linearly rather than exponentially.

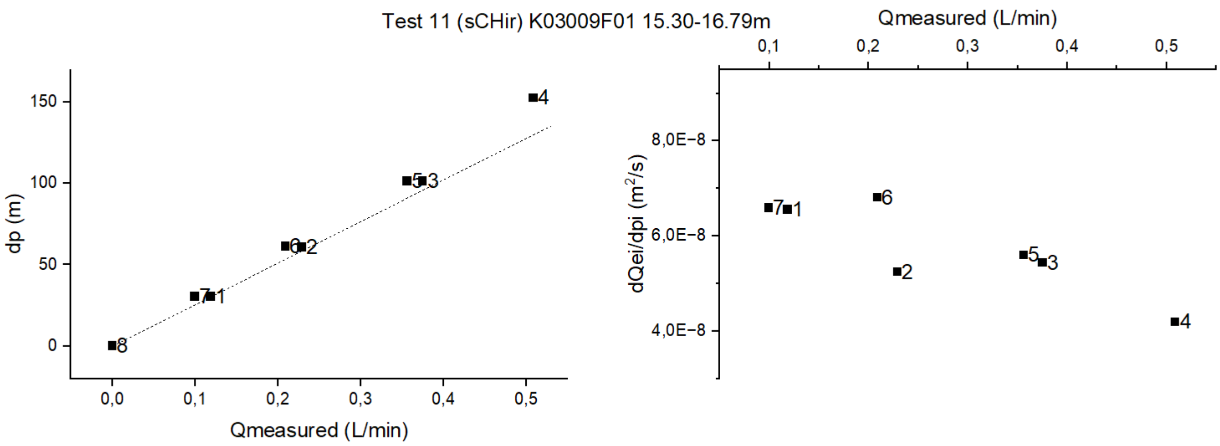

Figure 6-23. *Plot of pressure change (left) and specific capacity (right) as a function of the flow rate of the step withdrawal phases of Test 11 in section K03009F01 15.30-16.79m.*

7 Results K08028F01, Test 12-19.

The present chapter summarises the execution and presents results in each test section with separate chapters for each test. Basic and detailed test result, including all test plots, are presented in Appendix 4 and 5. Interpreted hydraulic formation parameters are compiled in Appendix 7.

7.1 Test section K08028F01 37.00-39.00m, Test 12-19

7.1.1 Test 12 Step constant head injection and recovery test (sCHir)

Test sequence and defined variables are shown in Figure 7-1. The test was conducted with fixed pressure perturbation relative formation pressure (*dp*), stepwise increasing from dp=7kPa up to a maximum of dp=1497kPa and then decreasing. The generated flows were in the interval 0.0038-0.22L/min. This was followed by a recovery phase with pressure eventually stabilizing at close static formation level (3177.6kPa).

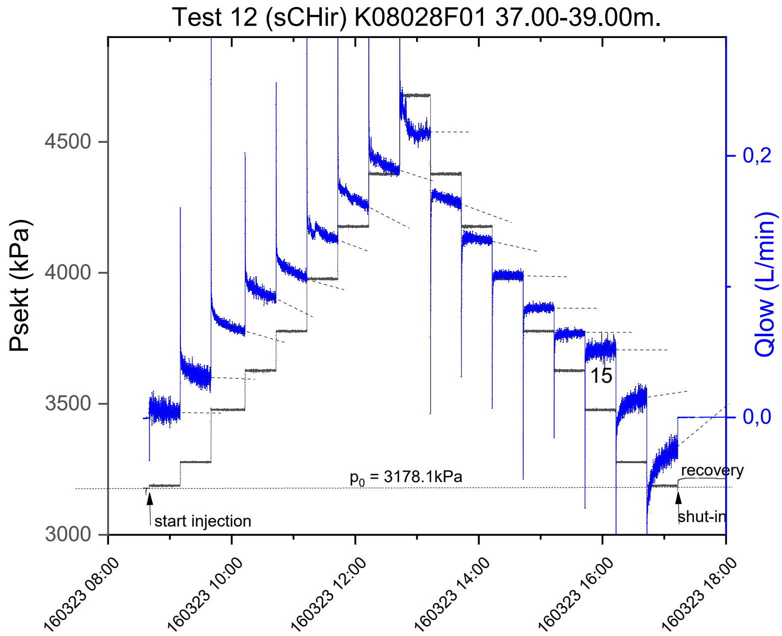

Figure 7-1. *Measured flow and pressure for the step constant head injection and recovery of test 12 in section 37.00-39.00m in borehole K08028F01.*

Q-p evaluation

Q-p results are compiled in the graphs of Figure 7-2, as pressure change versus flow and as specific capacity (dQi/dpi) versus flow. The latter were calculated for the dQi and dpi at the end of each step and plotted as a function of the flow rate. When flow rate did not stabilize it was linearly extrapolated from prior step (dashed lines in Figure 7-1) when calculating dp for the following step. As evident from Figure 7-1, the flow rate is often quite noisy. This makes the flow extrapolation, which is made subjectively through expert judgement, more uncertain which is carried forward to the estimated specific capacity (dQei/dpi) plotted in Figure 7-2.

The plot on the left of Figure 7-2 show that the flow regime deviates from linearity at quite low flow of about 0.05L/min.

The plots on the right of Figure 7-2 show that the specific capacity have clear trend of decreasing with increasing pressure (and flow), from 9E-8m2/s to a stabilised value of about 2E-8m2/s at a flow of 0.1L/min. The trend could be fitted quite well to an exponentially decreasing function with an adjusted coefficient of determination of R2 = 0.9782.

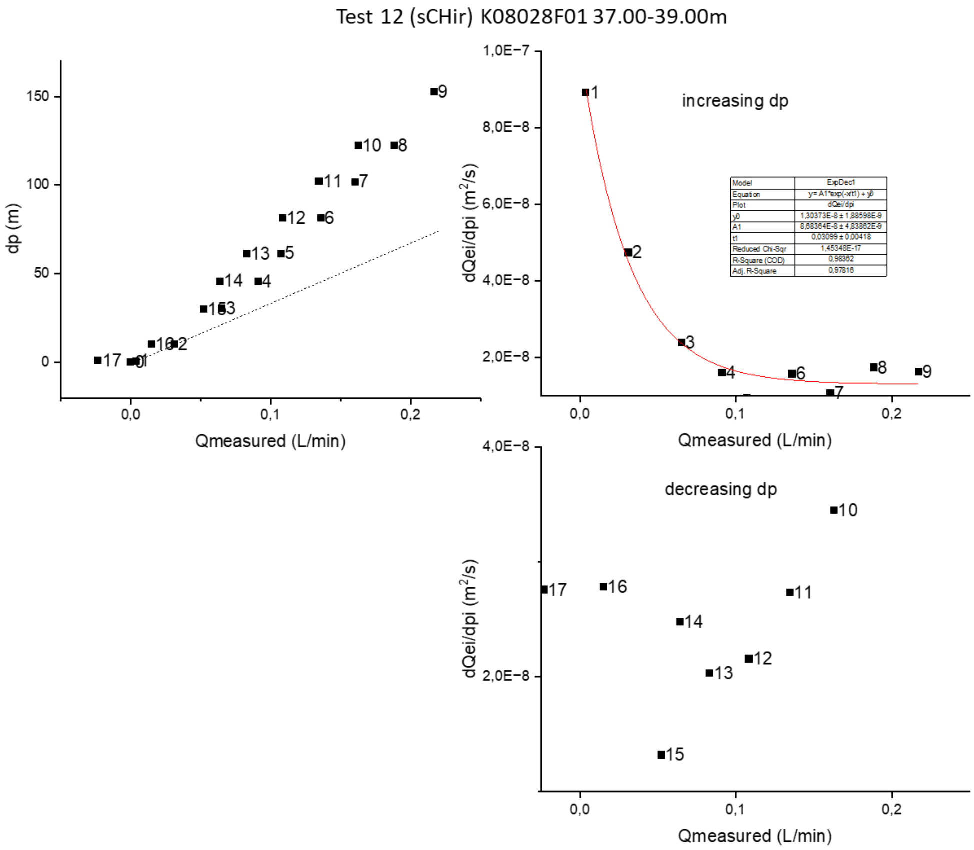

Figure 7-2. Plot of pressure change (left) and specific capacity (right) as a function of the flow rate of the step withdrawal phases of Test 9f in section K03009F01 15.30-16.79m.

7.1.2 Test 13 Step constant rate withdrawal and recovery test (sCRwr)

Test sequence is shown in Figure 7-3, conducted with imposed constant outflow in six steps from 0.05 to 0.3L/min, each of 30minutes duration. This generated a total drawdown of 679kPa, from 3174kPa (initial static formation pressure) to a total formation pressure of 2496kPa before shut-in. This was followed by a recovery phase of almost 16hours duration.

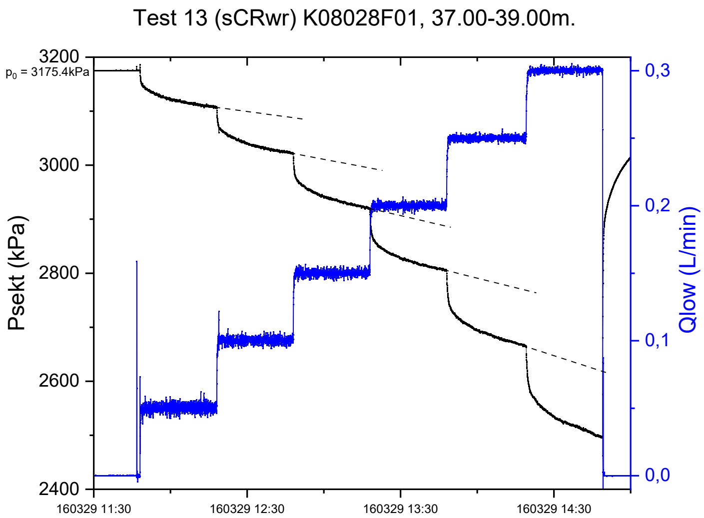

Figure 7-3. Measured flow and pressure for the step constant outflow and recovery test for section 37.00-39.00m in borehole K08028F01.

Q-p evaluation

The test was evaluated for its pressure change (*dp*) as a function of total outflow (*Q*) and specific capacity (*Q/dp*) at the end of each step as a function of the total outflow for the step, see Figure 7-4 left and right. This shows a deviation from linear flow starting at about 0.1L/min and a decrease in specific capacity (and hence transmissivity) with increasing flow, from 1.22E-7m^2/s at 0.05L/min to 0.72E-7m^2/s at 0.3L/min. The specific capacity shows an exponentially decreasing trend fitting well to such function with an adjusted coefficient of determination of $R^2 = 0.9974$.

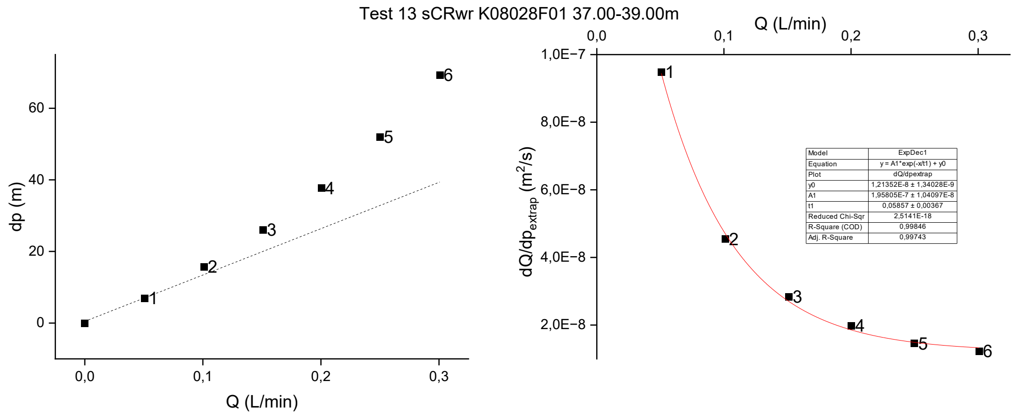

Figure 7-4. *Plot of pressure change (left) and specific capacity (right) as a function of the flow rate of the step withdrawal phases as a function of generated flow at the end of the perturbation periods for the step test (sCRwr) in section 37.00-39.00m in borehole K08028F01.*

Rorabaugh evaluation

Analysis according to Rorabaugh (1953) showed we do have a fully developed turbulent flow as evidenced in Rorabaugh plot of Figure 7-5 where the data resulted in an actual flow rate exponent of n=1.96 with a line fit determination coefficient of $R^2 = 0.99797$. This means that the proper analytical relation describing the drawdown for this test section should include a non-Darcy flow component according to

$$dp \approx BQ + CQ^n$$

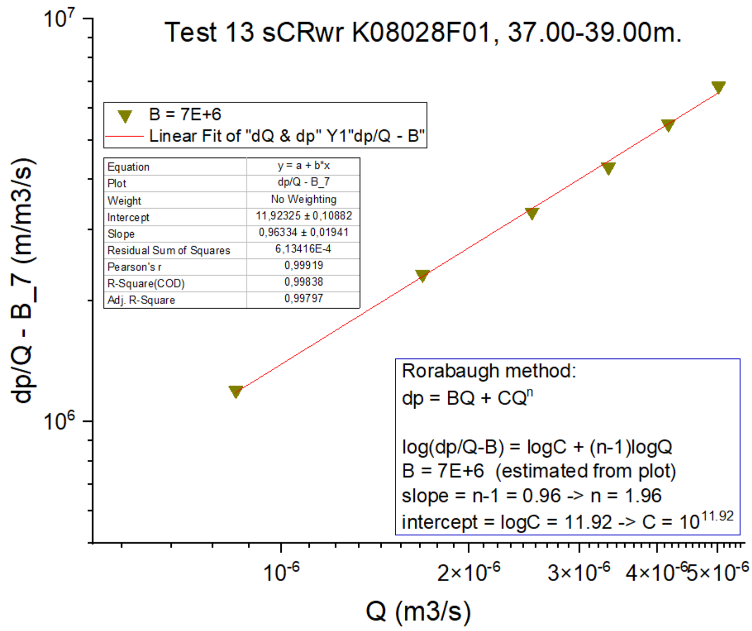

Figure 7-5. *Rorabaugh-plot for evaluation of the non-linear flow exponent for the step constant outflows and recovery test, Test 13 in section 37.00-39.00m in borehole K08028F01.*

7.1.3 Test 14-18 Constant head withdrawal and recovery test (CHwr)

These are five different tests conducted at different constant heads, with dp of 300 (Test 14), 600 (Test 15), 1000 (Test 16), 2000 (Test 17) and 3000kPa (Test18) respectively, with a duration of the perturbation and recovery phase of 1.5h each. The objective is to assess the flow rate related energy loss through the value of the obtained skin factors and transmissivities by means of well controlled transient tests.

Q-p evaluation

The composite Q-p results from these five tests are compiled in the two graphs of Figure 7-6, as pressure change versus flow and as specific capacity (*dQ/dp*) versus flow. The latter were calculated for the dQ at the end of each step and plotted as a function of the flow rate.

The plot on the left of Figure 6-13 show that flow appear to be linear up to 0.2L/min to when it starts to deviate from linearity, larger deviation the higher the rate.

The specific capacity is decreasing with increasing dQ (and dp), Figure 7-6 (right), from 6.7E-8 to 1.9E-8 m^2/s over the tested dQ interval. The decrease appear to be almost linear but was fitted to an exponential decreasing function, with an adjusted coefficient of determination of R^2 = 0.9470.

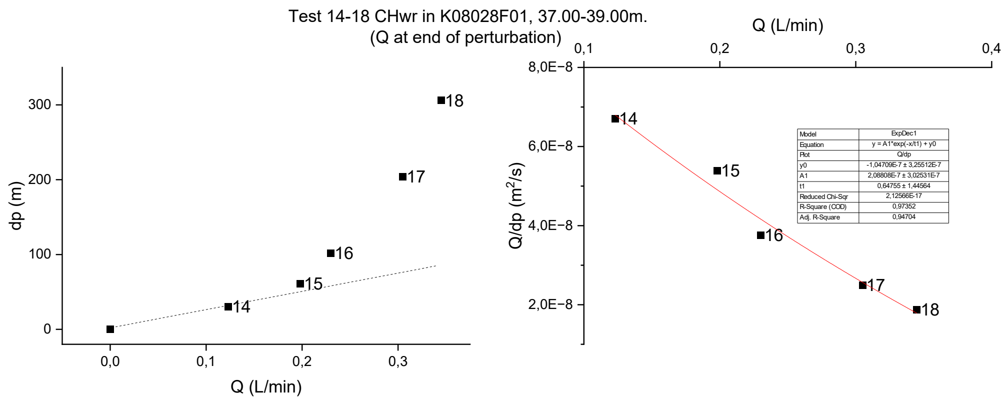

Figure 7-6. Plot of pressure change (left) and specific capacity (right) as a function of the flow rate of the step withdrawal phases as a function of generated flow at the end of the perturbation periods from Test 14-18 in section 37.00-39.00m in borehole K08028F01.

Transient evaluation

A transient evaluation was performed of the drawdown phase. Basic test data comprising with input variables, data plots and evaluated parameters are compiled in Appendix 4, (Test 14-18). The evaluation made for the withdrawal phase with resulting diagnostic plots compiled in Table 7-1 and Figure 7-7.

Log-log plots Figure 7-7 display a consistent diagnostic behaviour with an initial phase of convergence a few seconds towards specified dp. This is followed by a phase with transient flow change (10-100 s) towards a linear flow with a noisy but stable derivative interpreted as radial formation flow.

Table 7-1. Transmissivity and skin from transient interpretation from constant head withdrawal phase of Test 14-19.

Test no.	Test phase	p_i (kPa)	Applied dh (kPa)	dQ at shut-in (L/min)	Skin (m)	Transmissivity (m^2/s)	Comment
14	Withdrawal	3179.86	-300	0,12	-0.6	6.2E-08	
15	Withdrawal	3180.42	-600	0,20	1	6,7E-08	
16	Withdrawal	3168.25	-1000	0,23	5	7,3E-08	
17	Withdrawal	3178.35	-2000	0,30	6	4,0E-08	
18	Withdrawal	3182.40	-3000	0,35	4	2.9E-08	

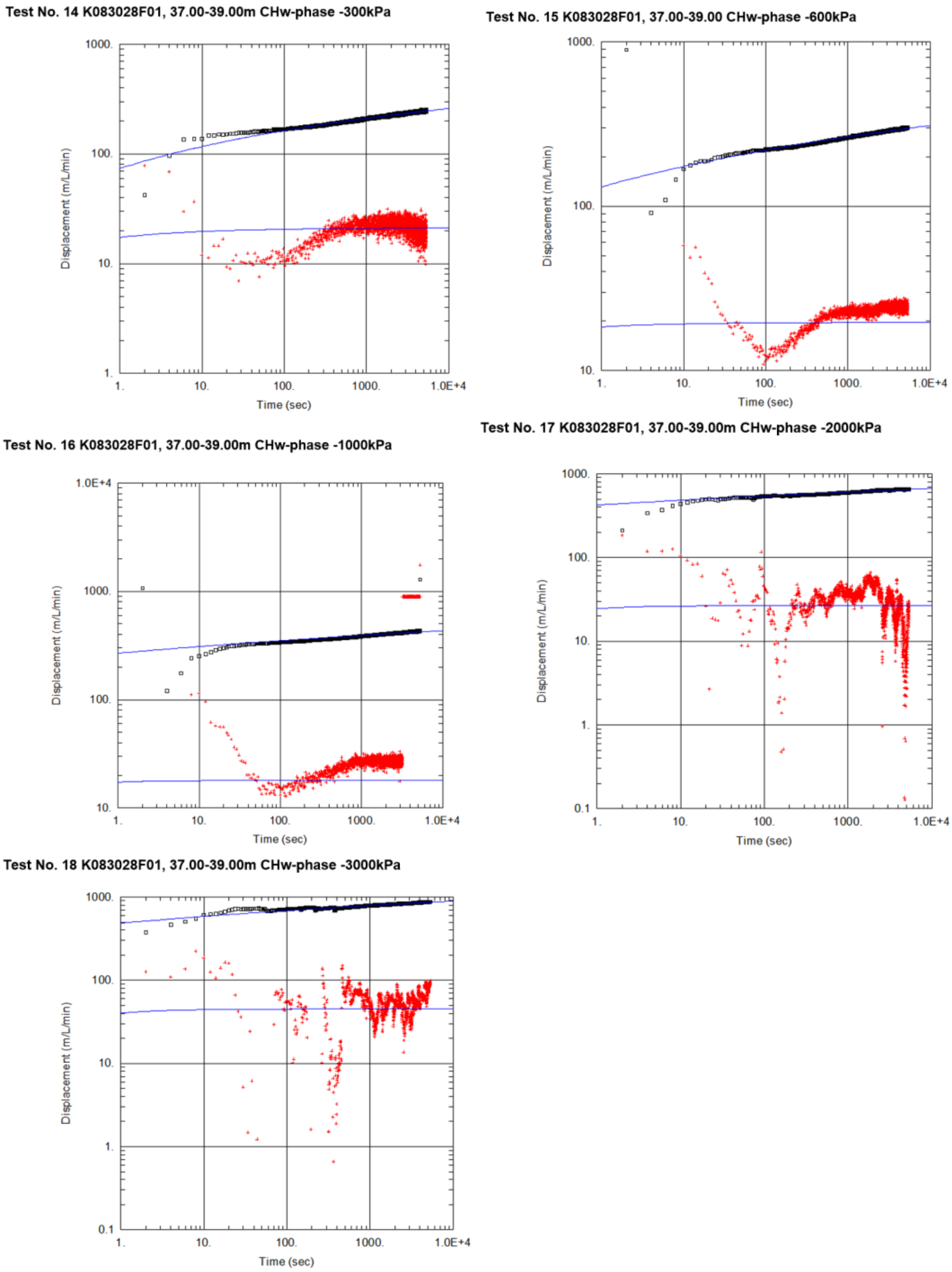

Figure 7-7. *Log-log diagnostic plots for the constant head withdrawal phase of tests no. 14-18 performed in section 37.00-39.00m in borehole K08028F0.*

The resulting transmissivities and skin factors as a function of the flowrate are compiled in Table 7-1 and Figure 7-8,The overall trend here is a rather consistent transmissivity ranging 3E-8 to 7E-8m^2/s and a generally increasing skin factor with increasing flow rate, from -1 to 4-6. This is taken as a support for increased energy losses with increased flow rate believed to be caused by non-linear flow according to the concept of Figure 5-2.

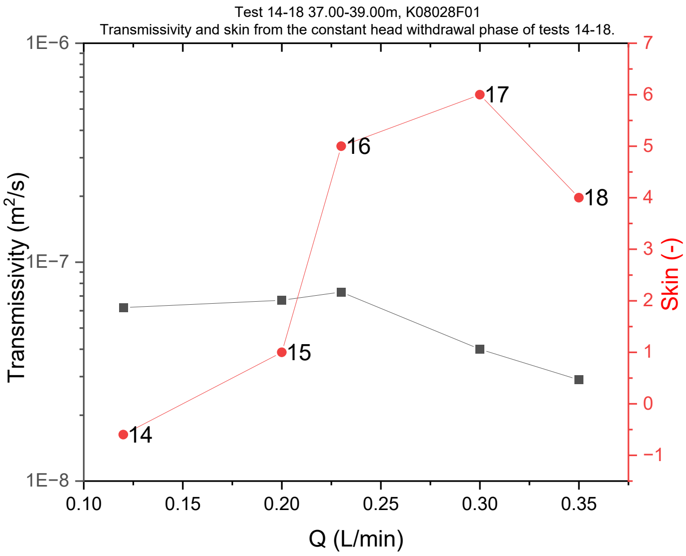

Figure 7-8. Resulting transmissivities and skin factors from the transient evaluation of the withdrawal phase of tests 14-18 as a function of flow rate (at shut-in) in section 37.00-39.00m in borehole K08028F01.

7.1.4 Test 19 Constant head injection and recovery test (CHir)

The test is conducted with a perturbation of constant pressure of dp=+1000kPa above initial formation pressure (3160kPa) for a duration of 1.5h followed by a longer recovery of 16h back to almost initial "static" formation pressure (3179kPa).

The primary objective with this test is to assess and relate to results from constant head withdrawal test (Test 16) under otherwise same conditions. This is done through the value of the obtained skin factors and transmissivities.

Transient evaluation

A transient evaluation is performed of the constant head injection phase. Basic test data comprising input variables, data plots and evaluated parameters are compiled in Appendix 4, (Test 19). The resulting diagnostic log-log plot is shown in Figure 7-9 which display an initial phase of convergence a few seconds towards specified dp. This is followed by a phase with transient flow change (10-100s) towards a linear flow with a noisy but stable derivative interpreted as radial formation flow. The test data was matched with a radial model providing an acceptable match for T=3.5E-8m^2/s and ξ=1.

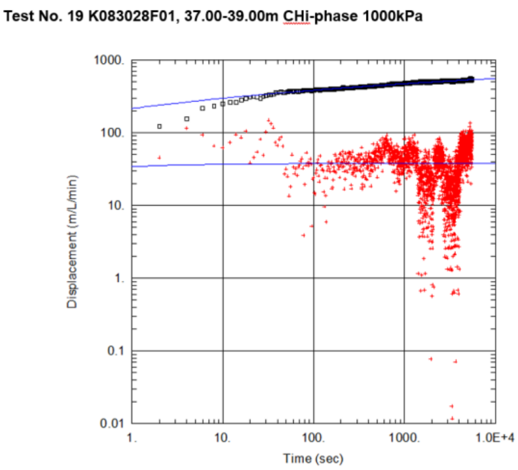

Figure 7-9. Diagnostic log-log plot of the constant head injection phase of Test 19 for section 37.00-39.00m in borehole K08028F01.

8 Discussion and conclusions

Step tests are performed in boreholes from a tunnel at 400m depth to identify and quantify non-linear flow during hydraulic borehole testing. To this effect a suite of hydraulic tests are undertaken. The tests target two types of hydro-structural features, two test sections intersecting discrete singular fractures apertures of 0.5/1.0 mm and one crush zone 27 mm wide. A pseudo steady-state step test was the main tool for assessing non-linearity. These are complemented with constant perturbation tests at different perturbations for transient analysis as a mean to check and validate the steady-state conditioned step test result. Adopted perturbations are ranging 100-3000kPa for pressure and 0.04-7L/min for flow. Non-linear flow is assessed by three means, through pseudo steady-state Q-p plots, through Rorabaugh analysis and through transient analysis. Interpreted hydraulic formation parameters are compiled in Appendix 7.

Issues of direct or general relevance which arose during the investigation are discussed/commented below. These concern non-linear flow, hydraulic parameters, flow regimes, test interpretation and section length. The chapter concludes with a short compilation of main findings.

8.1 Non-linear flow

The presence of non-linear flow was assessed through *dQ-dp* plots and through Rorabaugh analysis. All tests showed the presence of a non-linear flow domain and degree of non-linearity obtained through the flow exponent n in Q^n in the range $1.5 \leq n \leq 2$ (Appendix 5). The onset of non-linear flow was at relatively low perturbations. These comprised low to medium transmissive small open fractures and a crush zone. However, a highly transmissive crush zone at 10.5m in K03009F01 (Morosini, 2018) did not display any indications of non-linear flow as described in the Hydraulic parameters section below. For rock and fracturing tested in the present report the onset of non-linearity started from rather low flow of 0.05L/min for dp=20m, up to 3L/min for dp=45m, Table 8-1.

Well efficiency ranged 2-50% (Appendix 5). It is estimated that the non-linear energy loss causes a reduction in transmissivity of 11-65% (chapter 6 and 7, *dQ/dp*-plots). Furthermore, the reduction in T-value is of the exponentially decaying form for the discrete fracture sections while it is of a close to linearly decaying form for the crush zone section.

Table 8-1. Onset of non-linearity derived from the Q-p plots.

							Onset of non-linearity		
Test No.	**Test type**	**Test borehole/section**	**Geological environment**	**Well efficiency**	**dQ range**	**dp range**	**dQ**	**dp**	**dQ/dp**
				%	L/min	kPa	L/min	mH2O	m2/s
1	sCRw	K03009F01 14.20-17.19m	Small fractures with	6->2	0.08-0.7	100-1100	0,15	25	1,00E-07
2-6	CHw	K03009F01 14.20-17.19m	apertures 0.5, 1 and		0.12-0.75	300-3000	0,15	50	5,00E-08
7	sCHi	K03009F01 14.20-17.19m	1mm.		0.2-0.8	300-1500	0,3	40	1,30E-07
									--
9	sCRw	K03009F01 17.20-20.19m	Small fractures with	50->20	0.8-7	140-1300	1,7	40	7,10E-07
9a-9e	CHw	K03009F01 17.20-20.19m	apertures 0.5 and		1-7	300-3000	2	50	6,70E-07
9f	sCHi	K03009F01 17.20-20.19m	1mm.		2-6	300-1500	3	45	1,10E-06
									--
10	sCRw	K03009F01 15.30-16.79m	Small fractures with	95->75	0.05-0.5	140-700	0,18	50	6,00E-08
11	sCHi	K03009F01 15.30-16.79m	apertures 0.5, 1, 1mm.		0.1-0.5	300-1500	0,35	80	7,30E-08
									--
12	sCHi	K08028F01 37.00-39.00m			0.004-0.2	10-1500	0,05	20	4,20E-08
13	sCRw	K08028F01 37.00-39.00m	Crush zone 27mm wide.	85->50	0.05-0.3	70-700	0,1	18	9,30E-08
14-18	CRw	K08028F01 37.00-39.00m.			0.1-0.3	300-3000	0,17	50	5,70E-08

A somewhat less definitive picture is given from the transient interpretation of the constant head withdrawal phases for the test sections, tests 2-6, 9a-9e and 14-18. Evaluated skin factors as a function of final flow rates are plotted in Figure 8-1. These show linear trends for two the three sections

- 14.20-17.19m in K03009F01 with $d\xi/dQ=112(L/min)^{-1}$ with $R^2=0.86$ and in
- 37.00-39.00m in K08028F01 with $d\xi/dQ=25(L/min)^{-1}$ with $R^2= 0.52$.

while section 17.20-20.19m in K03009F01 do not appear to have any correlation.

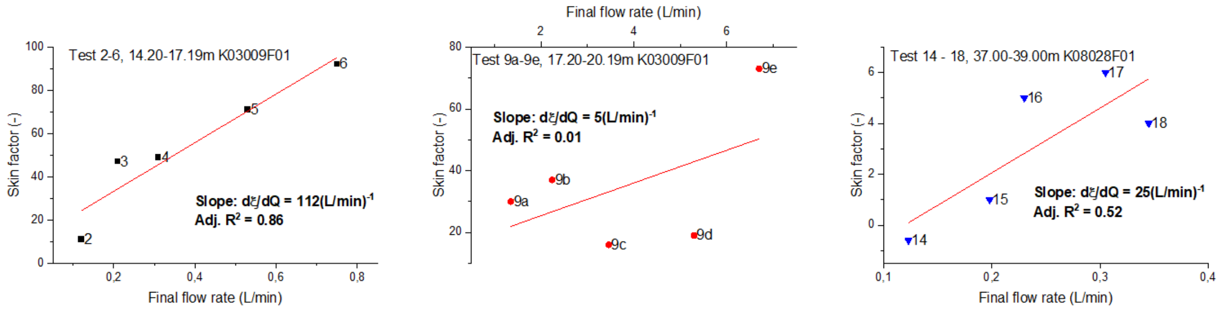

Figure 8-1. *Skin variation with flow rate for different test sections, 2-6 and 9a-9e are open fractures and 14-18 is a crush zone.*

Constant head tests are sensitive to non-linear flow. These are rate-transient with decreasing flow during the perturbation phase, the magnitude of which depends on the degree of non-linearity.

8.2 Hydraulic parameters

Interpreted transmissivities and skin factors are from transient evaluation of the constant perturbation phase of the tested borehole sections are presented in chapters 6.1.3 and 6.2.3 for the discrete singular fracture sections and chapter 7.1.3 for the crush zone section. Diagnostic plots and interpreted data are summarised in Appendix 4. All these tests exhibited a radial formation flow formation geometry.

The interpretation yielded consistent transmissivities for each section, within a relatively narrow range. Skin factors are however not as consistent and more varied. The following observations are made:

1) a flow rate related skin factor trend is apparent for two of the test sections (Tests 2-6 and 14-18), while no such trend for the third test section (Test 9a-9e) from transient evaluation,
2) the skin factors for the discrete singular fracture sections are considerably higher than for the crush zone, 10-100 times higher,
3) while skin values may be relatively low there can still be a non-linear flow component, as indicated by results from the crush zone section (Test 14-18).

Hence, presence and magnitude of nonlinear flow losses appear common and considerably high in small open fractures. These small conductive fractures are volumetrically dominating, i.e. occupying the rock between the high conductivity features. As a consequence, for steady-state tests there is a risk of systematically and considerably underestimating the hydraulic conductivity of that rock, by up to about one order of magnitude, particularly in rock around deep seated excavations/facilities where hydraulic gradients are high.

8.3 Tunnel skin

The findings and conclusions contained in this study are equally applicable to conditions around a tunnel. Hence, non-linear flow and head losses are most likely present around an underground excavation. Besides fracture properties, its quantitative effect is however also dependent on tunnel depth (i.e head difference) and degree of grouting.

The presence of a tunnel skin has sometimes been invoked into the model during numerical flow simulation as a matter of necessity for the simulation to agree with field measurements. Also, some pressure data from tunnel boreholes within the monitoring system at Äspö HRL show a large near-tunnel pressure drop. This is rock where no grouting was applied during tunnel construction. Such would suggest the possibility of the presence of a positive skin zone around the tunnel, being consistent the non-linear flow zone.

8.4 Fracture aperture

Fracture aperture refers to a change in the effective flow-through area of the fracture, either through physical displacement of the fracture surfaces or through a change in effective fracture porosity by means remobilisation of fracture gouge. The main avenue to assess fracture aperture effects is through stepwise injection tests to assess any effect of the applied head difference on the aperture of the fracture, and to distinguish it from non-linear flow effects. This type of assessment was done with tests 7, 9f, 11 and 12. Of the tested sections, a fracture closing effect was observed for the crush zone section, Test 12 where the specific capacity reduced from initial 8E-8m^2/s to 3E-8m^2/s after the step injection test, Figure 7-2. Test 9f and 11 which tested the same discrete fracture type of hydraulic features also show a reducing fracture aperture effect but slightly smaller than for the discrete fractures.

8.5 Flow regimes

For tests performed in this study transient and steady-state interpretations (Moye (1967), Thiem (1906)) were made. The basic difference between Moye and Thiem is the assumption on flow geometry, whereas Moye assumes radial spherical flow, Thiem assumes radial cylindrical flow. Actual flow geometry is revealed through the transient evaluation where radial cylindrical flow could be stated for all test sections. Physically all tests are transient progressing towards pseudo steady-state flow conditions, eventually reaching pseudo steady-state if duration is long enough. Transient evaluation is always superior to pseudo steady-state evaluation because it reveals much more about the tested formation than pseudo-steady state. Nevertheless, pseudo-steady state evaluation is a simple and low cost possibility, particularly if some exterior arguments are provided that support some assumptions in the pseudo steady-state theory and is extensively adopted in some of SKB:s hydraulic testing programme.

Comparing calculated transmissivities from constant perturbation phases, Table 8-2, we note that

a. pseudo steady-state transmissivities for the three test sections are in rather good agreement with transmissivities from the difference flow logging Ta_PFL,

b. pseudo steady-state transmissivities for the crushed zone test section (K08028F01 37-39m) agree with the transient transmissivities,

c. pseudo steady-state transmissivities for the small discrete fracture test sections (Tests 1-9e) are much lower than the transient transmissivities, by about 1 order of magnitude.

A transient evaluation is considered to provide more confidence and representative transmissivity than steady-state evaluation. Without further investigations, the reasons for observations b) and c) above is unknown.

With regards to item b) it is believed that the agreeing steady-state and transient transmissivities are due to little or no skin being present, since skin is not accounted for in steady-state evaluations.

The finding in item c) is consistent with basic fluid mechanics whereby energy losses for the same hydraulic head are distributed over more flow channels entering the borehole, hence increasing the flow-through area and decreasing the specific flow rate (Darcy velocity).

Table 8-2. Transmissivities from transient and pseudo steady-state evaluations of constant perturbation tests.

Test No.	Test section	Test type	Pertur-bation	Duration of pertur-bation	dQ/dp[2]	TT (transient)	T (Moye)	T (Thiem)	Ta_PFL (Thiem)
			kPa	h	m^2/s	m^2/s	m^2/s	m^2/s	m^2/s
2	K03009F01 14,20-17,19m	CHw	-300	1,5	6,5E-08	1,8E-07	1,0E-07	7,8E-08	
3	K03009F01 14,20-17,19m	CHw	-600	1,5	5,7E-08	5,1E-07	4,3E-08	3,2E-08	
4	K03009F01 14,20-17,19m	CHw	-1000	1,5	5,1E-08	4,6E-07	3,8E-08	2,8E-08	
5	K03009F01 14,20-17,19m	CHw	-2000	1,5	4,3E-08	5,5E-07	3,2E-08	2,4E-08	
6	K03009F01 14,20-17,19m	CHw	-3000	1,5	4,1E-08	6,4E-07	3,0E-08	2,3E-08	
8	K03009F01 14,20-17,19m	CHi	1000	1,5	8,5E-08	3,5E-07	6,3E-08	4,7E-08	
P-15-13[1]	K03009F01 14,20-17,19m	CHw	-463 to -512	c. 48					2,0E-08
9a	K03009F01 17,20-20,19m	CHw	-300	1,5	7,4E-07	4,6E-06	5,5E-07	4,1E-07	
9b	K03009F01 17,20-20,19m	CHw	-600	1,5	6,1E-07	4,5E-06	4,5E-07	3,4E-07	
9c	K03009F01 17,20-20,19m	CHw	-1000	1,5	5,7E-07	2,2E-06	4,2E-07	3,1E-07	
9d	K03009F01 17,20-20,19m	CHw	-2000	1,5	4,3E-07	1,9E-06	3,2E-07	2,4E-07	
9e	K03009F01 17,20-20,19m	CHw	-3000	1,5	3,7E-07	4,9E-06	2,7E-07	2,0E-07	
P-15-13[1]	K03009F01 17,20-20,19m	CHw	-463 to -512	c. 48					8,5E-09
14	K08028F01 37.00-39.00m	CHw	-300	1,5	6,7E-08	6.2E-08	4,6E-08	1,0E-07	
15	K08028F01 37.00-39.00m	CHw	-600	1,5	5,4E-08	6,7E-08	3,7E-08	8,1E-08	
16	K08028F01 37.00-39.00m	CHw	-1000	1,5	3,8E-08	7,3E-08	2,6E-08	5,7E-08	
17	K08028F01 37.00-39.00m	CHw	-2000	1,5	2,5E-08	4,0E-08	1,7E-08	3,8E-08	
18	K08028F01 37.00-39.00m	CHw	-3000	1,5	1,9E-08	2.9E-08	1,3E-08	2,8E-08	
19	K08028F01 37.00-39.00m	CHi	1000	1,5	3,0E-08	3.5E-08	2,0E-08	4,5E-08	
P-15-13[1]	K08028F01 37.00-39.00m	CHw	-530 to -603	c. 48					2,3E-08

1) P-15-13 is SKB's report number of difference flow logging.
2) Specifc capacity at end of perturbation phase.

8.6 Injection vs withdrawal

Tests are performed to compare and confirm that injection and withdrawal tests produce similar results in terms of skin factors and transmissivities when performed under otherwise same conditions. The perturbation phase tests are performed with the same constant dp of 1000kPa for a duration of 1.5h.

The tests are executed in two different hydrogeological settings, Test 4 and 8 on small open fractures and Test 16 and 19 on a crush zone setting.

Comparative results compiled in Appendix 6 show that transmissivities differ by about 100%. Transient transmissivity from withdrawal tests is twice that of injection while for pseudo steady-state it is half.

8.7 Inference on test interpretation

Lessons learned from the present study are feeding into SKB's standard methodology for hydraulic borehole testing. The toolbox consists a variety of different methods which can broadly be classified as transient or steady-state flow and as constant head or constant rate inner boundary. Here we highlight the more direct considerations of non-linear flow on the interpretation.

The presence of non-linear flow will have no impact on the derived transmissivity from constant rate tests. It will, however, cause a larger total skin factor, as the effect of geometrical skin and non-linear skin are lumped together. The impact also depends on whether the test is performed and evaluated according to transient flow or pseudo steady-state flow theory, of which the latter does not account for skin at all.

Constant head tests are sensitive to non-linear flow, these are, by definition, rate-transient and the specific capacity is impacted (decreased), the magnitude of which depends on the degree of non-linearity. The impact is on the transient flow since the targeted constant drawdown (dh) is, to a certain extent, composed of and exaggerated by non-linear losses. This requires additional flow to maintain the specified head giving a misrepresented transient flow evolution and, if not accounted for,underestimating the calculated transmissivity. The presence of non-linear flow may also have an impact on the diagnostic interpretation of the flow geometry. If an extensive non-linear flow regime develops near the borehole it may be interpreted as the formation being of lower transmissivity instead of a flow-induced effect. This is exhibited as a radial composite flow geometry leading to the identification of a lower transmissive zone near the wellbore rock when in fact it does not exist. Hence, this will give a wrong conceptualization and potentially also feed incorrect parameters into the statistics supporting the homogenization and parameterization process during the conceptual modelling exercise.

8.8 Section length

As mentioned in chapter 3.1,the same hydraulic features in K03009F01 at 15.42m and 16.10m, were tested with different positions of section seals in order to assess:

- if/how position of section seals might cause a redistribution of flow
- if flow below the lower detection limit might impact derived hydraulic parameters.

The sections that straddle the same hydraulic features are 15.30-16.79m and 14.20-17.19m. The latter is the same section as previously tested which resulted in very high skin factor when no consideration for non-linear flow was taken (Morosini, 2018).

Both sections were step tested through constant rate withdrawal (Test 1 and 10) and constant head injection (Test 7 and 11) with similar magnitudes of perturbation, Table 8-3.

The resulting transmissivity and skin factors are approximated and summarised in Table 8-3. The parameters derived through transient evaluation of the perturbation phase including a non-linear flow component are inconclusive in that the step constant head injection tests show similar parameters while the step withdrawal test yields considerable discrepancy, of one order by magnitude in transmissivity and threefold in skin factor.

Table 8-3. Transmissivity and skin factors derived for hydraulic features in K03009F01 at 15.42 m and 16.10 m from section delimitations.

Test section (m)	Constant rate withdrawal		Constant head injection	
	Parameters:			
	T (m^2/s)	ξ (-)	T (m^2/s)	ξ (-)
14.20-17.20	2,E-08	-3 to 3	4,E-07	12 to 20
15.30-18.80	1,E-07	6 to 10	4,E-07	28 to 33
	Perturbation:			
	dQ (L/min)	dp (m)	dQ (L/min)	dp (m)
14.20-17.20	0.08 to 0.7	10 to 100	0.24 to 0.82	30 to 150
15.30-18.80	0.05 to 0.47	14 to 67	0.12 to 0.51	30 to 150

8.9 Conclusions

On a general note, non-linear flow is identified in all tests in all section, from transitional flow to fully turbulent flow. It is much more pronounced in small open fractures than in a crush zone environment. The presence of non-linear flow is mainly impacting the skin factor/well loss component which may extend into the rock forming a two-regime flow system of non-linear/linear flow proximal to the borehole. Directly related to test objectives we found that

- non-linear flow is present in all test sections covering different hydraulic features small open fractures, crush zone and low transmissive deformation zone. The flow regime ranges from transitional to fully turbulent with a flow exponent of n = 1.5-2.0 which reduces the well efficiency to between 50 - 2%. (App. 5),
- for small open fractures high skin factors, up to 92, occur when non-linear flow is present during the test and not accounted for in the evaluation. (App.4),
- for the crush zone the skin factors are low, even non-linear flow is present. Suggesting the non-linear flow component is modest under otherwise same conditions. (App. 4),
- a distinct fracture aperture and/or gouge remobilisation effect was observed for the crushed zone section (Test 12) with decreased flow for same dp on recovery and decreased specific capacity after recovery,
- much higher skin factors are present in open fracture than in the crush zone, up to a ten-fold difference. (App 4.).

Also notable is that

- fracture closing effect are possibly present for discrete fractures features, each aperture 0.5 or 1 mm (Test 9f and 11). Here the uncertainty relates to the low resolution in dp at the beginning of the test. It is however definitely present for the crush zone (Test 12, 37-39m in K08028F01), (Q-p plots),
- the onset of non-linear flow is in the range 0.05-3L/min for perturbations in the range of 10-50m. This translates to specific capacities in the range of $4 \cdot 10^{-9}$ -$1.4 \cdot 10^{-5}$ m^2/s for the onset of non-linear flow. (Q-p plots),
- corresponding reduction in transmissivity over the adopted flow ranges due to nonlinear flow is in the interval 11-65%. (Q-p plots),
- the functional transmissivity reduction due to non-linear flow fits best to the exponential decay form, $T \approx T_0 + A_1 \cdot e^{-Q/t1}$, all with a coefficient of determination $R^2 > 0.99$. (Q-p plots),
- similar value of transmissivity and skin factor are obtained from withdrawal and injections tests (test 4 and 8) everything else being equal,
- small non-linear losses seem also be the case for a highly transmissive crush zone (Morosini, 2018) which yielded similarly low total skin factors as in this study for the low transmissive crush zone (Ch 7),
- transmissivities derived from steady-state evaluations are always prone to underestimate the actual transmissivity when positive skin is present. When the skin is caused by non-linear flow the estimated transmissivity can be exceptionally wrong, by order of magnitude,
- through analogy between borehole and tunnel, it is inferred that principles for non-linear flow and very high skin factors for boreholes in this investigation are equally applicable for tunnel inflow and associated head distribution around a tunnel.

References

SKB's (Svensk Kärnbränslehantering AB) publications can be found at www.skb.com/publications.

SKBdoc documents will be submitted upon request to document@skb.se.

Aarstad, K, 1987. Criteria for determining times for end of transient flow and start of pseudosteady state flow. Stanford Geothermal Program report SGP-TR-116. Stanford University, USA.

Batu, V, 1998. Aquifer hydraulics. John Wiley & Sons, Inc..

Bear, J, Zaslavsky, D., Irmay, S., 1968. Physical principles of water percolation and seepage. UNESCO.

Bear, J, 1972. Dynamics of fluids in porous media. Dover Publications reprint 1988.

Bear, J, 1979. Hydraulics of groundwater. McGraw-Hill, Inc.

Cooper, H H Jr, Jacob, C.E, 1946. A generalized graphical method for evaluating formation constants and summarizing well-field history. Transactions, American Geophysical Union. Vol.27, No.IV . August 1946.

da Prat, G, 1990. Well test analysis for fractured reservoir evaluation. Developments in petroleum science 27, Elsevier Publisher.

Doe, T.W, Geier, J.E, 1990. Interpretation of fracture system geometry using well test data. Stripa project report 91-03. Swedish Nuclear Fuel and Waste Management Co..

Dougherty, D.E and D.K. Babu, 1984. Flow to a partially penetrating well in a double-porosity reservoir, Water Resources Research, vol. 20, no. 8, pp. 1116-1122.

Forchheimer, P. 1901. Wasserbewegung durch Boden, Z. Ver. Deutsch. Ing. 45 pp1782-1788.

Hakami, H, 2003. Äspö Hard Rock Laboratory. Update of the rock mechanical model 2002. SKB report IPR-03-37. Svensk Kärnbränslehantering AB.

Hjerne, C, Ragvald, J, Palmfjord, E., 2016. Hydraulic interference tests in boreholes K03009F01 and K08028F01. SKB report P-15-04, Svensk Kärnbränslehantering AB.

Houben, G, 2015a. Hydraulics of water wells—head losses of individual components. Hydrogeology Journal, September 2015,Volume 23, pages 1659–1675

Houben, G, 2015b. Hydraulics of water wells—flow laws and influence of geometry. Hydrogeology Journal,October 2015 ,Volume 23, pages 1633–1657

Houlsby, A.C, 1976. Routine interpretation of the Lugeon water-test. Quarterly Journal of Engineering Geology, Vol 9 , pp303-313.

Hultgren, P, Mattsson, H, 2015. Geological single-hole interpretation of K03009F01. SKB Internal report SKBdoc id:1475597. Svensk Kärnbränslehantering AB.

HydroSOLVE, 2007. AQTESOLV Pro v4.5. Reston, VA., USA.

Jacob, C.E, 1946. Drawdown test to determine effective radius of artesian wells. Transactions American Society of Civil Engineers, vol 112, pp1047-1070.

Jacob, C.E, 1950. Flow of ground water. In Engineering hydraulics, Rouse, H. (ed.), 1950. Proceedings of the Fourth Hydraulics Conference, Iowa Institute of Hydraulic Research, June 12-15 1949. John Wiley & Sons Inc.

Jacob, C.E and S. W. Lohman (1952). Nonsteady flow to a well of constant drawdown in an extensive aquifer, Eos Trans. AGU, 33 (4), 559-569.

Komulainen, J, Pöllänen, J, 2016. Difference flow logging in boreholes K03009F01 and K08028F01. SKB report P-15-13. Svensk Kärnbränslehantering AB.

Kruseman, G.P, de Ridder, N.A., 1991. Analysis and evaluation of pumping test data. ILRI Publication 47. International Institute for Land Reclamation and Improvement, Wageningen, The Netherlands.

Mathias, S.A, Butler, A.P, Zhan, H. 2008. Approximate solutions for Forchheimer flow to a well. Journal of Hydraulic Engineering, ASCE, 134(9):1318-1325.

Mathias, S.A. and Todman, L.C, 2010. Step-drawdown test and the Forchheimer equation. Water Resources Research vol. 46. W07514 pp1-9. American Geophysical Union.

Morosini, M. Lindquist, A, Ragvald, J, Ludvigsson, J-E, Hjerne, C, 2018. Interferenstester och tolkning av borrningsresponser som underlag för hydrogeologisk modellering. SKB report P-17-36, Svensk Kärnbränslehantering AB.

Morosini, M, 2018. Hydraulic testing of borehole K03009F01. SKB report P-18-07. Svensk Kärnbränslehantering AB.

Morosini, M, 2026. Addressing non-Darcy flow through the rate-dependent skin concept. SKB report P-26-10. Svensk Kärnbränslehantering AB.

Moye, D G, 1967. Diamond drilling for foundation exploration. Civil Engineering Transactions, April, 1967.

OriginLab, 2025. Origin Pro 2023b. OriginLab Corporation, USA.

Quinn, P.M, B.L, Cherry, J.A, 2011. Using constant head step tests to determine hydraulic apertures in fractured rock. Journal of Contaminant Hydrology 126 pp85-99.

Rorabaugh, M.I, 1953. Graphical and theoretical analysis of step-drawdown tests of artesian wells. Proc. ASCE. 79, Separate No. 362. 1-23.

Rutqvist, J, Stephansson, O, 2003. The role of hydromechanical coupling in fractured rock engineering. Hydrogeology Journal 11:7-40.

Scheidegger, A 1974. The physics of flow through porous media. 3rd ed. University of Toronto Press.

SKB, 2013. Äspö Hard Rock Laboratory. Annual report 2012. TR-13-10. Svensk Kärnbränslehantering AB.

Stille, H, 2015. Rock grouting – Theories and Applications. . BEFO – Stiftelsen Bergteknisk Forskning, Sweden.

Theis CV, (1935). The relation between the lowering of the piezometric surface and the rate and duration of discharge of a well using groundwater storage. Trans Am Geophys Union 16:519–524.

Thiem, G, 1906. Hydrologische methoden, J. M. Gebhardt, Leipzig.

Nomenclature

Symbol	Description	Dimensions (L:length, T:time, M:mass)	SI-units
K	Hydraulic conductivity	L/T	m/s
T	Transmissivity	L^2/T	m2/s
S	Storage coefficient=storativity	-	-
S_s	Specific storage coefficient	1/L	1/m
ξ	Skin factor	-	-
t	Time	T	s
h	Hydraulic head	L	m
H	Formation thickness	L	m
L	Test section length	L	m
p	Pressure	$M/(LT^2)$	Pa ($kg/(ms^2)$)
r	Radius	L	m
R	Radius of influence	L	m
A	Area	L^2	m^2
Q	Volumetric flow rate	L^3/T	m^3/s
q	Specific discharge(=Q/A), aka Darcy velocity	L/T	m/s
ρ	Density	M/L^3	kg/m^3
C	Wellbore storage coefficient(=dV/dh)	L^2/T^2	m^2
C_D	Dimensionless wellbore storage coefficient	-	-
V	Volume	L^3	m^3
m	Slope of lin-log straight line, dh/dt (or dp/dt)	L/T	m/s
Prefixes & suffixes			
d	Finite difference of variable		
Δ	Finite difference of variable		
Subscripts & superscripts			
D	dimensionless		
M	match point		
i	initial condition		
0	natural,"static" condition at time prior to test , for variable (e.g. p_0, h_0, Q_0)		
0	for parameter at flow-rate extrapolated to zero (e.g. ξ_0)		
w	active well or borehole		
n	exponent		
e	extrapolated		
Constants			
g	Gravitational constant of acceleration(≈9.81m^2/s)	L^2/T)	m^2/s
π	Geometric constant of ratio circumference/diameter of a circle(≈3.14)	-	-
e	Euler's number(≈2.72), base of natural logarithms.	-	-

Appendix 1 - Test programme

Tests performed in borehole K03009F01

Test No.	Test type[3], acronym	Targeted perturb.[1] (kPa or L/min)	Measured response[1] (kPa or L/min)	Test start	Test stop	Duration perturb. / recovery (h)	Test aim
K03009F01 14,20-17,19m.							
		0,08 L/min	-100 kPa				
		0,16 L/min	-184 kPa				
1	sCRwr	0,27 L/min	-351 kPa	2015-03-30	2015-03-31	0.5/step /4[2)]	Assess rate dependent well loss
		0,53 L/min	-1127 kPa				
		0,7 L/min	-863 kPa				
2	CHwr	-300 kPa	0.12 L/min	2015-03-31	2015-03-31	1.5 /4	Test 2-6. Full transient evaluation without need for steady state. Assess dp effect on well loss. Relate to Test 7.
3	CHwr	-600 kPa	0.21 L/min	2015-03-31	2015-04-01	1.5 /4	
4	CHwr	-1000 kPa	0.31 L/min	2015-04-01	2015-04-01	1.5 /4	
5	CHwr	-2000 kPa	0.53 L/min	2015-04-01	2015-04-07	1.5 /4	
6	CHwr	-3000 kPa	0.75 L/min	2015-04-07	2015-04-08	1.5 /4	
		300 kPa [1)]	0,24 L/min				
		600 kPa	0,4 L/min				
		1000 kPa	0,57 L/min				
7	sCHir	1500 kPa	0,82 L/min	2015-04-08	2015-04-09	0.5/step /4[2)]	Assess dp dependent well loss, compare with Test 1.
		1000 kPa	0,57 L/min				
		600 kPa	0,37 L/min				
		300 kPa	0,2 L/min				
8	CHir	1000 kPa	0.52 L/min	2015-04-09	2015-04-09	1.5 /4	Compare/Assess injection/outflow effect with Test 4.
K03009F01 17,20-20,19m.							
		0,8 L/min	-138 kPa				
		1,6 L/min	-217 kPa				
9	sCRwr	2,7 L/min	-374 kPa	2015-04-15	2015-04-15	0.5/step /4[2)]	Identify onset of non-linear flow and assess rate dependent well loss.
		5,3 L/min	-1272 kPa				
		7 L/min	-1041 kPa				
9a	CHwr	-300 kPa	1,35 L/min	2015-04-16	2015-04-17	1.5 /4	Test 9a-9e: Full transient evaluation without need for steady state. Assess dp effect on well loss. Relate to Test 9f.
9b	CHwr	-600 kPa	2,24 L/min	2015-14-17 failed 2015-04-27 new	2015-04-20 failed 2015-04-28 new	1.5 /4	
9c	CHwr	-1000 kPa	3,46 L/min	2015-04-20 failed 2015-04-23 new	2015-04-20 failed 2015-04-23 new	1.5 /4	
9d	CHwr	-2000 kPa	5,30 L/min	2015-04-21 failed 2015-04-23 new	2015-04-21 failed 2015-04-27 new	1.5 /4	
9e	CHwr	-3000 kPa	6,75 L/min	2015-04-21	2015-04-22	1.5 /4	
		300 kPa	2,02 L/min				
		600 kPa	3,41 L/min				
		1000 kPa	4,86 L/min				
9f	sCHir	1500 kPa	6,27 L/min	2015-04-22	2015-04-23	0.5/step /4[2)]	Assess dp dependent well loss, compare with Test 9.
		1000 kPa	4,41 L/min				
		600 kPa	2,87 L/min				
		300 kPa	1,6 L/min				

Test No.	Test type[3]	Targeted perturb. (kPa or L/min)	Measured response (kPa or L/min)	Test start	Test stop	Duration perturb. / recovery (h)	Test aim
K03009F01 15,30 - 16,79m							
10	sCRwr	0,05 L/min 0,11 L/min 0,18 L/min 0,35 L/min 0,47 L/min	-136 kPa -176 kPa -235 kPa -670 kPa -566 kPa	2015-04-28	2015-04-29	0.5/step /4[2)]	Assess rate dependent well loss, as Test 9 but section narrowing on fractures. Lower dQ steps than Test 9.
11	sCHir	300kPa 600 kPa 1000 kPa 1500 kPa 1000 kPa 600 kPa 300 kPa	0,12 L/min 0,23 L/min 0,38 L/min 0,51 L/min 0,36 L/min 0,21 L/min 0,1 L/min	2015-04-29	2015-04-30	0.5/step /4[2)]	Assess dp dependent well loss and compare with Test 10, but also 9f. Lower dp than Test 9f

Tests performed in K08028F01

Test No.	Test type[3)]	Imposed perturbation (kPa or L/min)	Measured response (kPa or L/min)	Test start	Test stop	Duration perturb. / recovery (h)	Test aim (dp= change in pressure)
K08028F01 37.00-39.00m.							
12	sCHir	10kPa 100 kPa 300 kPa 450 kPa 600 kPa 800 kPa 1000 kPa 1200 kPa 1500 kPa 1200 kPa 800 kPa 600 kPa 450 kPa 300 kPa 100 kPa 10 kPa	-0,004 L/min -0,03 L/min -0,066 L/min -0,09 L/min -0,1 L/min -0,138 L/min -0,161 L/min -0,19 L/min -0,215 L/min -0,163 L/min -0,108 L/min -0,084 L/min -0,064 L/min -0,052 L/min -0,017 L/min 0,022 L/min	2016-03-23	2016-03-29	0.5/step /4[2)]	Assess dp dependent well loss and effect of higher dp resolution and smaller initial dp. - lower starting dp - denser dp frequency than Test1-11.
13	sCRwr	0,05L/min 0,1 L/min 0,15 L/min 0,2 L/min 0,25 L/min 0,3 L/min	69kPa 157 kPa 260 kPa 377 kPa 520 kPa 692 kPa	2016-03-29	2016-03-30	0.5/step /4[2)]	Assess rate dependent well loss, compare with Test 12.
14	CHwr	-300kPa	0,123 L/min	2016-03-30	2016-03-31	1.5 /4	Assess dp dependent well loss, Test 14-18. Compare with Test 13
15	CHwr	-600 kPa	0,198 L/min	2016-03-31	2016-03-31	1.5 /4	
16	CHwr	-1000 kPa	0,23 L/min	2016-03-31	2016-04-01	1.5 /4	
17	CHwr	-2000 kPa	0,305 L/min	2016-04-01	2016-04-04	1.5 /4	
18	CHwr	-3000 kPa	0,345 L/min	2016-04-04	2016-04-04	1.5 /4	
19	CHir	1000 kPa	-0,184 L/min	2016-04-04	2016-04-05	1.5 /4	Assessing effect of injection and outflow effect with test Test 16.

1) Momentary change after each step

2) Time when all steps are executed

3) CRwr : Constant Rate Withdrawal and Recovery
CHwr : Constant Head Withdrawal and Recovery
CHir : Constant Head Injection and Recovery
sCRwr : step Constant Rate Withdrawal and Recovery
sCHir : step Constant Head Injection and Recovery

Appendix 2 - Test site and equipment

Figure A6-1. *Test platform for K08028F01 in tunnel TAS08.*

Figure A6-2. *Borehole collar K08028F01*

Figure A6-3. *Tunnel TAS08 where K08028F01 was drilled in the tunnel face. Photo from SKB (2013).*

Appendix 3 – Atmospheric pressure and groundwater pressure above/below test sections

For definition of measured sections see Table 3-4.

A3.1 - Atmospheric pressure.

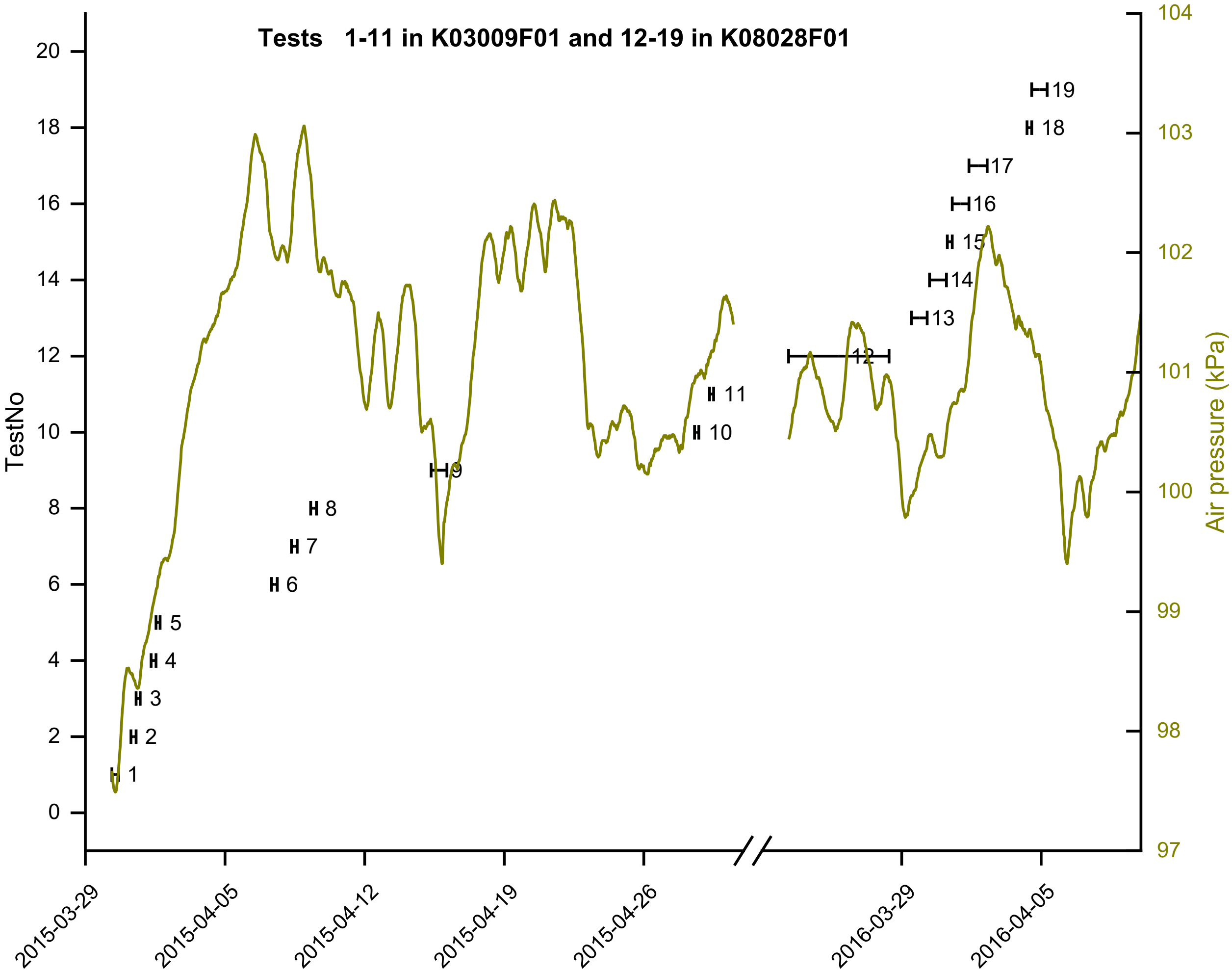

Figure A7-1. *Test with duration in real time and air pressure from meteorological station at Äspö Norra. The fluctuation of air pressure during a test is maximum 0.5kPa and consequently the barometric amplitude is 0.25kPa (tests 9,12,16,17). Whereas the tidal amplitude is about 0.5kPa (e.g. for Test 7).*

A3.2 - K03009F01, groundwater pressure above/below test section

Unfortunatelly pressure data from inner and outer observation sections in K03009F01 during test #9a-11 went missing. This noted in chapter 3.7 Nonconformities.

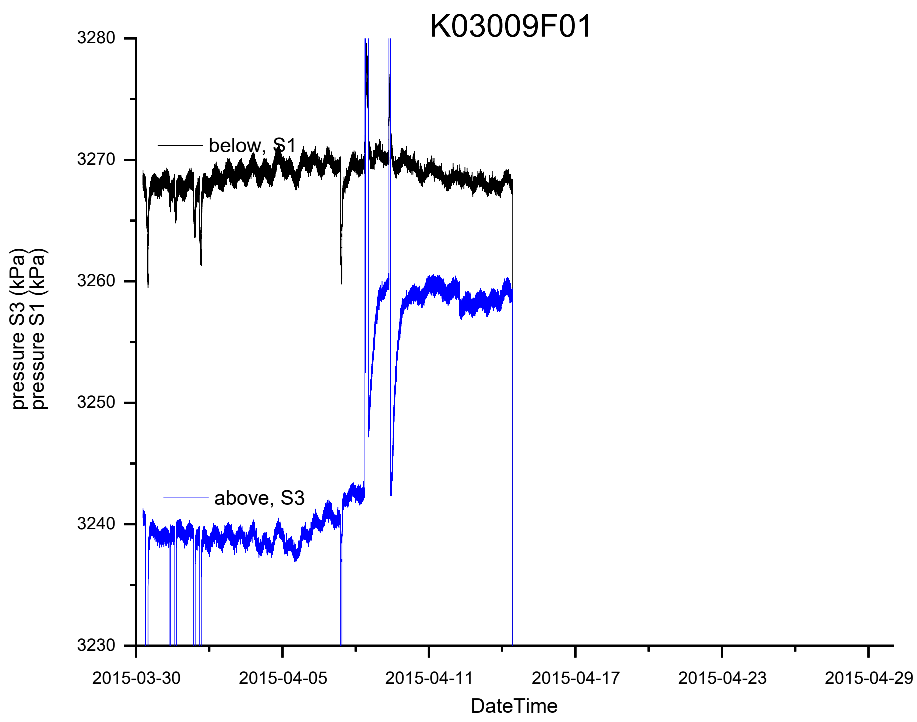

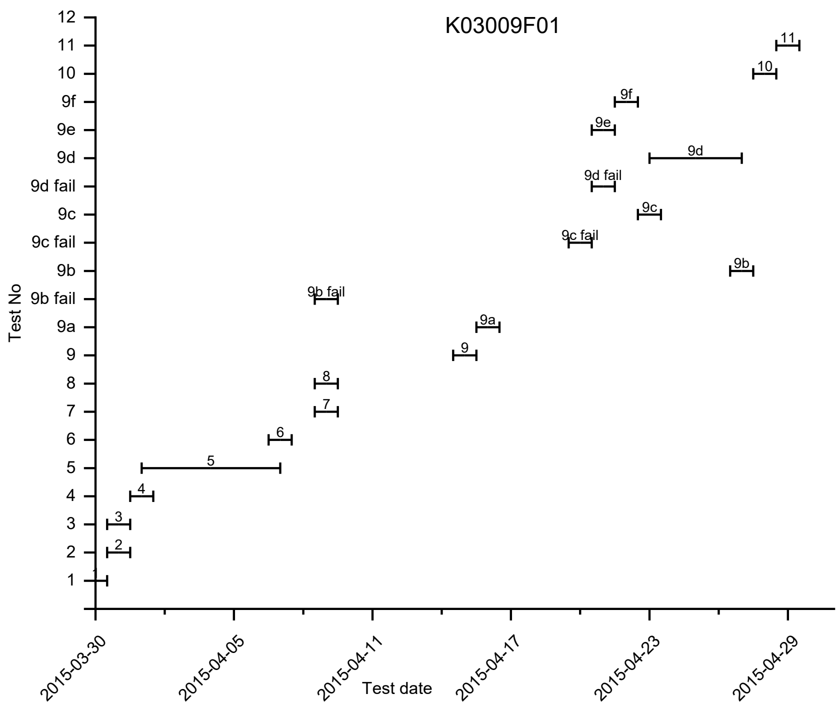

Figure A7-2. *Groundwater pressure in test sections above and below the test section (top) and tests periods (bottom) in borehole K03009F01.*

A3.3 - K08028F01, groundwater pressure above/below test section

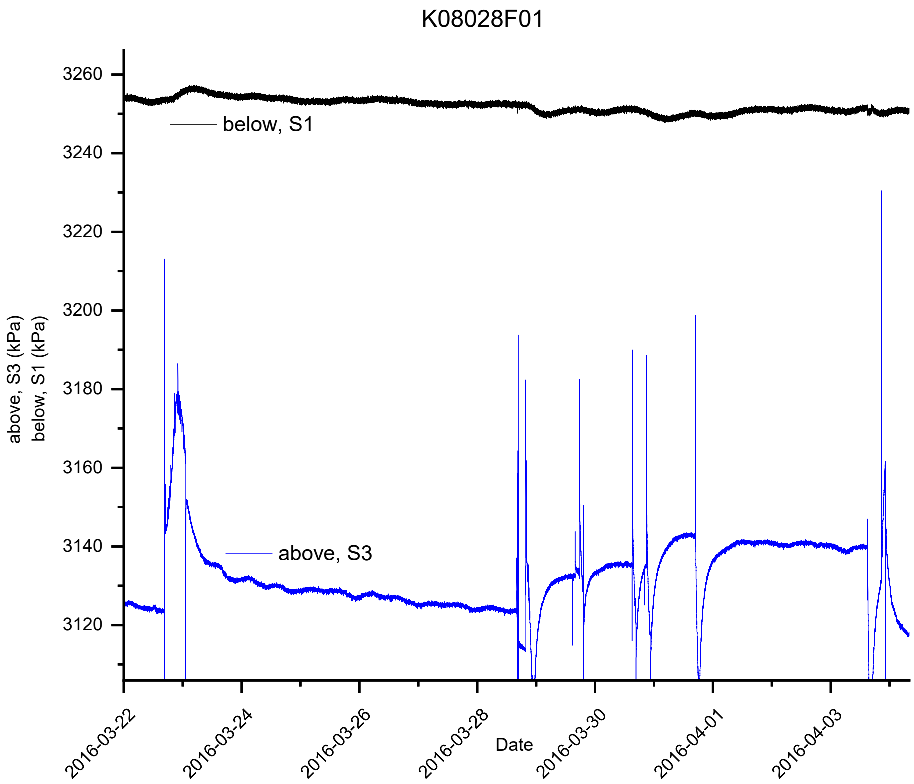

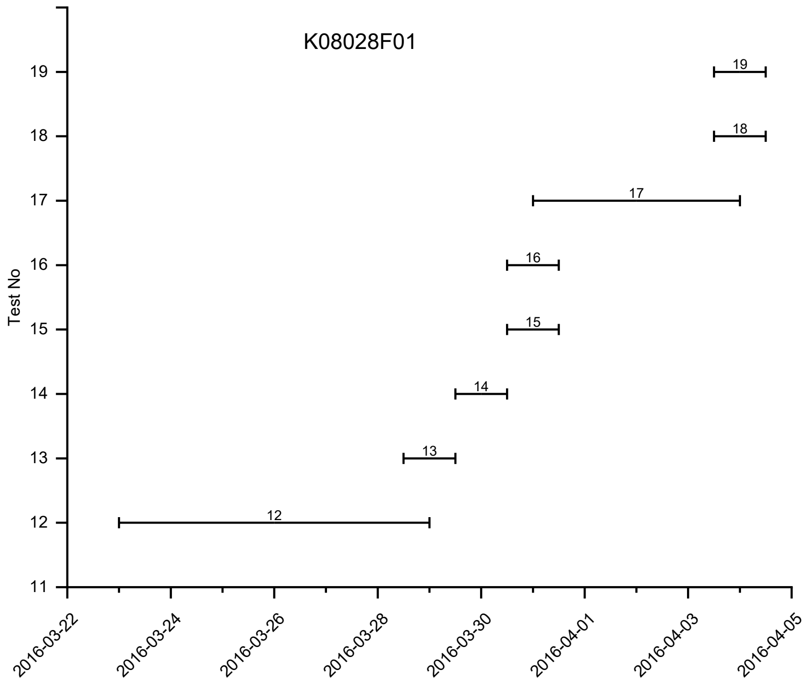

Figure A7-3. *Groundwater pressure in test sections above and below the test section (top) and tests periods (bottom) in borehole K08028F01.*

Appendix 4 - Constant head solution

The constant head tests were also evaluated with the constant head solution of Dougherty & Babu (1984) implemented in Aqtesolv (Hydrosolve, 2007) are summarised in Table A4-1 with log-log plots in chapter A4.2.

A4.1. Summary table and plot

Table A4-1 Calculated transmissivity and skin for the constant head perturbation phases (CHw and CHi), with constant head solution.

				Perturbation phase Constant head solution (Aqtesolv)	
Test No.	**Test Type[1)]**	**Targeted perturbation (kPa)**	**Measured response prior to shut-in (L/min)**	**Transmissivity (m^2/s)**	**Skin factor (-)**
K03009F01 14,20-17,19m.					
2	CHwr	-300	0.12	1,8E-07	11
3	CHwr	-600	0.21	5,1E-07	47
4	CHwr	-1000	0.31	4,6E-07	49
5	CHwr	-2000	0.53	5,5E-07	71
6	CHwr	-3000	0.75	6,4E-07	92
8	CHir	1000	0.52	3,5E-07	18
K03009F01 17,20-20,19m.					
9a	CHwr	-300	1,35	4,6E-06	30
9b	CHwr	-600	2,24	4,5E-06	37
9c	CHwr	-1000	3,46	2,2E-06	16
9d	CHwr	-2000	5,30	1,9E-06	19
9e	CHwr	-3000	6,75	4,9E-06	73
K08028F01 37.00-39.00m.					
14	CHwr	-300	0,12	6.2E-08	-0.6
15	CHwr	-600	0,20	6,7E-08	1
16	CHwr	-1000	0,23	7,3E-08	5
17	CHwr	-2000	0,30	4,0E-08	6
18	CHwr	-3000	0,35	2.9E-08	4
19	CHir	1000	-0,18	3.5E-08	1

1) CRwr : Constant Rate Withdrawal and Recovery
CHwr : Constant Head Withdrawal and Recovery
CHir : Constant Head Injection and Recovery
sCRwr : step Constant Rate Withdrawal and Recovery
sCHir : step Constant Head Injection and Recovery

A4.2. Log-log diagnostic plots for constant head solution

Test No. 2 K03009F01, 14.20-17.19m CHw-phase -300kPa.

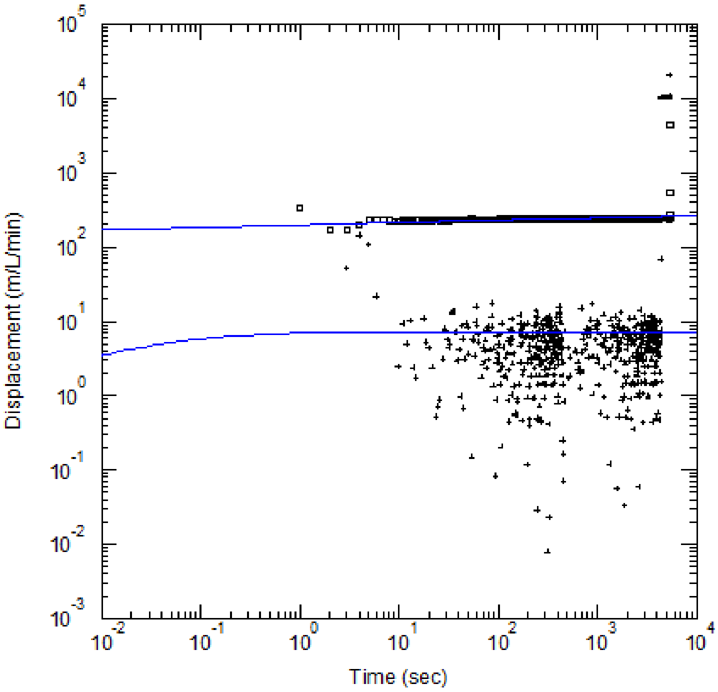

WELL TEST ANALYSIS

Data Set: D:\...\Test2 Dd.aqt
Date: 07/09/25 Time: 12:51:18

PROJECT INFORMATION

Company: SKB
Client: Test No. 2
Project: Test type: CHr -300kPa
Location: Äspö HRL
Test Well: K03009F01, 14.20-17.19m

AQUIFER DATA

Saturated Thickness: 1000. m

WELL DATA

Pumping Wells

Well Name	X (m)	Y (m)
K03009F01, 14.20-17.19m	0	0

Observation Wells

Well Name	X (m)	Y (m)
▫ K03009F01, 14.20-17.19m	0	0

SOLUTION

Aquifer Model: Confined
Solution Method: Dougherty-Babu

T = 1.819E-7 m^2/sec
Kz/Kr = 1.
r(w) = 0.038 m
C = 0. sec^2/m^5

S = 2.74E-6
Sw = 11.22
r(c) = 0.038 m
P = 2.

Test No. 3 K03009F01, 14.20-17.19m CHw-phase -600kPa

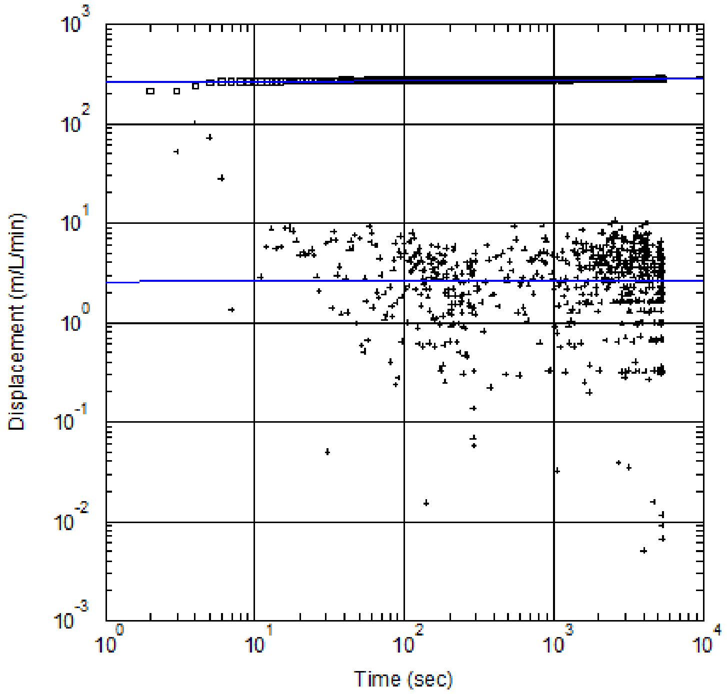

WELL TEST ANALYSIS	
Data Set: D:\...\Test3 Dd.aqt	
Date: 07/09/25	Time: 12:59:53

PROJECT INFORMATION

Company: SKB
Client: Test No. 3
Project: Test type: CHw -600kPa
Location: Äspö
Test Well: K03009F01, 14.20-17.19m

AQUIFER DATA

Saturated Thickness: 1000. m

WELL DATA

Pumping Wells

Well Name	X (m)	Y (m)
K03009F01	0	0

Observation Wells

Well Name	X (m)	Y (m)
▫ K03009F01	0	0

SOLUTION

Aquifer Model: Confined
Solution Method: Dougherty-Babu

T = 5.078E-7 m^2/sec
Kz/Kr = 1.
r(w) = 0.038 m
C = 0. sec^2/m^5
S = 2.74E-6
Sw = 46.64
r(c) = 0.038 m
P = 2.

Test No. 4 K03009F01, 14.20-17.19m CHw-phase -1000kPa

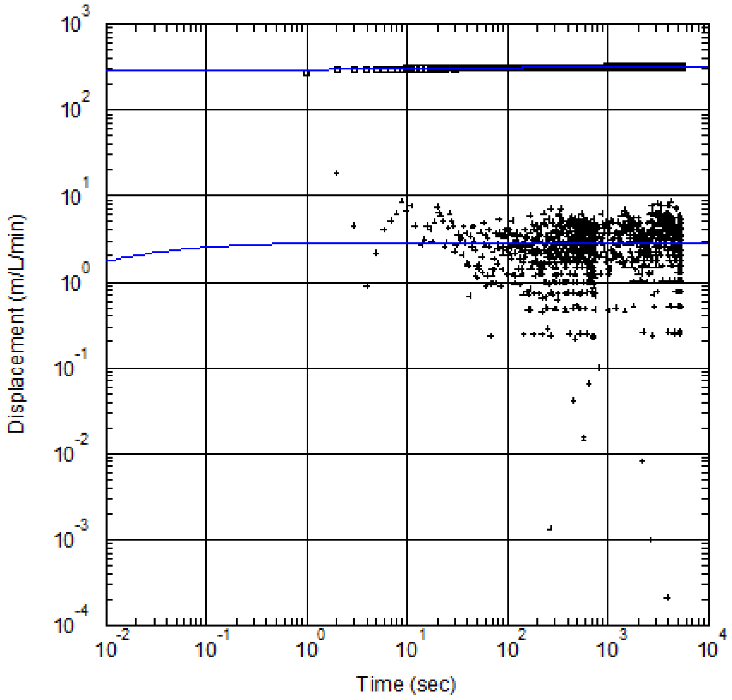

WELL TEST ANALYSIS

Data Set: D:\...\Test 4 Dd 201227.aqt
Date: 07/09/25 Time: 13:55:35

PROJECT INFORMATION

Company: SKB
Client: Test No.4
Project: CHw -1000kPa
Location: Äspö
Test Well: K03009F01,14.20-17.19m

AQUIFER DATA

Saturated Thickness: 1000. m

WELL DATA

Pumping Wells

Well Name	X (m)	Y (m)
K03009F01, 14.20-17.19m	0	0

Observation Wells

Well Name	X (m)	Y (m)
K03009F01, 14.20-17.19m	0	0

SOLUTION

Aquifer Model: Confined
Solution Method: Dougherty-Babu

T = 4.638E-7 m^2/sec
Kz/Kr = 1.
r(w) = 0.038 m
C = 0. sec^2/m^5

S = 2.74E-6
Sw = 48.99
r(c) = 0.038 m
P = 2.

Test No. 5 K03009F01, 14.20-17.19m CHw-phase -2000kPa

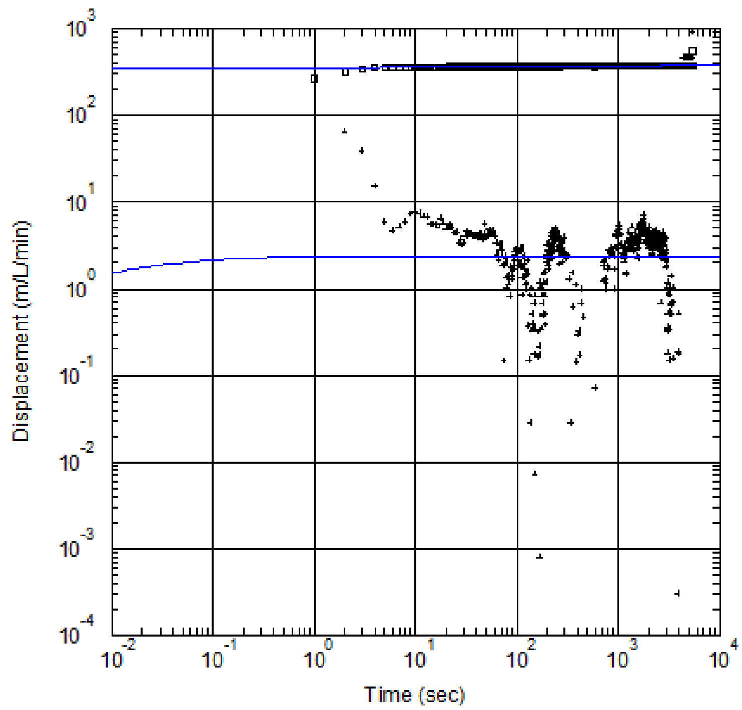

WELL TEST ANALYSIS	
Data Set: D:\...\Test 5 Dd 201227.aqt	
Date: 07/09/25	Time: 14:02:53

PROJECT INFORMATION

Company: SKB
Client: Test No. 5
Project: CHw -2000kPa
Location: Äspö
Test Well: K03009F01, 14.20-17.19m

AQUIFER DATA

Saturated Thickness: 1000. m

WELL DATA

Pumping Wells

Well Name	X (m)	Y (m)
New Well	0	0

Observation Wells

Well Name	X (m)	Y (m)
▫ New Well	0	0

SOLUTION

Aquifer Model: Confined

Solution Method: Dougherty-Babu

T = 5.545E-7 m^2/sec
Kz/Kr = 1.
r(w) = 0.038 m
C = 0. sec^2/m^5

S = 2.74E-6
Sw = 71.24
r(c) = 0.038 m
P = 2.

Test No. 6 K03009F01, 14.20-17.19m CHw-phase -3000kPa

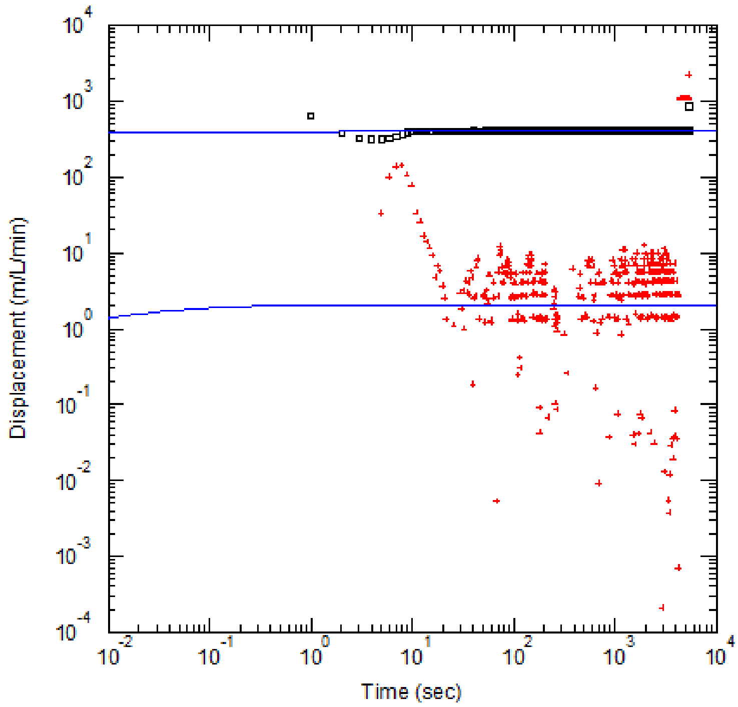

WELL TEST ANALYSIS

Data Set: D:\...\K03009F01 Test6.aqt
Date: 07/09/25 Time: 14:24:37

PROJECT INFORMATION

Company: SKB
Client: Test No.6
Project: Test Type: CHw -3000kPa
Location: Äspö
Test Well: K03009F01 14.20-17.19m

AQUIFER DATA

Saturated Thickness: 1000. m

WELL DATA

Pumping Wells

Well Name	X (m)	Y (m)
K03009F01 Test 6	0	0

Observation Wells

Well Name	X (m)	Y (m)
▫ K03009F01 Test 6	0	0

SOLUTION

Aquifer Model: Confined

Solution Method: Dougherty-Babu

T = 6.353E-7 m^2/sec

Kz/Kr = 1.

r(w) = 0.038 m

C = 0. sec^2/m^5

S = 2.74E-6

Sw = 91.72

r(c) = 0.038 m

P = 2.

Test No. 8 K03009F01, 14.20-17.19m CHi-phase 1000kPa

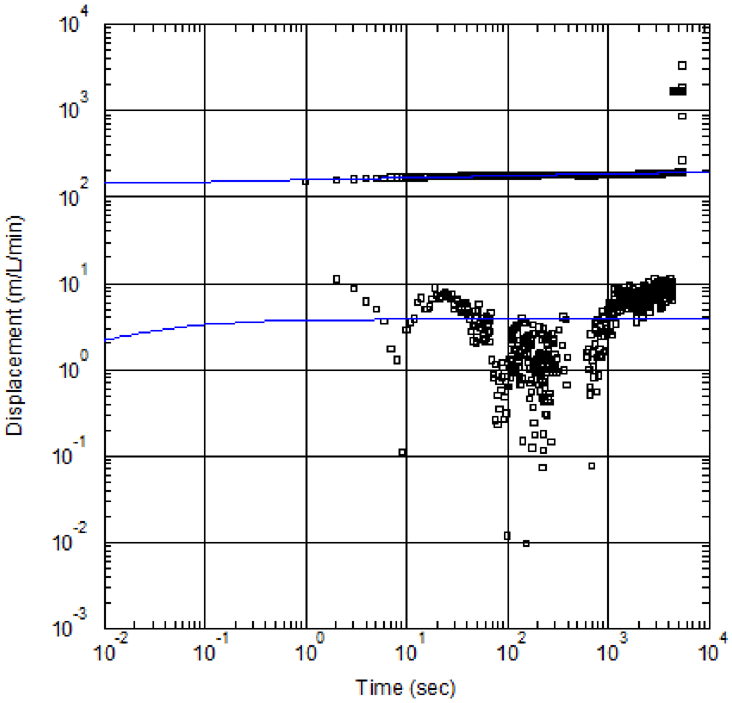

WELL TEST ANALYSIS

Data Set: D:\...\8 Dd aqt 201227.aqt
Date: 07/09/25 Time: 14:23:00

PROJECT INFORMATION

Company: SKB
Client: Test No. 8
Project: CHi 1000kPa
Location: Äspö
Test Well: K03009F01, 14.20-17.19m

AQUIFER DATA

Saturated Thickness: 1000. m

WELL DATA

Pumping Wells

Well Name	X (m)	Y (m)
New Well	0	0

Observation Wells

Well Name	X (m)	Y (m)
▫ New Well	0	0

SOLUTION

Aquifer Model: Confined

Solution Method: Dougherty-Babu

T = 3.484E-7 m^2/sec
Kz/Kr = 1.
r(w) = 0.038 m
C = 0. sec^2/m^5

S = 2.74E-6
Sw = 18.07
r(c) = 0.038 m
P = 2.

Test No. 9a K03009F01, 17.20-20.19m CHw-phase -300kPa

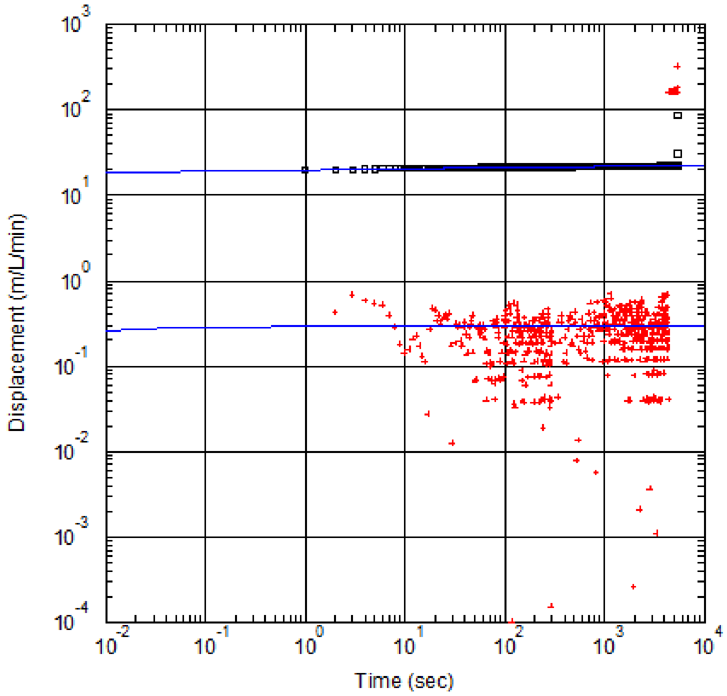

WELL TEST ANALYSIS

Data Set: D:\...\9a Dd CHw.aqt
Date: 07/09/25 Time: 14:31:00

PROJECT INFORMATION

Company: SKB
Client: Test No.9a
Project: Test type: CHw -300kPa
Location: Äspö
Test Well: K03009F01 17.20-20.19m

AQUIFER DATA

Saturated Thickness: 1000. m

WELL DATA

Pumping Wells

Well Name	X (m)	Y (m)
New Well	0	0

Observation Wells

Well Name	X (m)	Y (m)
New Well	0	0

SOLUTION

Aquifer Model: Confined

Solution Method: Dougherty-Babu

T = 4.556E-6 m^2/sec
Kz/Kr = 1.
r(w) = 0.038 m
C = 0. sec^2/m^5

S = 2.74E-6
Sw = 29.91
r(c) = 0.038 m
P = 2.

Test No. 9b K03009F01, 17.20-20.19m CHw-phase -600kPa

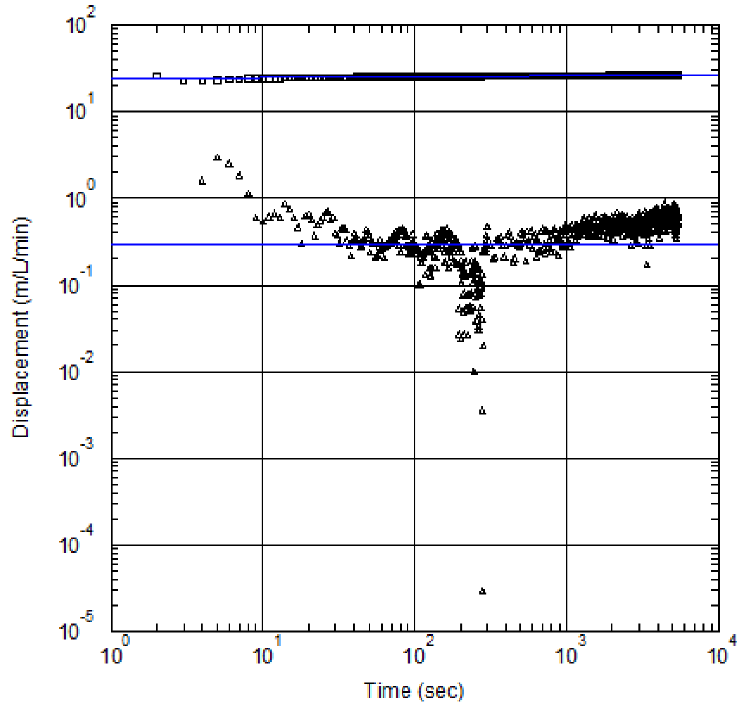

WELL TEST ANALYSIS

Data Set: D:\...\9b Dd CHw.aqt
Date: 07/09/25 Time: 16:24:03

PROJECT INFORMATION

Company: SKB
Client: Test 9b.
Project: CHw -600kPa
Location: Äspö
Test Well: K03009F01, 17.20-20.19m

AQUIFER DATA

Saturated Thickness: 1000. m

WELL DATA

Pumping Wells

Well Name	X (m)	Y (m)
New Well	0	0

Observation Wells

Well Name	X (m)	Y (m)
□ New Well	0	0

SOLUTION

Aquifer Model: Confined

Solution Method: Dougherty-Babu

T = 4.478E-6 m^2/sec
Kz/Kr = 1.
r(w) = 0.038 m
C = 0. sec^2/m^5

S = 2.74E-6
Sw = 36.7
r(c) = 0.038 m
P = 2.

Test No. 9c K03009F01, 17.20-20.19m CHw-phase -1000kPa

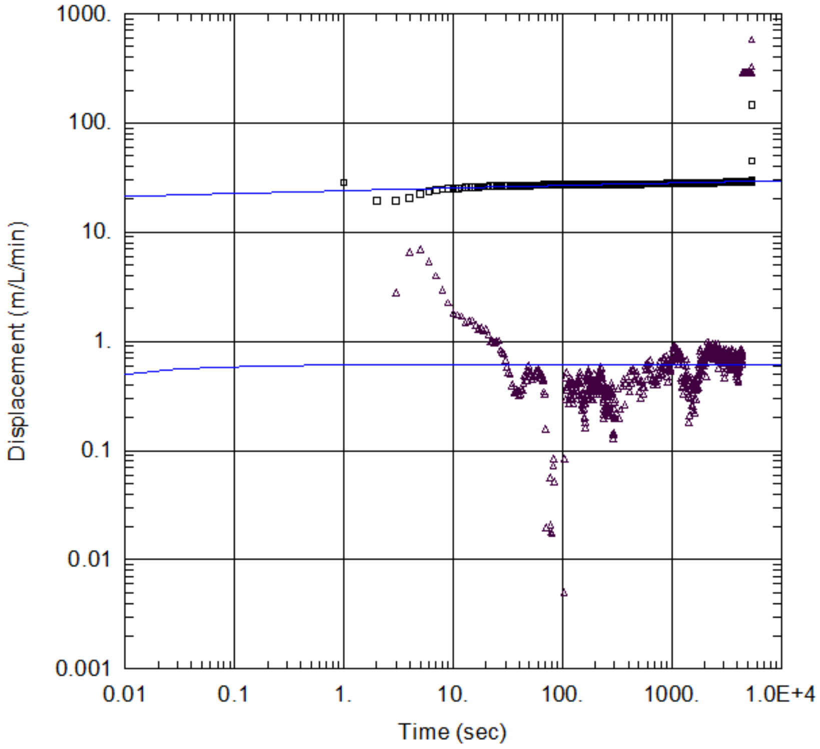

WELL TEST ANALYSIS

Data Set: D:\..\9c Dd CHw.aqt
Date: 07/10/25 Time: 09:45:51

PROJECT INFORMATION

Company: SKB
Client: Test 9c
Project: Test type: CHw -1000kPa
Location: Äspö
Test Well: K03009F01, 17.20-20.19m

AQUIFER DATA

Saturated Thickness: 1000. m

WELL DATA

Pumping Wells

Well Name	X (m)	Y (m)
New Well	0	0

Observation Wells

Well Name	X (m)	Y (m)
▫ New Well	0	0

SOLUTION

Aquifer Model: Confined

Solution Method: Dougherty-Babu

$T = 2.181E\text{-}6\ m^2/sec$
$Kz/Kr = 1.$
$r(w) = 0.038\ m$
$C = 0.\ sec^2/m^5$

$S = 2.74E\text{-}6$
$Sw = 16.09$
$r(c) = 0.038\ m$
$P = 2.$

Test No. 9d K03009F01, 17.20-20.19m CHw-phase -2000kPa

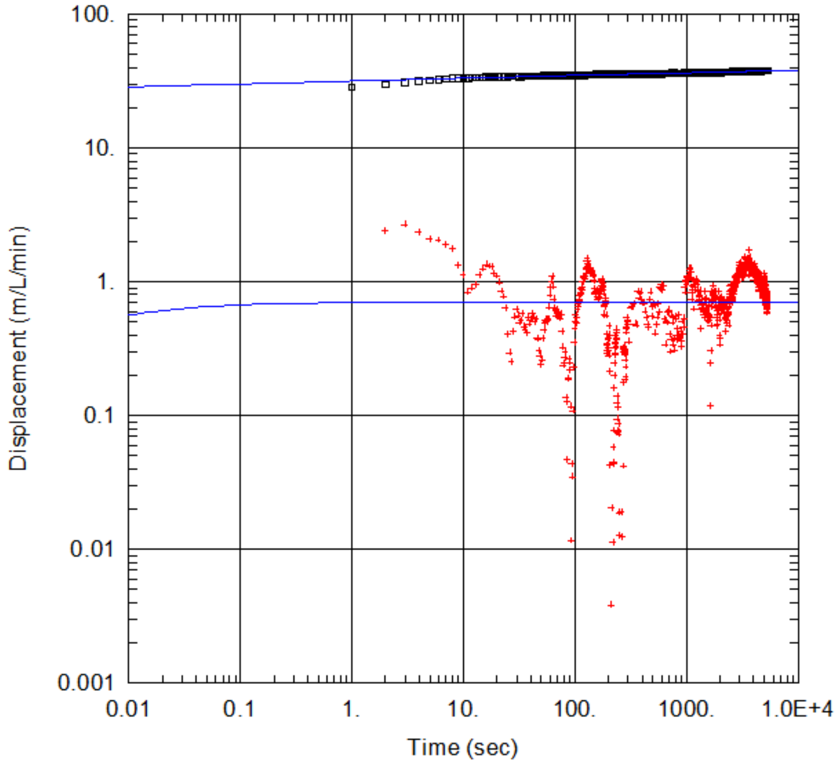

WELL TEST ANALYSIS

Data Set: D:\..\9d Dd CHw.aqt
Date: 07/10/25 Time: 09:51:02

PROJECT INFORMATION

Company: SKB
Client: Test No. 9d
Project: Test type: CHw -2000kPa
Location: Äspö
Test Well: K03009F01, 17.20-20.19m

AQUIFER DATA

Saturated Thickness: 1000. m

WELL DATA

Pumping Wells

Well Name	X (m)	Y (m)
New Well	0	0

Observation Wells

Well Name	X (m)	Y (m)
▫ New Well	0	0

SOLUTION

Aquifer Model: Confined

Solution Method: Dougherty-Babu

T = 1.887E-6 m^2/sec
Kz/Kr = 1.
r(w) = 0.038 m
C = 0. sec^2/m^5

S = 2.74E-6
Sw = 18.98
r(c) = 0.038 m
P = 2.

Test No. 9e K03009F01, 17.20-20.19m CHw-phase -3000kPa

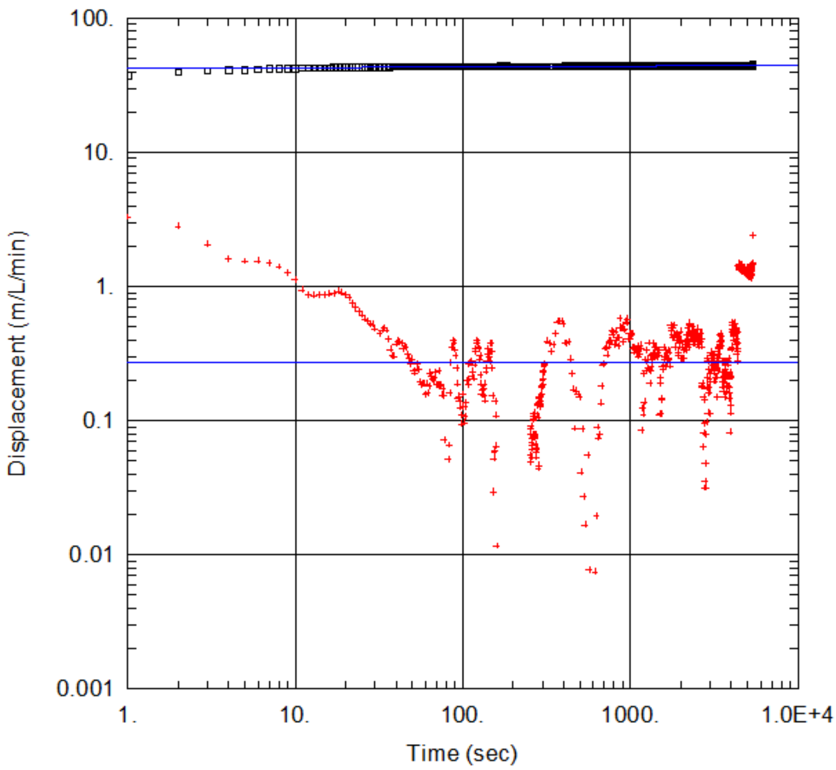

WELL TEST ANALYSIS

Data Set: D:\...\9e Dd CHw.aqt
Date: 07/10/25 Time: 09:56:04

PROJECT INFORMATION

Company: SKB
Client: Test No. 9e
Project: Test tyoe: CHw -3000kPa
Location: Äspö
Test Well: K03009F01, 17.20-20.19m

AQUIFER DATA

Saturated Thickness: 1000. m

WELL DATA

Pumping Wells

Well Name	X (m)	Y (m)
New Well	0	0

Observation Wells

Well Name	X (m)	Y (m)
□ New Well	0	0

SOLUTION

Aquifer Model: Confined

Solution Method: Dougherty-Babu

T = 4.835E-6 m^2/sec
Kz/Kr = 1.
r(w) = 0.038 m
C = 0. sec^2/m^5

S = 2.74E-6
Sw = 72.77
r(c) = 0.038 m
P = 2.

Test No. 14 K083028F01, 37.00-39.00m CHw-phase -300kPa

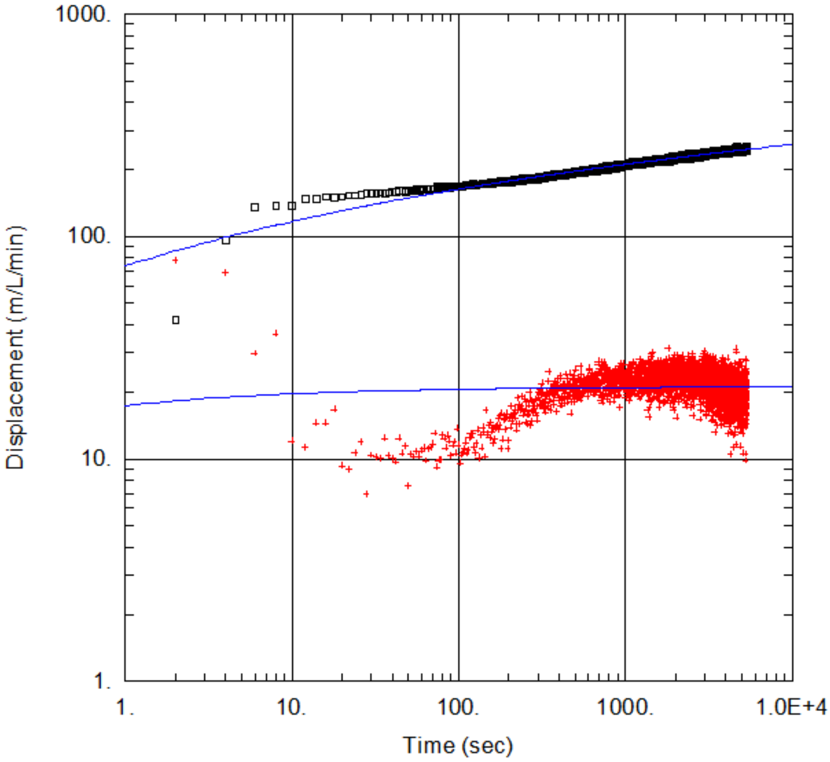

WELL TEST ANALYSIS

Data Set: D:\...\Test 14 Chwr withdrawal phase dt & Q.aqt
Date: 07/10/25 Time: 10:05:16

PROJECT INFORMATION

Company: SKB
Client: Test No. 14
Project: Test type: CHw - 300kPa
Location: Äspö
Test Well: K08028F01, 37-39m

AQUIFER DATA

Saturated Thickness: 1000. m

WELL DATA

Pumping Wells

Well Name	X (m)	Y (m)
K08028F01, 37-39m	0	0

Observation Wells

Well Name	X (m)	Y (m)
□ K08028F01, 37-39m	0	0

SOLUTION

Aquifer Model: Confined

Solution Method: Dougherty-Babu

T = 6.195E-8 m^2/sec
Kz/Kr = 1.
r(w) = 0.038 m
C = 0. sec^2/m^5

S = 2.023E-6
Sw = -0.5576
r(c) = 0.038 m
P = 2.

Test No. 15 K083028F01, 37.00-39.00 CHw-phase -600kPa

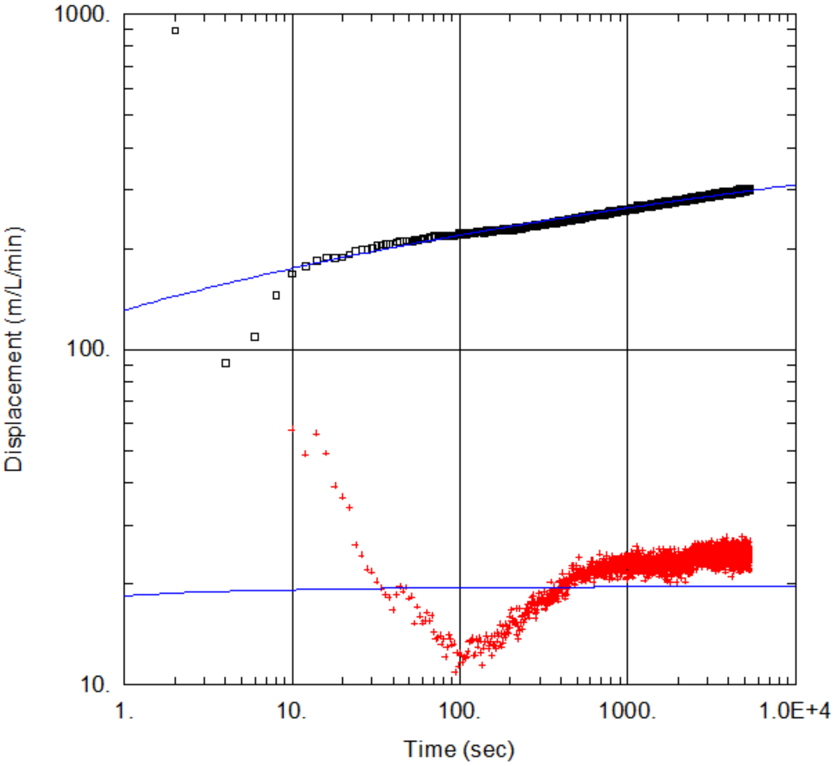

WELL TEST ANALYSIS

Data Set: D:\..\Test 15 Chwr withdrawal phase dt & Q.aqt
Date: 07/10/25 Time: 10:07:14

PROJECT INFORMATION

Company: SKB
Client: Test No. 15
Project: CHw -600kPa
Location: Äspö
Test Well: K08028F01, 37-39m

AQUIFER DATA

Saturated Thickness: 1000. m

WELL DATA

Pumping Wells

Well Name	X (m)	Y (m)
K08028F01, 37-39m	0	0

Observation Wells

Well Name	X (m)	Y (m)
▫ K08028F01, 37-39m	0	0

SOLUTION

Aquifer Model: Confined

Solution Method: Dougherty-Babu

T = 6.686E-8 m^2/sec
Kz/Kr = 1.
r(w) = 0.038 m
C = 0. sec^2/m^5

S = 1.496E-6
Sw = 1.013
r(c) = 0.038 m
P = 2.

Test No. 16 K083028F01, 37.00-39.00m CHw-phase -1000kPa

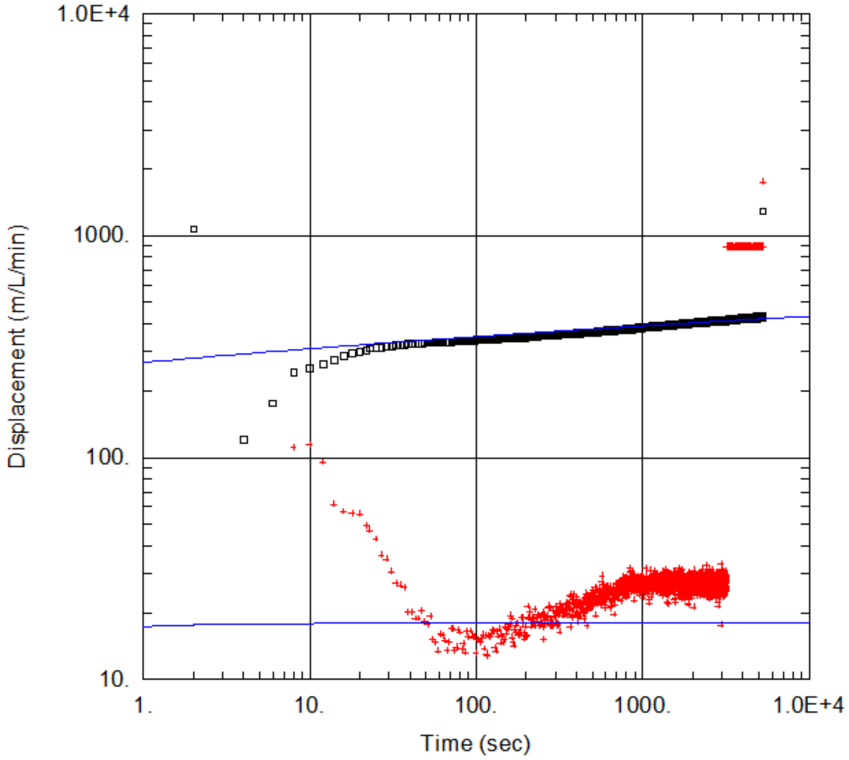

WELL TEST ANALYSIS

Data Set: D:\..\Test 16 Chwr withdrawal phase dt & Q.dat.aqt
Date: 07/10/25 Time: 10:14:52

PROJECT INFORMATION

Company: SKB
Client: Test No. 16
Project: Tests type: CHw 1000kPa
Location: Äspö
Test Well: K08028F01, 37.00-39.00m

AQUIFER DATA

Saturated Thickness: 1000. m

WELL DATA

Pumping Wells

Well Name	X (m)	Y (m)
New Well	0	0

Observation Wells

Well Name	X (m)	Y (m)
□ New Well	0	0

SOLUTION

Aquifer Model: Confined

Solution Method: Dougherty-Babu

T = 7.34E-8 m^2/sec
Kz/Kr = 1.
r(w) = 0.038 m
C = 0. sec^2/m^5

S = 1.019E-6
Sw = 5.
r(c) = 0.038 m
P = 2.

Test No. 17 K083028F01, 37.00-39.00m CHw-phase -2000kPa

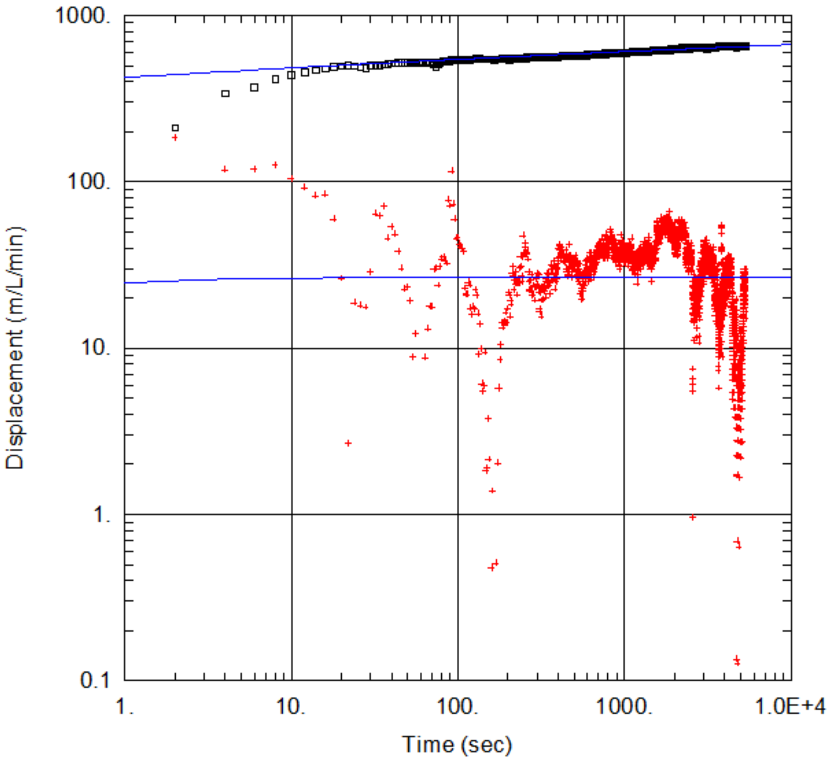

WELL TEST ANALYSIS

Data Set: D:\..\Test 17 Chwr withdrawal phase dt & Q.aqt
Date: 07/10/25 Time: 10:18:24

PROJECT INFORMATION

Company: SKB
Client: Test No. 17
Project: Test type: CHw -2000kPa
Location: Äspö
Test Well: K08028F01, 37-39m

AQUIFER DATA

Saturated Thickness: 1000. m

WELL DATA

Pumping Wells

Well Name	X (m)	Y (m)
K08028F01, 37-39m	0	0

Observation Wells

Well Name	X (m)	Y (m)
□ K08028F01, 37-39m	0	0

SOLUTION

Aquifer Model: Confined

Solution Method: Dougherty-Babu

T = 4.956E-8 m^2/sec
Kz/Kr = 1.
r(w) = 0.038 m
C = 0. sec^2/m^5

S = 2.0E-6
Sw = 6.
r(c) = 0.038 m
P = 2.

Test No. 18 K083028F01, 37.00-39.00m CHw-phase -3000kPa

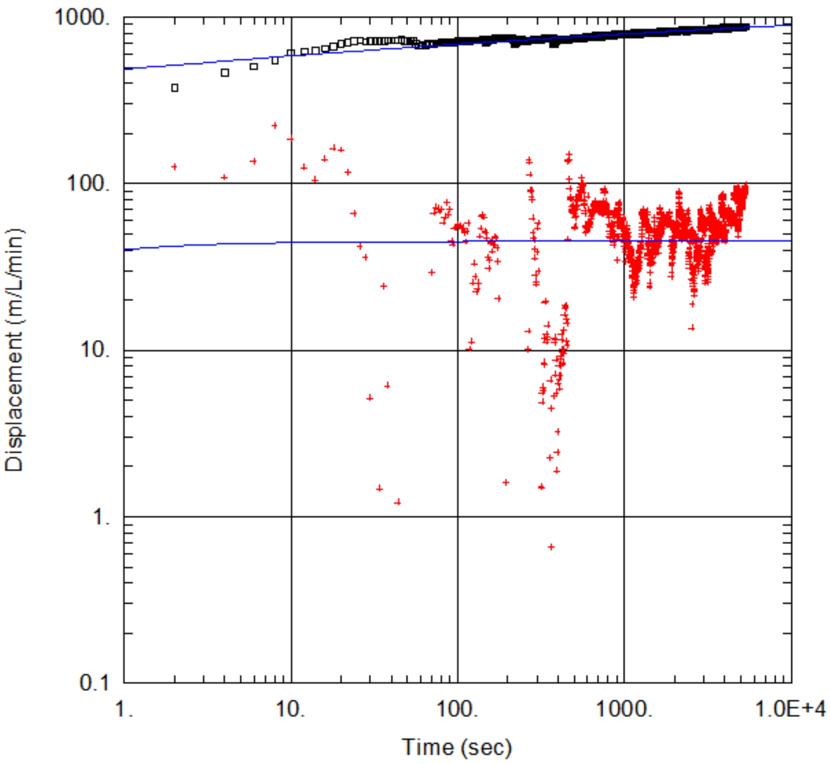

WELL TEST ANALYSIS

Data Set: D:\..\Test 18 Chwr withdrawal phase dt & Q.aqt
Date: 07/10/25 Time: 10:21:05

PROJECT INFORMATION

Company: SKB
Client: Test No. 18
Project: Test type: CHw -3000kPa
Location: Äspö
Test Well: K08028F01, 37-39m

AQUIFER DATA

Saturated Thickness: 1000. m

WELL DATA

Pumping Wells

Well Name	X (m)	Y (m)
K08028F01, 37-39m	0	0

Observation Wells

Well Name	X (m)	Y (m)
□ K08028F01, 37-39m	0	0

SOLUTION

Aquifer Model: Confined

Solution Method: Dougherty-Babu

T = 2.92E-8 m^2/sec
Kz/Kr = 1.
r(w) = 0.038 m
C = 0. sec^2/m^5

S = 2.0E-6
Sw = 3.64
r(c) = 0.038 m
P = 2.

Test No. 19 K083028F01, 37.00-39.00m CHi-phase 1000kPa

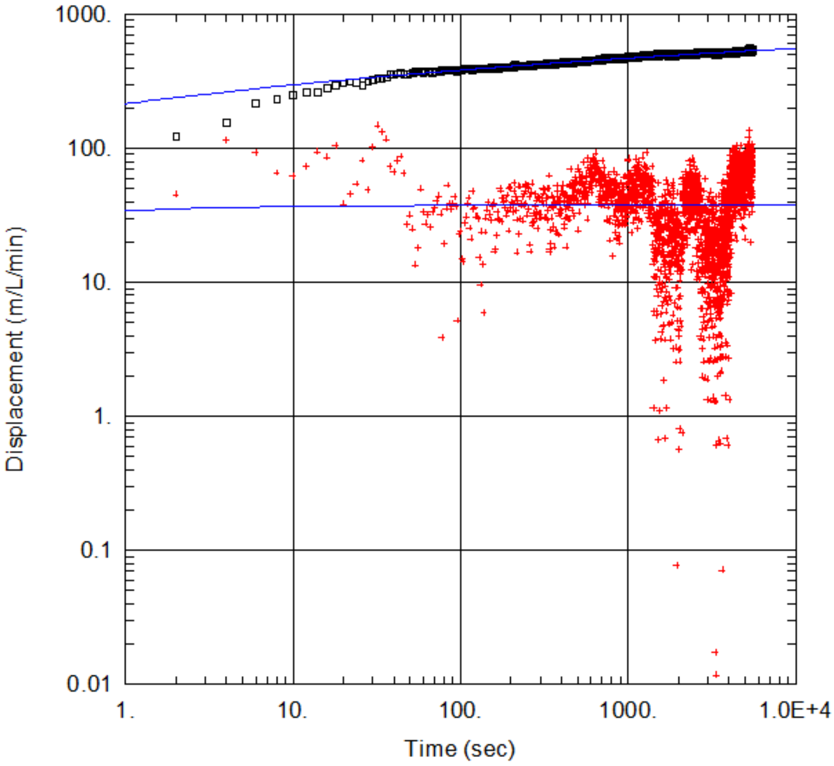

WELL TEST ANALYSIS
Data Set: D:\...\Test 19 Chir injection phase dt & Q.aqt
Date: 07/10/25 Time: 10:23:07

PROJECT INFORMATION

Company: SKB
Client: Test No.19
Project: Test type: CHi 1000kPa
Location: Äspö
Test Well: K08028F01, 37-39m

AQUIFER DATA

Saturated Thickness: 1000. m

WELL DATA

Pumping Wells

Well Name	X (m)	Y (m)
K08028F01, 37-39m	0	0

Observation Wells

Well Name	X (m)	Y (m)
▫ K08028F01, 37-39m	0	0

SOLUTION

Aquifer Model: Confined

Solution Method: Dougherty-Babu

T = 3.447E-8 m^2/sec
Kz/Kr = 1.
r(w) = 0.038 m
C = 0. sec^2/m^5

S = 2.305E-6
Sw = 1.011
r(c) = 0.038 m
P = 2.

Appendix 5 - Rorabaugh analysis

Results of Rorabaugh analysis for the step constant rate withdrawal and recovery tests (sCRwr) number 1,9,10 and 13, each comprising the following plots:

- Rorabaugh B-plot
- Rorabaugh linear best fit plot
- Well efficiency plot, linear and non-linear components
- Measured and simulated step drawdown plot
- Measured and simulated total drawdown

Test 1 sCRwr K03009F01, 14.20-17.19m

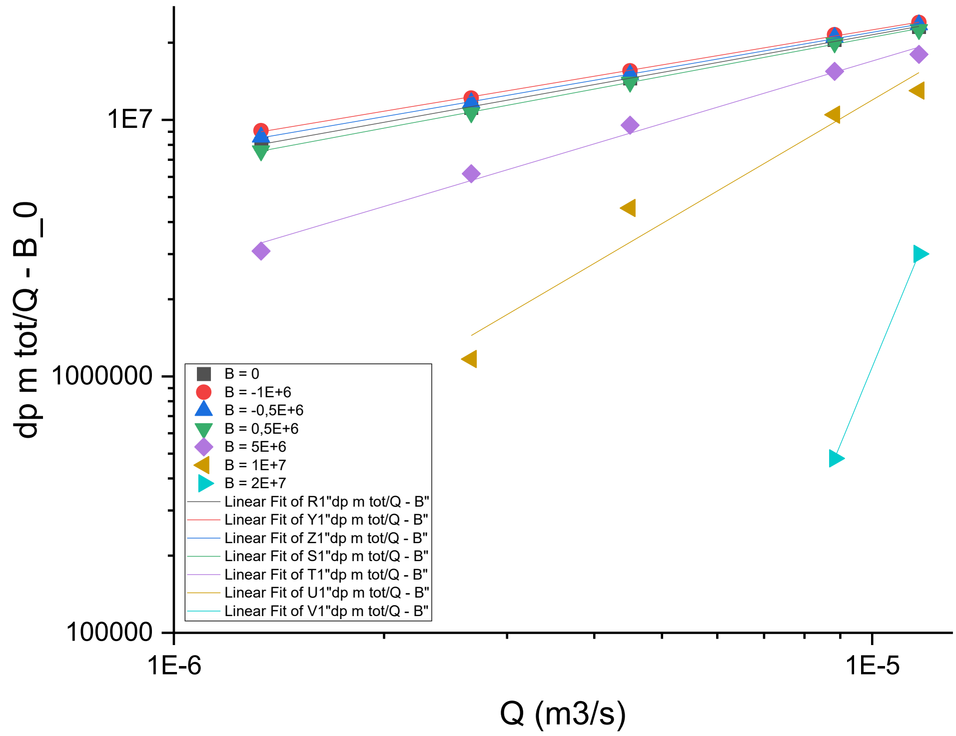

Equation	y = a + b*x						
Plot	dp m tot/Q - B_0	dp m tot/Q - B_-1	dp m tot/Q - B_-0.5	dp m tot/Q - B_0.5	dp m tot/Q - B_5	dp m tot/Q - B_1	dp m tot/Q - B_
Weight	No Weighting						
Intercept	9,77282 ± 0,03142	9,62158 ± 0,03652	9,69398 ± 0,03361	9,85902 ± 0,03089	11,28497 ± 0,23761	15,07758 ± 1,3213	39,04291 ± --
Slope	0,48812 ± 0,00585	0,45406 ± 0,0068	0,47043 ± 0,00626	0,50732 ± 0,00575	0,81104 ± 0,04427	1,59998 ± 0,2525	6,60144 ± --
Residual Sum of Squares	6,03631E-5	8,15484E-5	6,90865E-5	5,83351E-5	0,00345	0,03202	6,70532E-29
Pearson's r	0,99978	0,99966	0,99973	0,99981	0,99556	0,97599	1
R-Square (COD)	0,99957	0,99933	0,99947	0,99961	0,99114	0,95255	1
Adj. R-Square	0,99942	0,9991	0,99929	0,99949	0,98819	0,92883	--

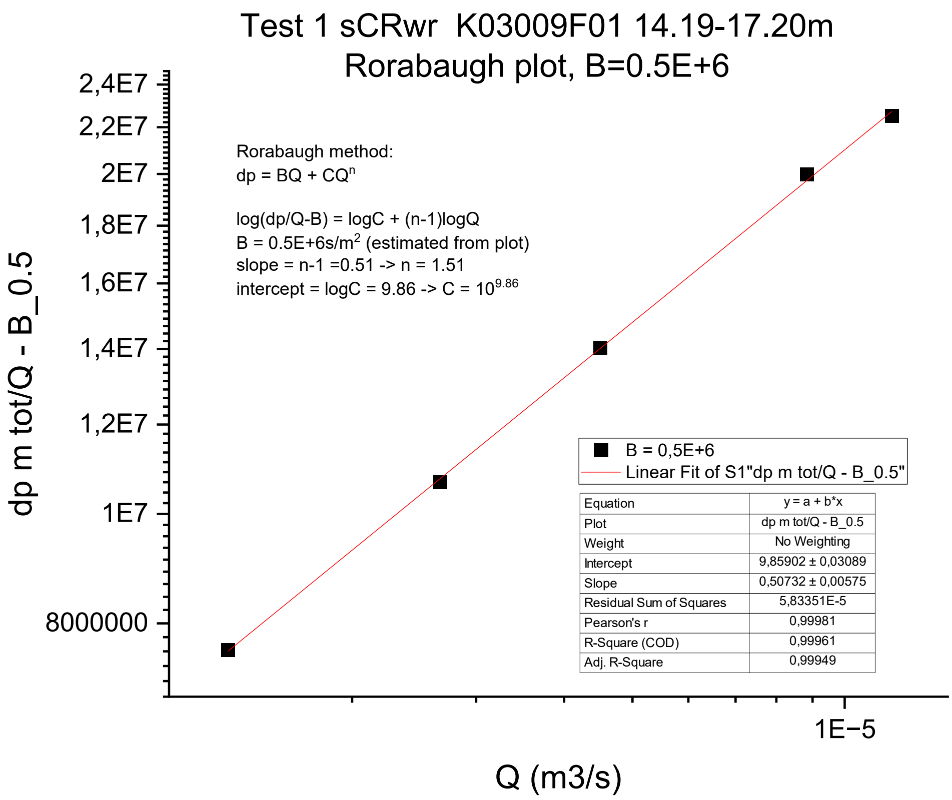
Test 1 sCRwr K03009F01 14.19-17.20m
Rorabaugh plot, B=0.5E+6
Rorabaugh method:
dp = BQ + CQ^n
log(dp/Q-B) = logC + (n-1)logQ
B = 0.5E+6s/m^2 (estimated from plot)
slope = n-1 =0.51 -> n = 1.51
intercept = logC = 9.86 -> C = 10^9.86
B = 0,5E+6
Linear Fit of S1"dp m tot/Q - B_0.5"
Equation y = a + b*x
Plot dp m tot/Q - B_0.5
Weight No Weighting
Intercept 9,85902 ± 0,03089
Slope 0,50732 ± 0,00575
Residual Sum of Squares 5,83351E-5
Pearson's r 0,99981
R-Square (COD) 0,99961
Adj. R-Square 0,99949
dp m tot/Q - B_0.5
2,4E7
2,2E7
2E7
1,8E7
1,6E7
1,4E7
1,2E7
1E7
8000000
1E−5
Q (m3/s)

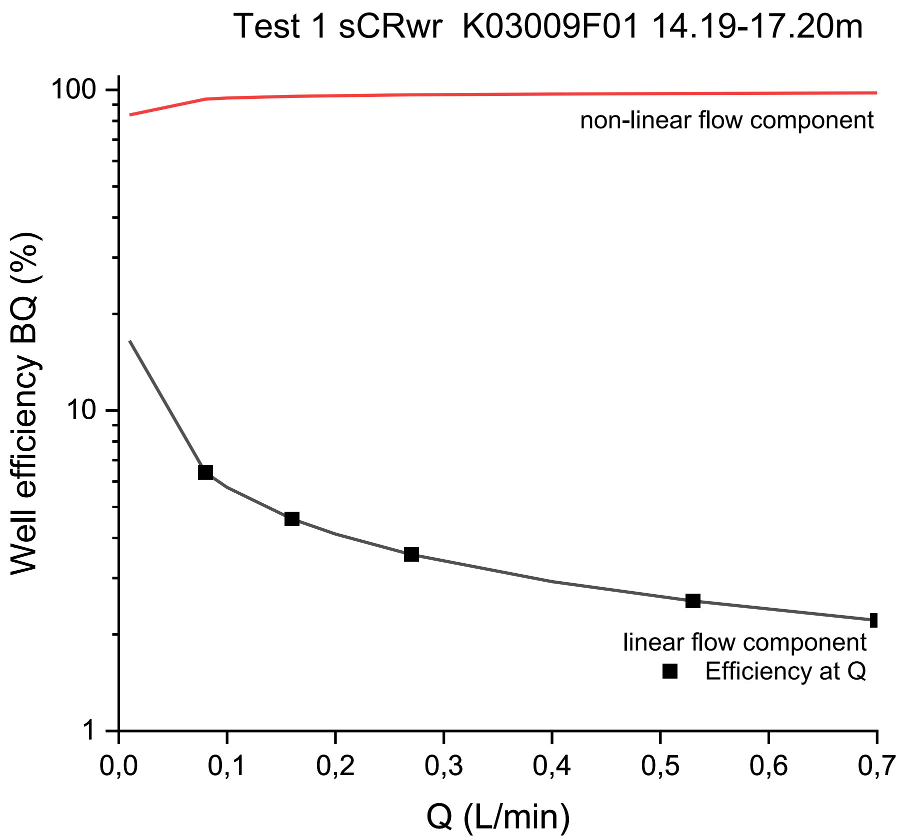
Test 1 sCRwr K03009F01 14.19-17.20m
non-linear flow component
linear flow component
Efficiency at Q
Well efficiency BQ (%)
100
10
1
0,0
0,1
0,2
0,3
0,4
0,5
0,6
0,7
Q (L/min)

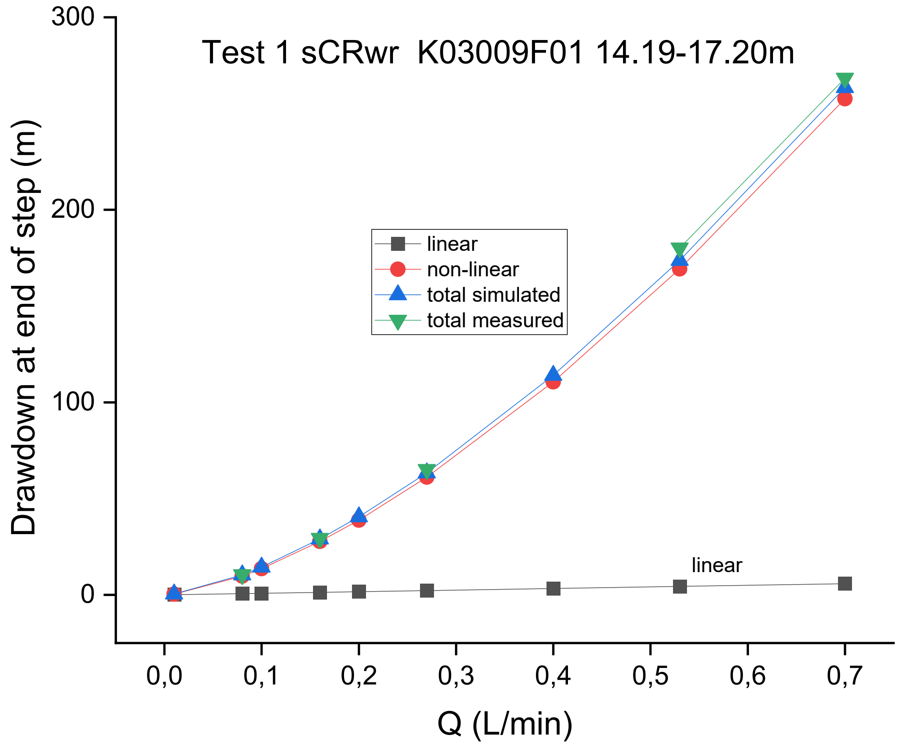
Test 1 sCRwr K03009F01 14.19-17.20m
Drawdown at end of step (m)
Q (L/min)
linear
non-linear
total simulated
total measured
linear
300
200
100
0
0,0
0,1
0,2
0,3
0,4
0,5
0,6
0,7

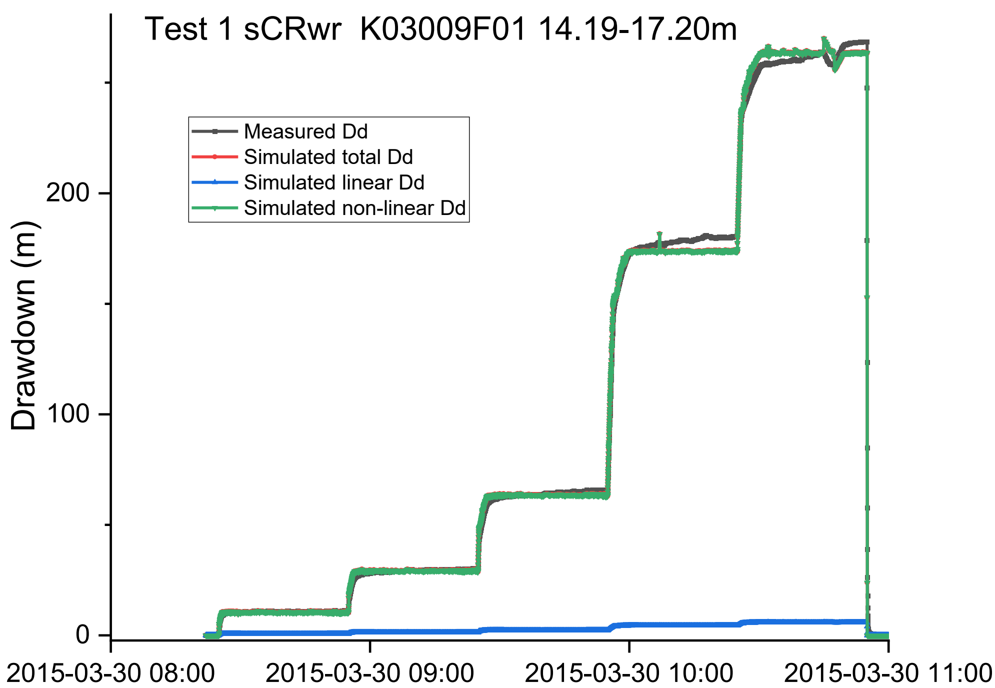
Test 1 sCRwr K03009F01 14.19-17.20m
Drawdown (m)
Measured Dd
Simulated total Dd
Simulated linear Dd
Simulated non-linear Dd
200
100
0
2015-03-30 08:00
2015-03-30 09:00
2015-03-30 10:00
2015-03-30 11:00

Test 9 sCRwr K03009F01, 17.20-20.19m

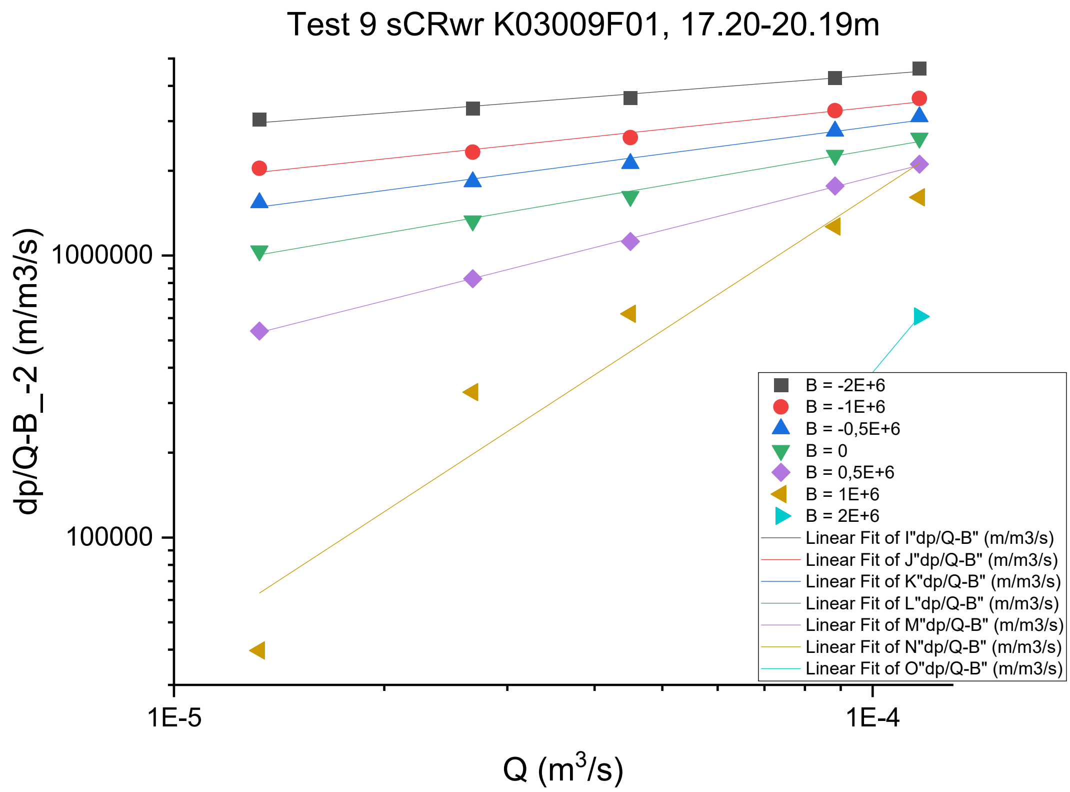

Equation	y = a + b*x						
Plot	dp/Q-B_-2	dp/Q-B_-1	dp/Q-B_-0.5	dp/Q-B_0	dp/Q-B_0.5	dp/Q-B_1	dp/Q-B_2
Weight	No Weighting						
Intercept	7,41019 ± 0,07473	7,58384 ± 0,08875	7,75916 ± 0,09463	8,07837 ± 0,09188	8,78834 ± 0,04145	12,67232 ± 1,15405	17,46926 ± --
Slope	0,1925 ± 0,0171	0,26408 ± 0,02031	0,32525 ± 0,02165	0,42555 ± 0,02102	0,62756 ± 0,00948	1,61333 ± 0,26407	2,971 ± --
Residual Sum of Squares	5,16969E-4	7,2906E-4	8,28868E-4	7,81534E-4	1,59051E-4	0,12328	6,31089E-30
Pearson's r	0,98837	0,99125	0,99342	0,99636	0,99966	0,96208	1
R-Square (COD)	0,97688	0,98257	0,98688	0,99273	0,99932	0,92561	1
Adj. R-Square	0,96917	0,97676	0,98251	0,99031	0,99909	0,90081	--

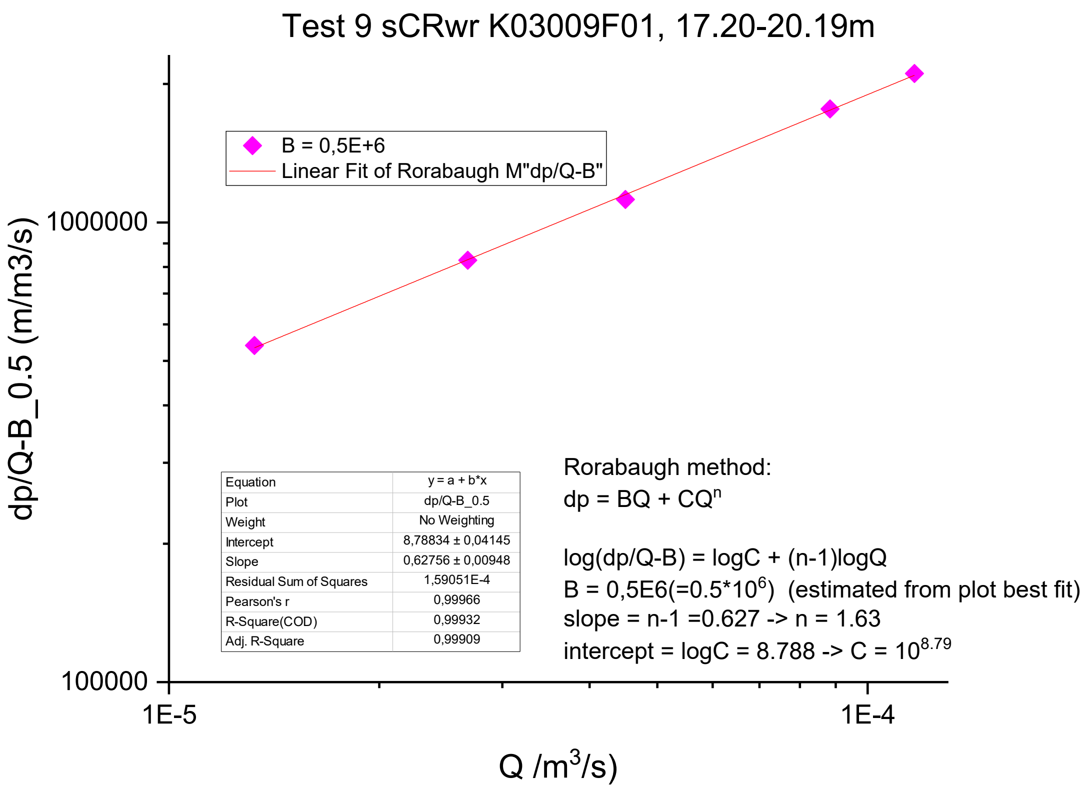
Test 9 sCRwr K03009F01, 17.20-20.19m
B = 0,5E+6
Linear Fit of Rorabaugh M"dp/Q-B"
dp/Q-B_0.5 (m/m3/s)
1000000
100000
1E-5
1E-4
Q /m3/s)
Equation y = a + b*x
Plot dp/Q-B_0.5
Weight No Weighting
Intercept 8,78834 ± 0,04145
Slope 0,62756 ± 0,00948
Residual Sum of Squares 1,59051E-4
Pearson's r 0,99966
R-Square(COD) 0,99932
Adj. R-Square 0,99909
Rorabaugh method:
dp = BQ + CQn
log(dp/Q-B) = logC + (n-1)logQ
B = 0,5E6(=0.5*106) (estimated from plot best fit)
slope = n-1 =0.627 -> n = 1.63
intercept = logC = 8.788 -> C = 108.79

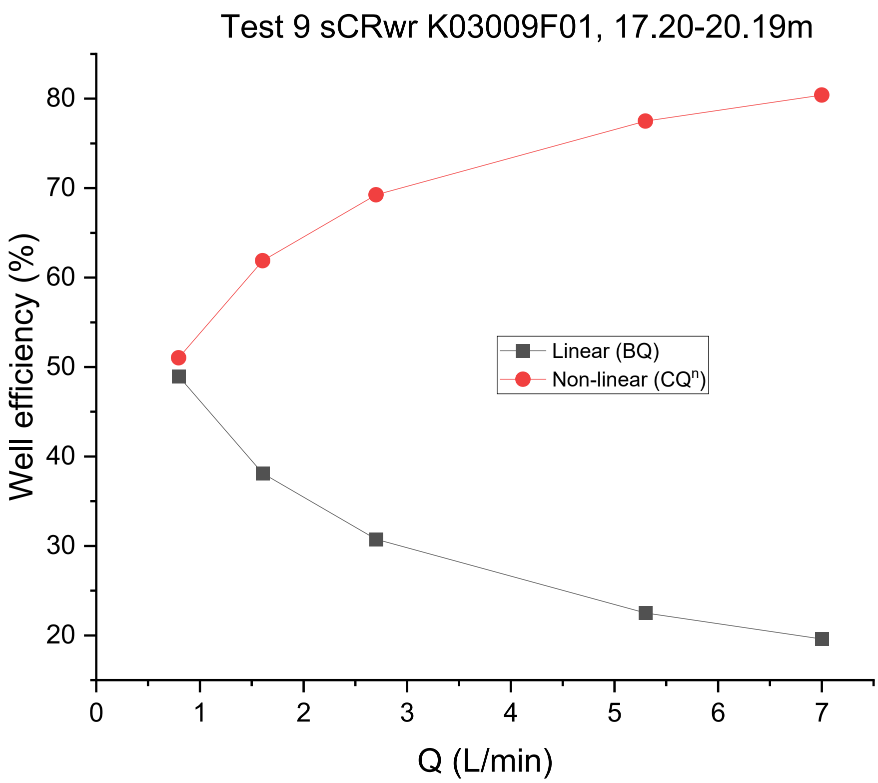
Test 9 sCRwr K03009F01, 17.20-20.19m
Well efficiency (%)
80
70
60
50
40
30
20
Linear (BQ)
Non-linear (CQn)
0
1
2
3
4
5
6
7
Q (L/min)

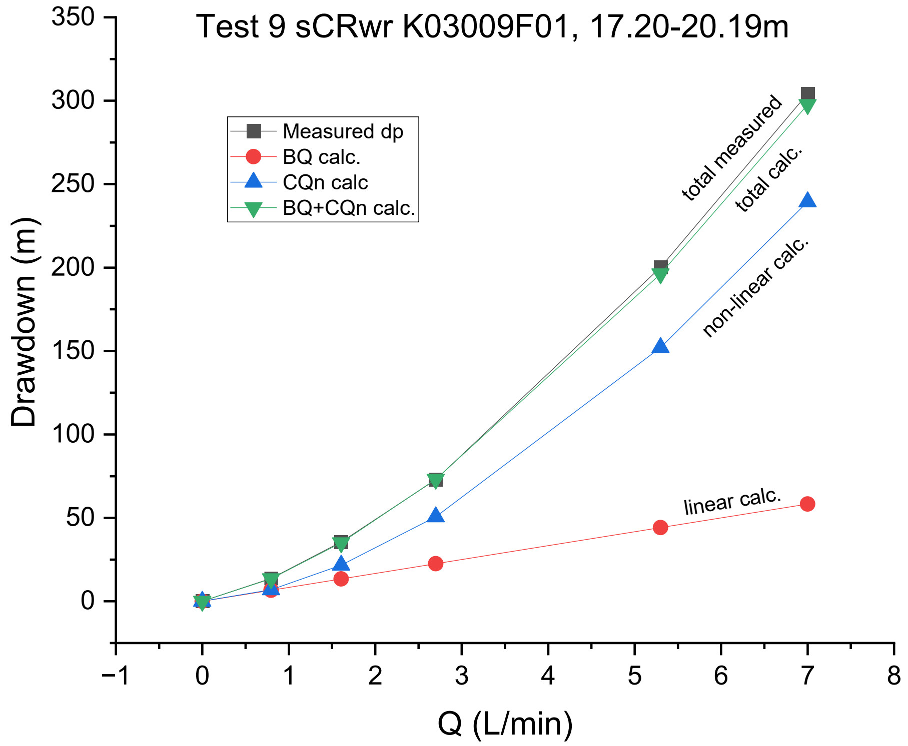
Test 9 sCRwr K03009F01, 17.20-20.19m
Measured dp
BQ calc.
CQn calc
BQ+CQn calc.
total measured
total calc.
non-linear calc.
linear calc.
Drawdown (m)
Q (L/min)
350
300
250
200
150
100
50
0
−1
0
1
2
3
4
5
6
7
8

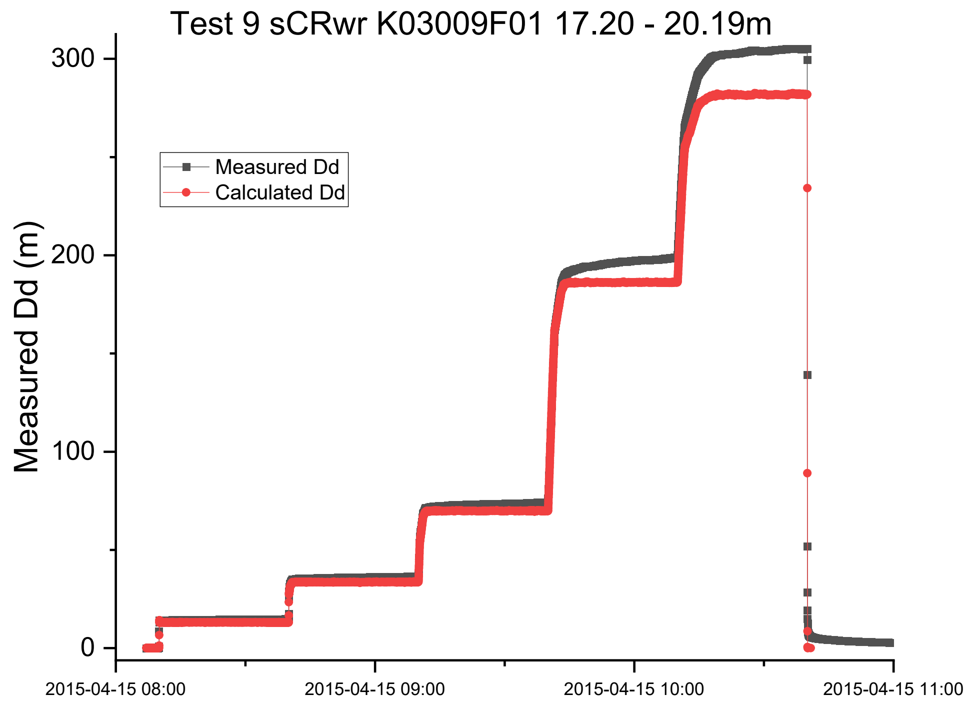
Test 9 sCRwr K03009F01 17.20 - 20.19m
Measured Dd
Calculated Dd
Measured Dd (m)
300
200
100
0
2015-04-15 08:00
2015-04-15 09:00
2015-04-15 10:00
2015-04-15 11:00

Test 10 sCRwr K03009F01, 15.30-16.79m

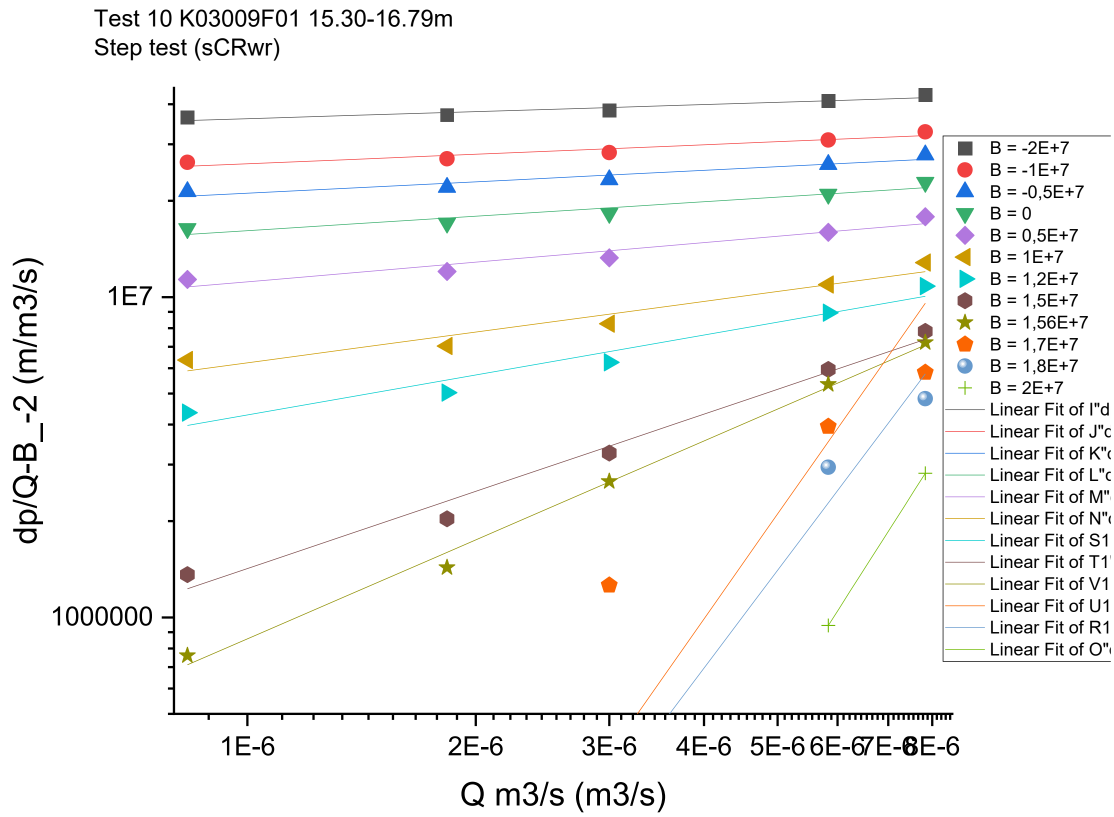

Equation	y = a + b*x						
Plot	dp/Q-B_-2	dp/Q-B_-1	dp/Q-B_-0.5	dp/Q-B_0	dp/Q-B_0.5	dp/Q-B_1	dp/Q-B_1.2
Weight	No Weighting						
Intercept	7,99639 ± 0,07302	8,00626 ± 0,09601	8,03639 ± 0,11393	8,10618 ± 0,13997	8,26748 ± 0,1811	8,70484 ± 0,25381	9,11758 ± 0,29797
Slope	0,0732 ± 0,01316	0,09829 ± 0,01731	0,11866 ± 0,02054	0,14975 ± 0,02523	0,20325 ± 0,03265	0,31828 ± 0,04576	0,41419 ± 0,05372
Residual Sum of Squares	3,17903E-4	5,49691E-4	7,73912E-4	0,00117	0,00196	0,00384	0,00529
Pearson's r	0,95476	0,95649	0,95788	0,95995	0,96341	0,97037	0,97568
R-Square (COD)	0,91157	0,91488	0,91753	0,9215	0,92815	0,94162	0,95196
Adj. R-Square	0,88209	0,88651	0,89004	0,89534	0,9042	0,92216	0,93595

y = a + b*x						
dp/Q-B_1	dp/Q-B_1.2	dp/Q-B_1.5	dp/Q-B_1.56	dp/Q-B_1.7	dp/Q-B_1.8	dp/Q-B_2
No Weighting						
8,70484 ± 0,25381	9,11758 ± 0,29797	10,95584 ± 0,32284	12,08894 ± 0,23379	24,22199 ± 5,23175	22,82501 ± 2,45028	25,40747 ± --
0,31828 ± 0,04576	0,41419 ± 0,05372	0,80051 ± 0,0582	1,02593 ± 0,04215	3,37656 ± 0,96785	3,14621 ± 0,46314	3,7127 ± --
0,00384	0,00529	0,00621	0,00326	0,4542	0,01956	2,52435E-29
0,97037	0,97568	0,99216	0,99748	0,92675	0,98934	1
0,94162	0,95196	0,98439	0,99496	0,85887	0,97879	1
0,92216	0,93595	0,97918	0,99328	0,7883	0,95758	--

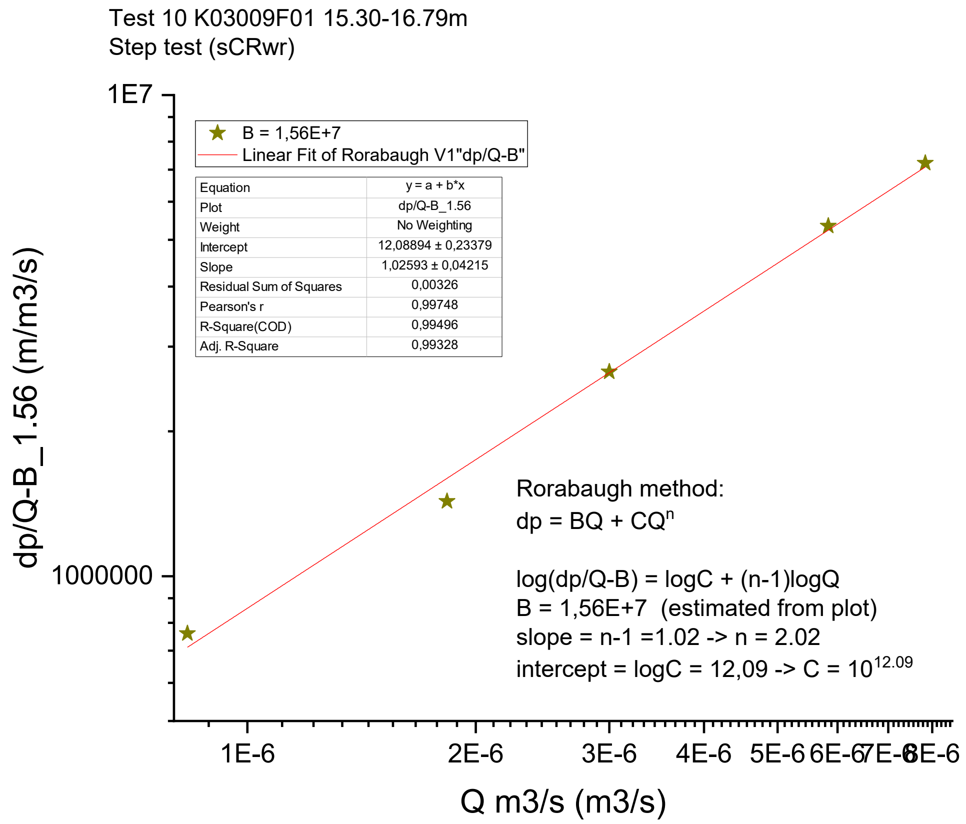

Test 10 K03009F01 15.30-16.79m
Step test (sCRwr)
B = 1,56E+7
Linear Fit of Rorabaugh V1"dp/Q-B"
Equation y = a + b*x
Plot dp/Q-B_1.56
Weight No Weighting
Intercept 12,08894 ± 0,23379
Slope 1,02593 ± 0,04215
Residual Sum of Squares 0,00326
Pearson's r 0,99748
R-Square(COD) 0,99496
Adj. R-Square 0,99328
Rorabaugh method:
dp = BQ + CQn
log(dp/Q-B) = logC + (n-1)logQ
B = 1,56E+7 (estimated from plot)
slope = n-1 =1.02 -> n = 2.02
intercept = logC = 12,09 -> C = 1012.09
dp/Q-B_1.56 (m/m3/s)
1E7
1000000
1E-6
2E-6
3E-6
4E-6
5E-6
6E-6
7E-6
8E-6
Q m3/s (m3/s)

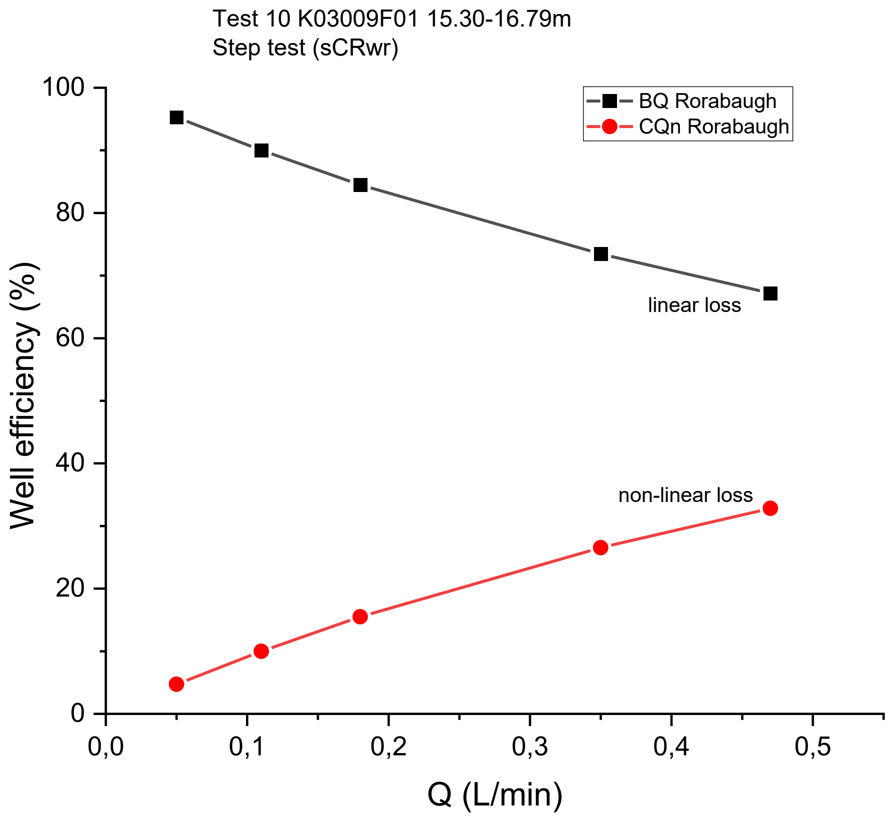

Test 10 K03009F01 15.30-16.79m
Step test (sCRwr)
BQ Rorabaugh
CQn Rorabaugh
linear loss
non-linear loss
Well efficiency (%)
100
80
60
40
20
0
0,0
0,1
0,2
0,3
0,4
0,5
Q (L/min)

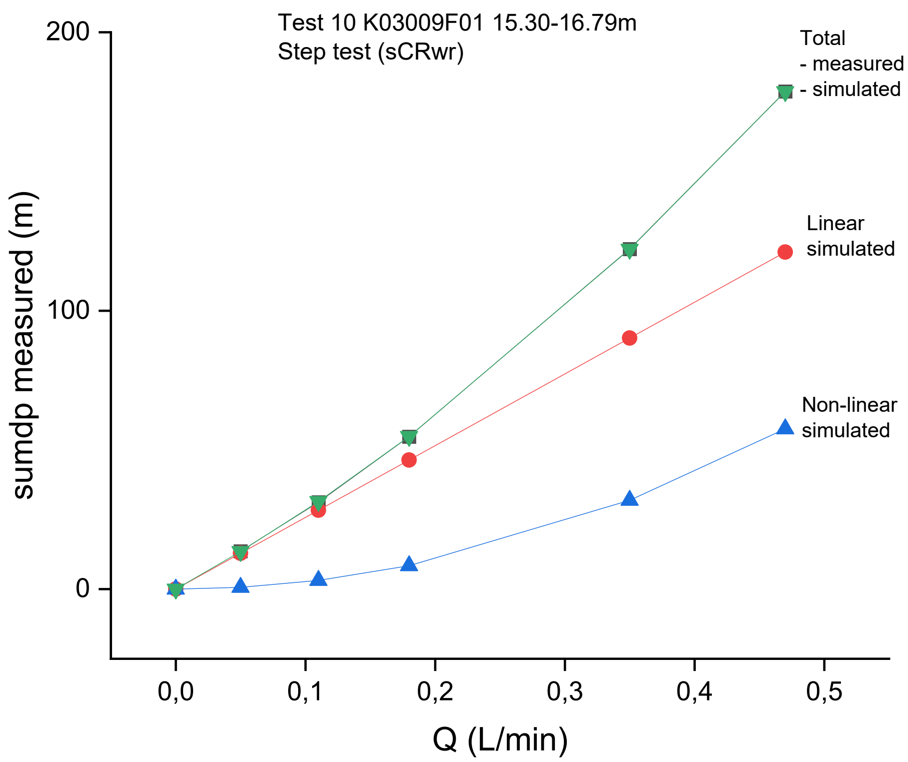

Test 10 K03009F01 15.30-16.79m
Step test (sCRwr)
Total
- measured
- simulated
Linear
simulated
Non-linear
simulated
sumdp measured (m)
200
100
0
0,0
0,1
0,2
0,3
0,4
0,5
Q (L/min)

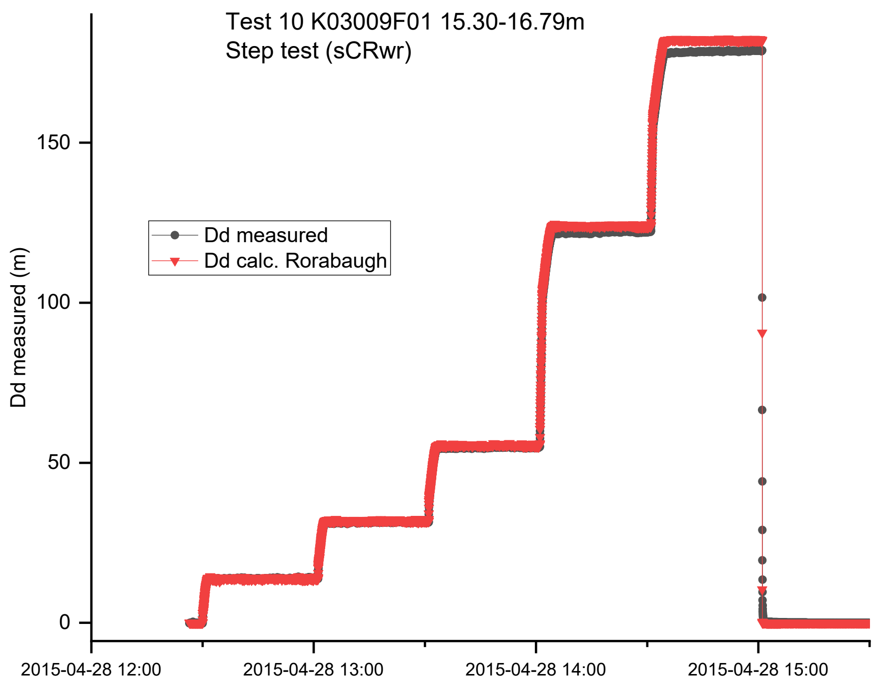

Test 10 K03009F01 15.30-16.79m
Step test (sCRwr)
Dd measured
Dd calc. Rorabaugh
Dd measured (m)
150
100
50
0
2015-04-28 12:00
2015-04-28 13:00
2015-04-28 14:00
2015-04-28 15:00

Test 13 sCRwr K08028F01, 37.00-39.00m

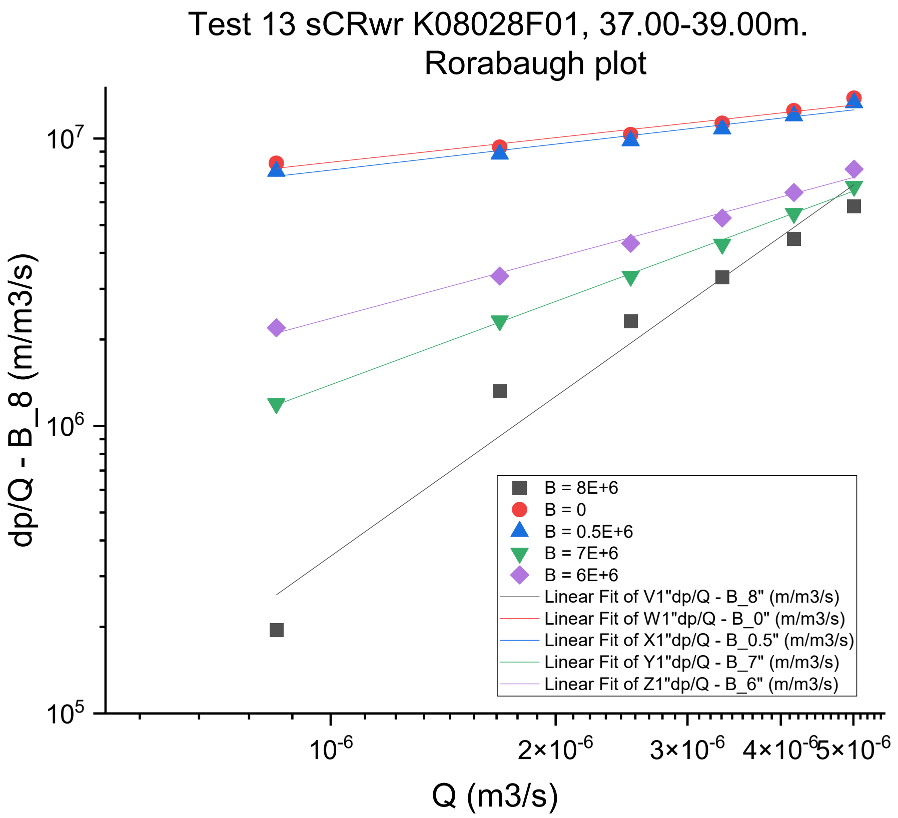

Equation	y = a + b*x				
Plot	dp/Q - B_8	dp/Q - B_0	dp/Q - B_0.5	dp/Q - B_7	dp/Q - B_6
Weight	No Weighting				
Intercept	16,62853 ± 1,00702	8,62778 ± 0,17151	8,68767 ± 0,17674	11,92325 ± 0,10882	10,5858 ± 0,19643
Slope	1,84695 ± 0,17962	0,28512 ± 0,03059	0,29957 ± 0,03152	0,96334 ± 0,01941	0,70199 ± 0,03504
Residual Sum of Squares	0,05253	0,00152	0,00162	6,13416E-4	0,002
Pearson's r	0,9816	0,97774	0,97856	0,99919	0,99505
R-Square (COD)	0,96355	0,95598	0,95758	0,99838	0,99013
Adj. R-Square	0,95443	0,94497	0,94698	0,99797	0,98767

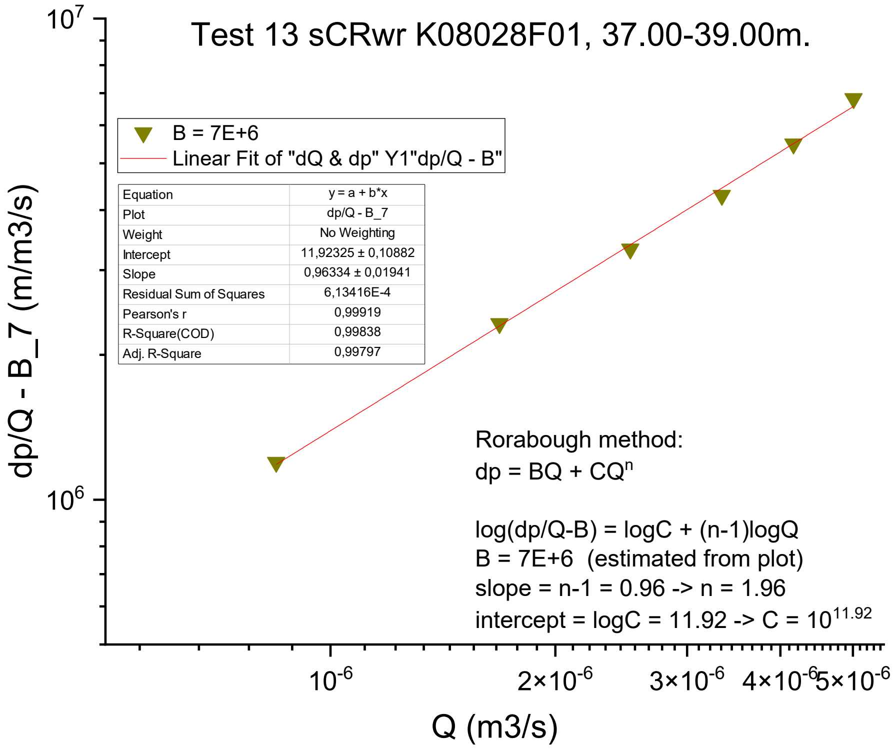
Test 13 sCRwr K08028F01, 37.00-39.00m.
B = 7E+6
Linear Fit of "dQ & dp" Y1"dp/Q - B"
Equation y = a + b*x
Plot dp/Q - B_7
Weight No Weighting
Intercept 11,92325 ± 0,10882
Slope 0,96334 ± 0,01941
Residual Sum of Squares 6,13416E-4
Pearson's r 0,99919
R-Square(COD) 0,99838
Adj. R-Square 0,99797
Rorabough method:
dp = BQ + CQ^n
log(dp/Q-B) = logC + (n-1)logQ
B = 7E+6 (estimated from plot)
slope = n-1 = 0.96 -> n = 1.96
intercept = logC = 11.92 -> C = 10^11.92
dp/Q - B_7 (m/m3/s)
Q (m3/s)

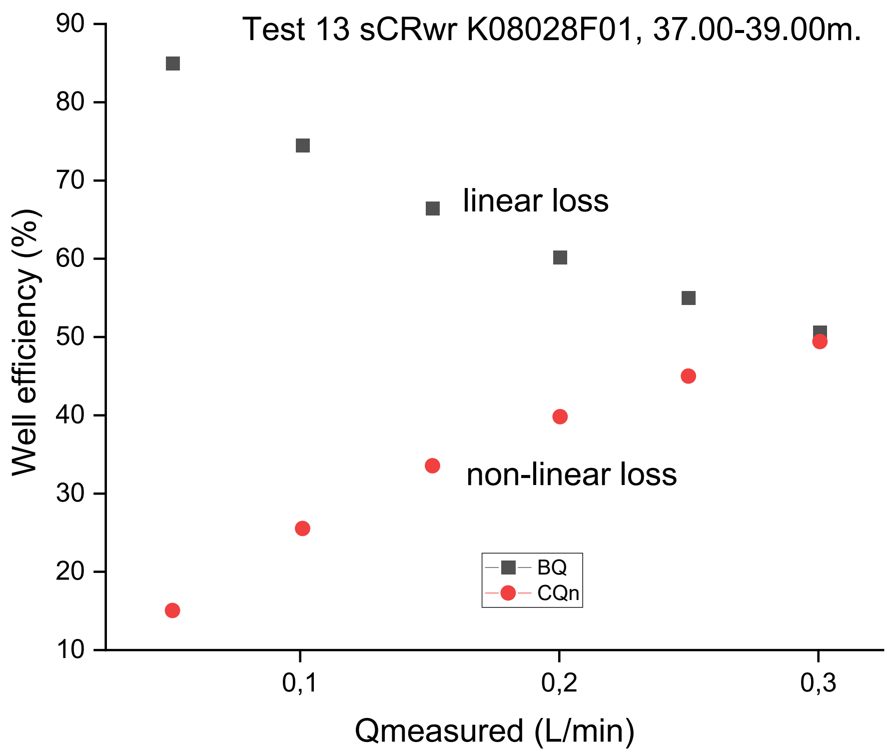
Test 13 sCRwr K08028F01, 37.00-39.00m.
linear loss
non-linear loss
BQ
CQn
Well efficiency (%)
Qmeasured (L/min)

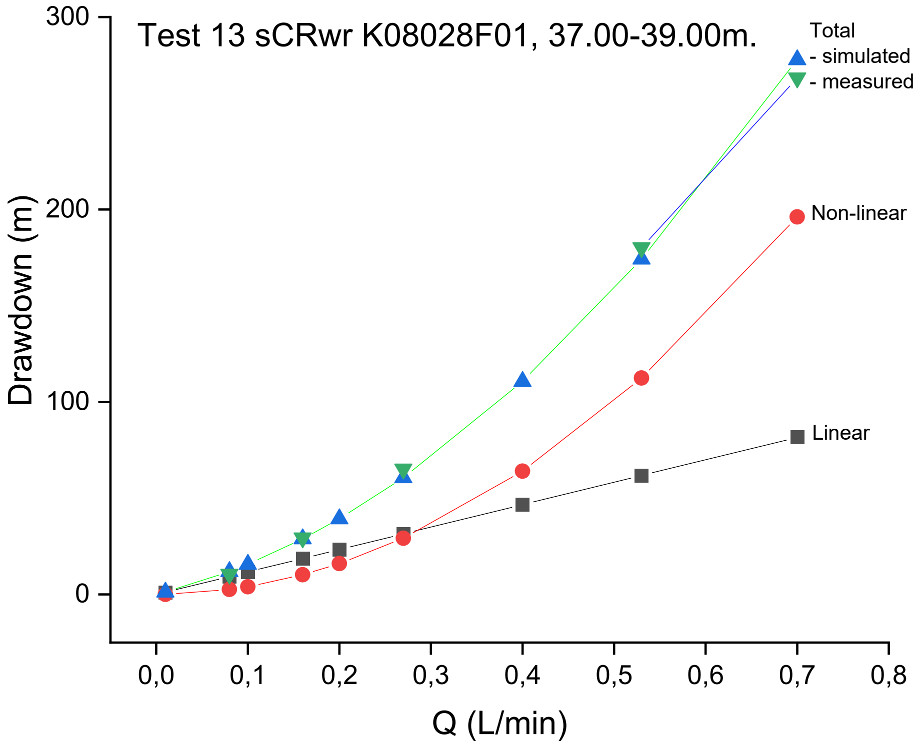
Test 13 sCRwr K08028F01, 37.00-39.00m.
Total
- simulated
- measured
Non-linear
Linear
Drawdown (m)
Q (L/min)
300
200
100
0
0,0
0,1
0,2
0,3
0,4
0,5
0,6
0,7
0,8

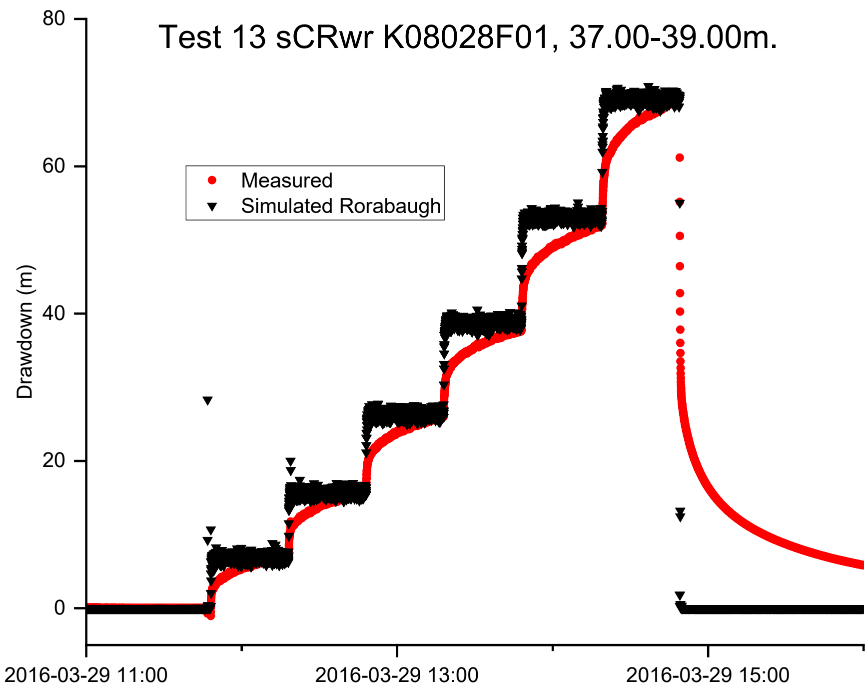
Test 13 sCRwr K08028F01, 37.00-39.00m.
Measured
Simulated Rorabaugh
Drawdown (m)
80
60
40
20
0
2016-03-29 11:00
2016-03-29 13:00
2016-03-29 15:00

Appendix 6 - Withdrawal vs injection

The main rationale of these tests is to compare and confirm that injection and withdrawal tests produce similar results in terms of skin factors and transmissivities, when performed under otherwise same conditions. They are performed with the same constant *dp* of 1000kPa.

The tests are executed in two different hydrogeological settings, Test 4 and 8 in a discrete open fracture setting and Test 16 and 19 in a crush zone setting.

Test 4 and 8, Fractures in section 14.20-17.19m in K03009F01

These tests are performed with same duration of 1.5h and same pressure disturbance of 1000kPa. Figure A6-1 shows the perturbation phase of the two tests: compiled results in Table A6-1. We note that it required a much higher flow rate during injection than during withdrawal to maintain the same constant change in pressure . For the injection Q_i = 0.55L/min with a total injected volume of V = 47.9L and for the withdrawal Q_w = 0.32L/min with a total extracted volume of V = 28.8L.

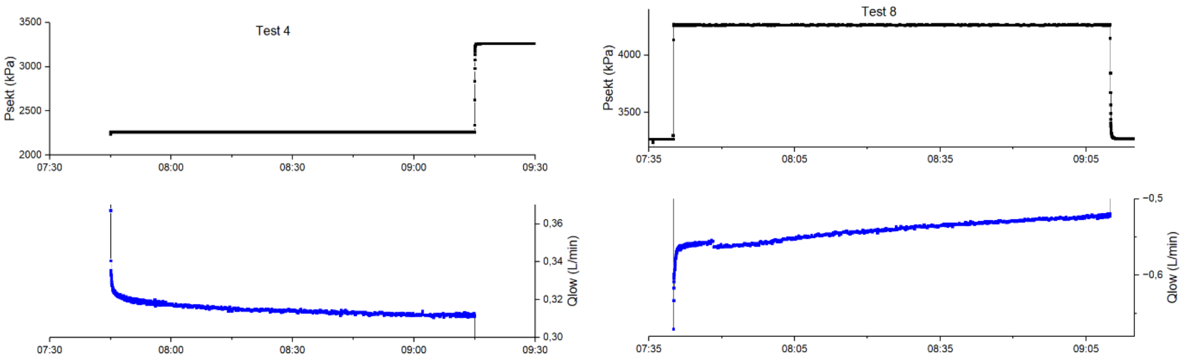

Figure A6-1. *Linear history plots of the flow rate of perturbation phase, Test 4 withdrawal (left) and Test 8 injection (right).*

This difference in flow rates and volumes is believed to be caused mainly by higher *dp* during injection than withdrawal. Note that pre-perturbation pressure data is missing for Test 4 which gives additional uncertainty to the adopted constant *dp*.

Table A6-1 Specific capacity and transmissivities for the perturbation phase of Test 4 and Test 8.

Test no.	Test type	Perturbation	Stabilized flow rate	Total flowed volume	dQ/dp	T_{Moye}	T_{Thiem}	TT (transient)	Skin factor
	units:	kPa	L/min	L	m^2/s	m^2/s	m^2/s	m^2/s	-
4	Withdrawal	c. 1000[a]	0,32	28,8	5,1E-08	3,6E-08	8,0E-08	4,6E-07	49
8	Injection	1000,309	0,52	47,9	8,5E-08	6,0E-08	1,3E-07	3,5E-07	18
	ratio w/i		0,6	0,6	0,6	0,6	0,6	1,3	2,7

a) Unfortunately pre-perturbation pressure data is missing and dp is an estimated approximation

Evaluated parameters (Table A6-1) show consistent and similar transmissivity values between the withdrawal and injection phase respectively, pseudo steady-state evaluation by a factor 0.6 and transient a factor 1.3 and skin 2.7.

The diagnostic derivative is quite noisy (Figur 8-4) due to noisy flow rate signal, (Figure 8-3), which is carried forward to the dependent variable (*dp/dQ*). Generally, the smoothing factor for the dependent variable (*dp/dQ*) of the diagnostic derivative is held as low as possible but sufficiently high to extract a diagnostic signature without distorting the underlying information. Usually, a smoothing factor of 0.2 up to 0.5 is used. In the evaluating software (Aqtesolv) a constant value is given for dp, 100m for these tests.

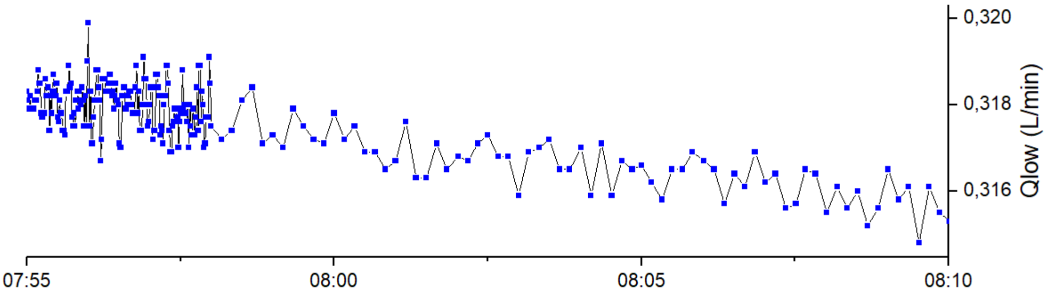

Figure A6-2. *Time series of measured flow rate of the constant head phase of Test 4, extracted from Figure 8-2.*

From the perturbation phase (injection) the log-log diagnostic plot shows a fluctuating derivative, possibly reminiscent of a double porosity signature but is interpreted as a radial flow geometry consistent with Test 4, although its derivative is quite noisy as well, Figure 8-4. The transient interpretation yielded similar transmissivity but different skin factors for withdrawal and injection respectively, Table 8-3.

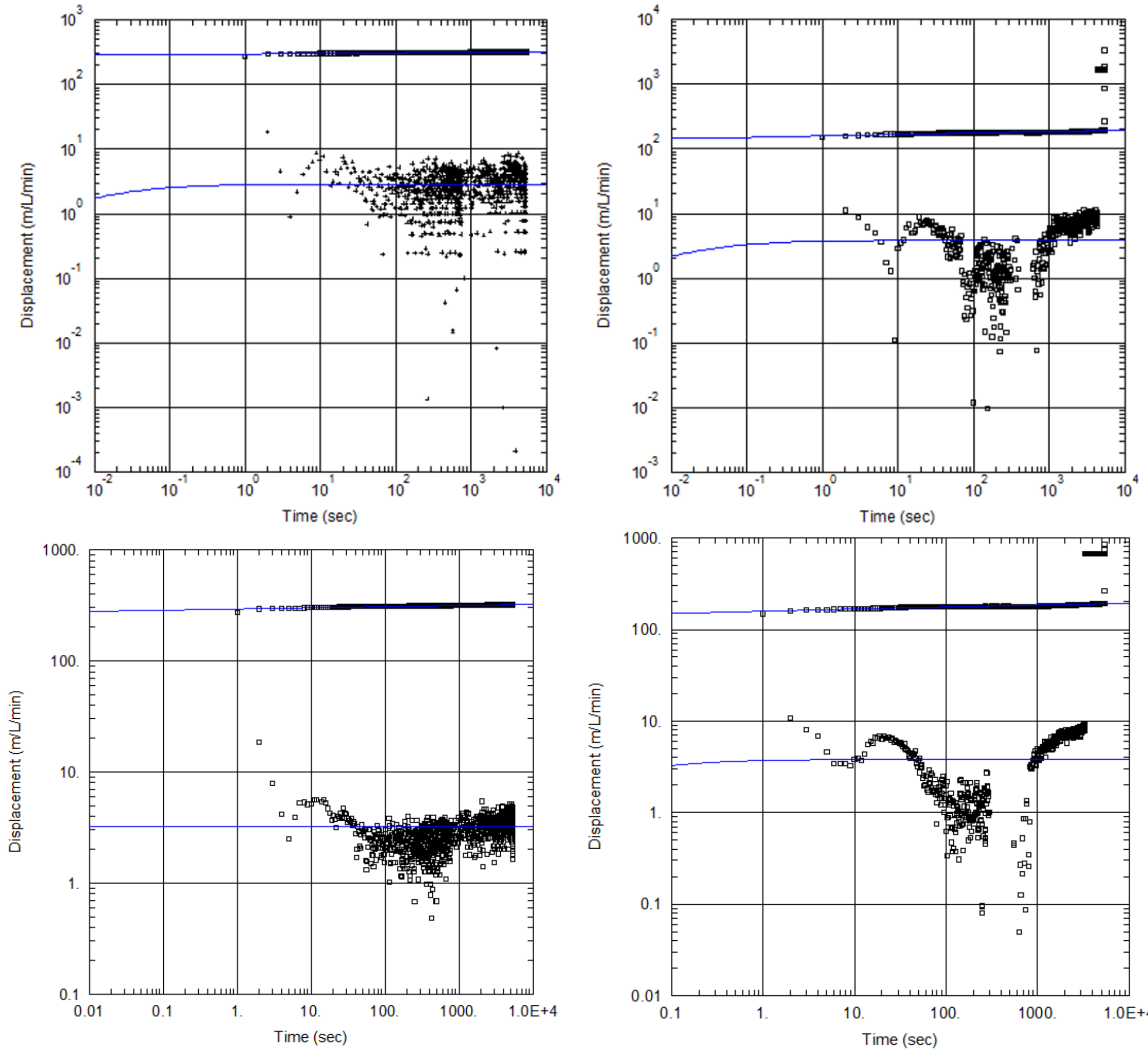

Figure A6-3 *Log-Log diagnostic plot of perturbation Test 4 withdrawal (left) and Test 8 injection (right), both with constant head of 1000kPa relative the initial formation pressure. Plots above with a smoothing factor 0.2 and those below 0.5.*

Test 16 and 19, Crush zone in section 37-39m K08028F01

The perturbation phase of the two tests are shown in Figure A6-4, performed with same duration of 1.5 h and same pressure disturbance of 1000kPa. It required similar but slightly lower flow rates during injection than withdrawal, to maintain the same constant dp. For Test 19 injection Q_i = 0.18L/min with a total injected volume of V = 18.4L and for Test 16 the withdrawal Q_w = 0.23L/min with a total extracted volume of V = 21.9L, Table 6-2.

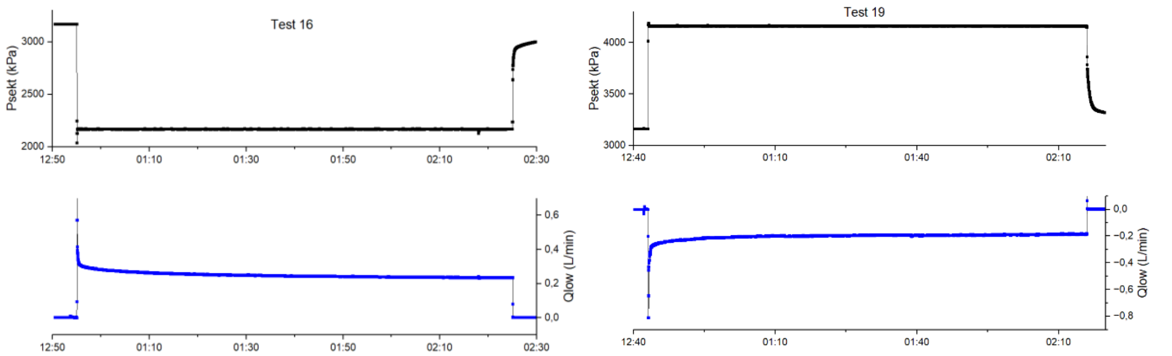

Figure A6-4. *Linear history plots of the flow rate of perturbation phase, Test 16 withdrawal (left) and Test 19 injection (right).*

This difference in flow rates and volumes is attributed to the slightly higher dp by about 2kPa during withdrawal than injection, but possibly also on how the control unit (HWIC) works when regulating valves and pumps through the algorithms in response to the formations ability to transmit water, towards targeted head. Table A6-2.

Table A6-2 Steady state evaluated specific capacity and transmissivity Test 16 and Test 19.

Test no.	Test type	Perturbation	Stabilized flow rate	Total flowed volume	dQ/dp	T_{Moye}	T_{Thiem}	TT (transient)	Skin factor (transient)
	units:	kPa	L/min	L	m^2/s	m^2/s	m^2/s	m^2/s	(-)
16	Withdrawal	1001,131	0,23	21,9	3,8E-08	5,7E-08	5,7E-08	7,3E-08	6
19	Injection	999,01	0,18	18,4	2,9E-08	4,5E-08	4,4E-08	3,5E-08	1
	ratio w/i		1,3	1,2	1,3	1,3	1,3	2,1	6,0

Evaluated parameters (Table A6-2) show consistent and similar transmissivity values between the withdrawal and injection phase respectively, pseudo steady-state evaluation by a factor 1.3 and transient a factor 2.1 and skin 6.

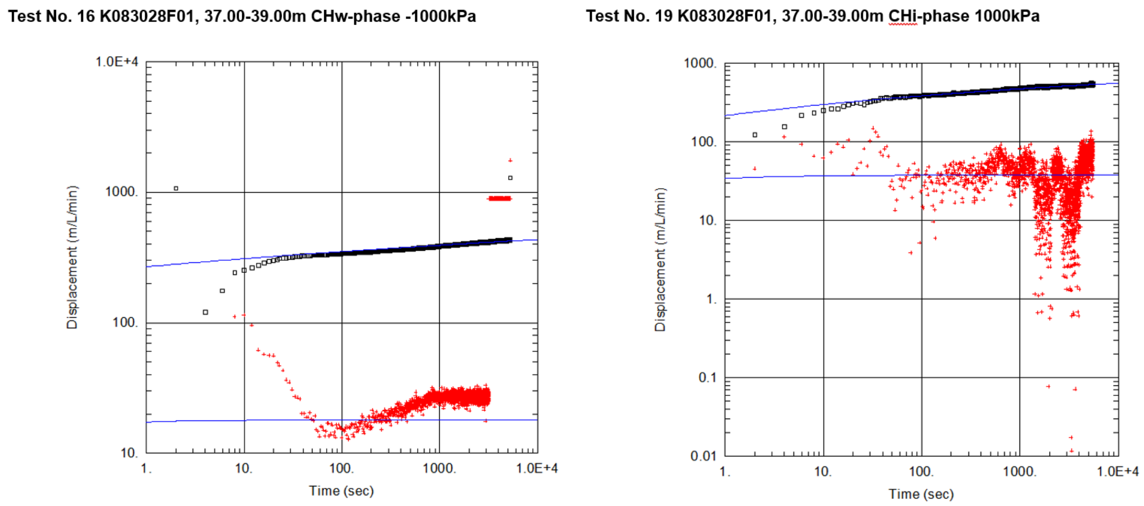

Figure A6-5 *Log-Log diagnostic plot of perturbation Test 16 withdrawal (left) and Test 19 injection (right), both with constant head of 1000kPa relative the initial formation pressure.*

Appendix 7 - Interpreted hydraulic formation parameters

Test No.	Test type[1]	Pertur-bation	Perturbation	Durat. perturb.	dQ/dp^2	TT (transient)	Skin, ξ (transient)	T_{Moye} (PSS)	T_{Thiem} (PSS)	Flow regime (n)	On-set nonlinearity dQ	On-set nonlinearity dp	Well efficiency
		L/min	kPa	h	m^2/s	m^2/s	-	m^2/s	m^2/s	-	L/min	mH_2O	%
K03009F01 14,20-17,19m													
1	sCRwr	0.08->0.7		5x0.5						1,51	0,15	25	6->2
2	CHw		-300	1,5	6,5E-08	1,8E-07	11	1,0E-07	7,8E-08				
3	CHw		-600	1,5	5,7E-08	5,1E-07	47	4,3E-08	3,2E-08				
4	CHw		-1000	1,5	5,1E-08	4,6E-07	49	3,8E-08	2,8E-08		0,15	50	
5	CHw		-2000	1,5	4,3E-08	5,5E-07	71	3,2E-08	2,4E-08				
6	CHw		-3000	1,5	4,1E-08	6,4E-07	92	3,0E-08	2,3E-08				
7	sCHir		300->1500->300	7x0.5							0,3	40	
8	CHi		1000	1,5	8,5E-08	3,5E-07	18	6,3E-08	4,7E-08				
K03009F01 17,20-20,19m													
9	sCRwr	0.8->7		5x0.5						1,63	1,7	40	49->20
9a	CHw		-300	1,5	7,4E-07	4,6E-06	30	5,5E-07	4,1E-07				
9b	CHw		-600	1,5	6,1E-07	4,5E-06	37	4,5E-07	3,4E-07				
9c	CHw		-1000	1,5	5,7E-07	2,2E-06	16	4,2E-07	3,1E-07		2	50	
9d	CHw		-2000	1,5	4,3E-07	1,9E-06	19	3,2E-07	2,4E-07				
9e	CHw		-3000	1,5	3,7E-07	4,9E-06	73	2,7E-07	2,0E-07				
K03009F01 15.30-16.79m													
10	sCRwr	0.05->0.47		5x0.5						2,02	0,18	50	95->67
11	sCHir		300->1500->300	7x0.5							0,35	80	
K08028F01 37.00-39.00m													
12	sCHir		10->1500->10	16x0.5							0,05	20	
13	sCRwr	0.05->0.3		5x0.5						1,96	0,1	18	85->51
14	CHw		-300	1,5	6,7E-08	6.2E-08	-0,6	4,6E-08	1,0E-07				
15	CHw		-600	1,5	5,4E-08	6,7E-08	1	3,7E-08	8,1E-08				
16	CHw		-1000	1,5	3,8E-08	7,3E-08	5	2,6E-08	5,7E-08		0,17	50	
17	CHw		-2000	1,5	2,5E-08	4,0E-08	6	1,7E-08	3,8E-08				
18	CHw		-3000	1,5	1,9E-08	2.9E-08	4	1,3E-08	2,8E-08				
19	CHi		1000	1,5	3,0E-08	3.5E-08	1	2,0E-08	4,5E-08				

1) CRw r: Constant Rate Withdraw al and Recovery
CHw r: Constant Head Withdraw al and Recovery
Chir: Constant Head Injection and Recovery
sCRw r: step Constant Rate Withdraw al and Recovery
sCHir: step Constant Head Injection and Recovery
2) At end of perturbation phase

PSS= pseudo steady-state

n=1 linear flow
n=2 turbulent flow